UNIVERSITY OF NAPLES FEDERICO II
DEPARTMENT OF PHARMACY

PLANT- DERIVED COMPOUNDS IN EXPERIMENTAL INFLAMMATORY BOWEL DISEASE AND COLON CARCINOGENESIS

by

INES FASOLINO

Ph.D. Thesis
25th Cycle

TUTOR	**COORDINATOR**
Prof. Angelo A. Izzo	**Prof. Maria Valeria D'auria**

Ph.D. Programme in Pharmaceutical Sciences

2010-2013

INDEX **Page**

ABBREVIATIONS

ACF, aberrant crypt foci; AOM, azoxymethane; BHT, 2,6-di-tert-butyl-4-methylphenol; CAM, complementary/alternative medicine; CB_1, cannabinoid receptor type 1; CB_2, receptor cannabinoid type 2; CBD, cannabidiol; CBG, cannabigerol; CD, Crohn's disease; COX-1, cyclooxygenase type 1; COX-2, cyclooxygenase type 2; CRC, colorectal cancer; DADS, diallyl disulfide; DAN, 2,3-iaminonaphtalene; DAPI, 2-(4-amidinophenyl)-1H-indole-6-carboxamidine; DAS, diallyl sulfide; DMEM, Dulbecco's Modified Eagle Medium; DMPO, 5,5-dimethyl-1-pyrroline-N-oxide; DMSO, dimethyl sulfoxide; DNBS, dinitrobenzenesulphonic acid; DTT, dithiothreitol; ENMD-1068, N^1-3-methylbutyryl-N^4-6-aminohexanoyl-piperazine; ERKs, extracellular-signal-related kinases; FBS, Fetal Bovine Serum; FITC, fluorescein isothiocyanate conjugated dextran; H_2DCF-DA, 2′,7′-dichlorfluorescein-diacetate; H_2O_2, hydrogen peroxide; IBD, inflammatory bowel disease; IFN-γ, interferon-gamma; IL-10, interleukin-10; IL-1β, interleukin-1β; IL-6, interleukin-6; iNOS, inducible nitric oxide synthase; ip, intraperitoneally; IP-10, Interferon-γ-induced protein 10; LDH, lactate dehydrogenase; LPS, lipopolysaccharide; MAPK, mitogen-activated protein kinase; MDA, malondialdehyde; MTT, 3-(4,5-dimethylthiazol-2-yl)-2,5-diphenyltetrazolium bromide; MPO, Myeloperoxidase; NF-kB, nuclear-factor kappa B; NO, nitric monoxide; NR, neutral red; PAR-2, protease-activated receptors type 2; PBS, phosphate buffer saline; ROS, reactive oxygene species; SDS, sodium dodecyl sulphate; SOD, superoxide dismutase; TBA, thiobarbituric acid; TBARs, thiobarbituric acid reactive substances; TCA, trichloroacetic acid; TRP, transient receptor potential channels; TRPA1, transient receptor potential ankyrin type 1;TRPV1, transient receptor potential vanilloid type 1; WST-8, 2-(2-methoxy-4-nitrophenyl)-3-(4-nitrophenyl)-5-(2,4disulfophenyl)-2H-tetrazolium, monosodium salt; Δ^9-THC, Δ^9-tetrahydrocannabinol.

1.0 INTRODUCTION

1.1 Inflammatory bowel disease (IBD) and colorectal cancer (CRC)

Inflammatory bowel disease (IBD) and colorectal cancer (CRC) are widespread intestinal diseases. The link between these two diseases is highlighted by the observation that patients with IBD are at increased risk for CRC. The risk is related to the duration and anatomic extent of the disease (Ekbom et al., 1990). The mortality in patients diagnosed with CRC in the setting of IBD is higher than for sporadic CRC (Triantafillidis et al., 2009). IBD, which includes Crohn's disease (CD) and ulcerative colitis (UC), has a high incidence in industrialized countries (Hou et al., 2009). IBD was previously considered to be diseases of Caucasian patients, but recent studies have documented the increasing burden of this disease among non-white populations outside the United States (Cosnes et al., 2011; Molodecky et al., 2012). The incidence and prevalence of IBD has increased in the past 50 years, up to 8–14/100,000 and 120–200/100,000 cases, respectively, for UC and 6–15/100,000 and 50–200/100,000 cases, respectively, for CD (Cosnes et al., 2011). While CD and UC involve different genetic vulnerabilities, pathological abnormalities, and different regions of involvement in the intestinal tract, both are characterized by gastrointestinal symptoms such as bloody diarrhea, weight loss, and abdominal pain, as well as extra-intestinal manifestations such as joint pain, uveitis, and erythema nodosum. IBD can be alleviated with medications that induce and maintain remission since a cure remains elusive. Steroids, 5-ASA, and biologicals have been a mainstay in its treatment (Sewell et al., 2010; Jones et al., 2011). Although these drugs may be effective, their long-termuse can induce severe side effects that have detrimental impact on life quality of patients (Blonski et al., 2011). Hence, it is required to

develop new therapeutic approaches with fewer side effects for the treatment of IBD.

CRC is a major cause of morbidity and mortality in western countries. In 2013, an estimated 142,82 new cases of colorectal cancer were diagnosed in the USA, with 50,830 estimated deaths (Siegel at al., 2013). CRC is thought to arise as the result of a series of histopathologic and molecular changes that transform normal colonic epithelial cells into a colorectal carcinoma, with aberrant crypt foci (ACF) and polyps as intermediate steps in this process (Markowitz at al., 2009). This multi-step process spans 10 to 15 years, thereby providing an opportunity for prevention (Half et al., 2009). Surgery is the cornerstone for cure in localized colorectal cancer (Sargent et al., 2007). Chemotherapy after surgery (adjuvant chemotherapy, in high risk stage II and stage III CRC patients) versus surgery alone reduced the risk of cancer relapse (Cunningham et al., 2010; Wolpin and Meyer, 2008). Drugs used in colorectal cancer chemotherapy include fluorouracil, irinotecan, oxaliplatin, angiogenesis inhibitors (i.e. bevacizumab) and epidermal growth factor receptor inhibitors (i.e. cetuximab and and panitumumab) (Wolpin and Mayer, 2008). Despite many progresses, and improvement of overall survival to nearly 2 years for non-resectable disease, cures for this kind of neoplasia remain unsatisfactory (Cunningham et al., 2010). Also, the new chemotherapeutic agents (i.e. the biologicals cetuximaband, panitumumab and bevacizumab) have not come without a significant cost to the health care system (Wolpin and Meyer, 2008).

1.2 Ancient and modern use of plant products: focus on inflammatory bowel disease and colorectal cancer

Plants have been traditionally used in folk medicine and are actually practiced in industrialized countries where their use is often integrated into conventional medicine (Capasso et al. 2003). Throughout human history, plants have formed the basis of traditional medicine systems, with the earliest records, dating from around 2600 BC, documenting the uses of approximately 1000 plant-derived substances in Mesopotamia (Cragg and Newmann, 2013). Egyptian medicine dates from about 2900 B.C., but the best known record is the "Ebers Papyrus" dating from 1500 BCE, documenting over 700 drugs, mostly of plant origin (Borchardt et al., 2002). The Chinese *Materia Medica* has been extensively documented over the centuries **(**Huang et al., 1999) with the first record dating from about 1100 B. C. A substantial contribution to the rational development of medicinal herbs in Western countries came from Greeks and Romans**.** Dioscorides, the first century Greek physician, who served as a medical doctor in the Roman army, accurately recorded the collection, storage, and use of medicinal herbs during his travels with Roman armies, whilst Galen (130–200 CE.), a prominent Roman (of Greek ethnicity) physician, surgeon and philosopher, is well known for his complex prescriptions and formulae used in compounding drugs (Cragg and Newman, 2013). During the Middle Age, very little progress was made in the development of the subject. The Arabs preserved much of the Greco-Roman expertise during the Middle Age and expanded it to include the use of their own resources, together with Chinese and Indian herbs unknown to the Greco-Roman world**.** During the 16^{th} and 17^{th} centuries, the era of European exploration overseas, many new crude herbs were brought to Europe. In the 18^{th} century, Linnaeus made an important contribution to the use of herbal remedies, throught the introduction of his new system of naming and classifying plants (Samuelsson, 1999). At the beginning of the 20th century, however, when

scientific method predominated, ‘modern medicine’ relegated herbal medicines to the level of charlatanism. By contrast, today, patients have become enlightened consumers and are again embracing herbal remedies. It is estimated that they are now used by approximately 20% of the general population in the USA (Bent, 2008). Herbal use is often motivated by dissatisfaction with conventional therapies and synthetic drug side effects, or by a desire to be proactive against a disabling disorder.

Most survey agree that digestive tract ailments cure, including IBD and CRC, is one of the most frequent reasons for trying plant medicines. For example, in a Canadian survey, 2,847 IBD patients were asked whether they used a form of complementary/alternative medicine (CAM). Current or past use of CAM for IBD was reported by 47%. Herbal therapies were the most commonly used (41% of CAM users). Improvements in sense of well-being, IBD symptoms, and sense of control over the disease were the most commonly reported benefits (Hilsden et al., 2003). Herbal therapies are claimed to exert benefit in managing IBD by different mechanisms such as immune system regulation, antioxidant activity, inhibition of leukotriene B4, inhibition of nuclear factor-kappa B (NF-kB), and antiplatelet activity (Rahimi et al., 2009).

Plant products are also used by cancer patients, who, being desperate, may feel tempted to use one of the many therapies on offer. A distinction should be made between alleged cures and preventive measures. While none of “natural cures" have been shown to do what they promise (Ernst et al., 2009), the use of herbs and/or dietary treatments for cancer prevention is an important issue (Capasso et al 2003). For example, a recent report from the Shanghai Men's Health Study evaluated the association between green tea consumption and CRC risk in a population-based prospective cohort study. The analysis included 60,567 Chinese

men aged 40-74 years at baseline. During ~5 years of follow-up, it was found that regular green tea consumption (ever drank green tea at least three times per week for more than six consecutive months) was associated with reduced risk of CRC, with the risk decreasing as the amount of green tea consumption increased. Each 2 g increment of intake of dry green tea leaves per day (approximately equivalent to the amount of tea in a tea bag) was associated with a 12% reduction in risk. Overall, the study suggested that regular consumption of green tea may reduces CRC risk (Yang et al., 2011).

In addition to their use as phytotherapeutic agents (i.e. as a mixture of many ingredients, mostly in form of extracts), plants continue to be a source for new drugs or lead compounds for the synthesis of new drugs. In this regard, neoplastic diseases, including CRC, remain one of the greatest health challenges confronting humankind, and the search for better drugs, both in terms of efficacy and safety, is a global health imperative (Cragg and Newman, 2005). An important example of drug used in CRC therapy, which derives from a chemical modification of a plant compound, is irinotecan. This anticancer drug is a semi-synthetically derived from camptothecin, which is isolated from the Chinese ornamental tree, *Camptotheca acuminata* (Fam. Nyssaceae) (Rahier et al., 2005). Camptothecin (as its sodium salt) was advanced to clinical trials by the NCI in the 1970s, but was dropped because of severe bladder toxicity (Cragg and Newmann, 2005). Nevertheless, extensive research led to the development of more effective derivatives such as irinotecan.

1.3 Plant compounds evaluated in the present study

Plant compounds here evaluated for their effect in experimental IBD and colon carcinogenesis are: 1) cannabigerol (CBG), a non-psychotropic plant-derived

cannabinoid isolated from the marijuana plant *Cannabis sativa*; 2) diallyl-sulfide (DAS), diallyl disulfide (DADS), contained in *Allium sativum*; 3) Bromelain, a cysteine protease derived from the stem of the pineapple plant, *Ananas comosus* and boeravinone G, extract from the Ayurvedic plant *Boerhaavia diffusa* . These compounds were selected because a) they are contained in plants traditionally used for the treatment of digestive diseases, including IBD and CRC and 2) possess pharmacological properties which may predict their possible efficacy in intestinal inflammation and cancer. Details of such compounds are reported below:

1.3.1 Cannabigerol *(Cannabis sativa)*

The marijuana plant (Fig. 1A) *Cannabis sativa* has a long medical history (Mechoulam et al., 1999). Extracts of *Cannabis* were indicated for the treatment of diarrhea a century ago in the USA, and there are several anecdotal accounts of the effective use of *Cannabis*-based products against IBD (Mechoulam et al., 1999). Anecdotal reports suggest that IBD patients experience relief by smoking marijuana (Izzo et al., 2009; Alhouayek et al., 2012). Recent retrospective observational studies, by showing that *Cannabis* use is common in patients with IBD for symptom relief, have confirmed such reports (Naftali et al., 2011; Lal et al., 2011). Also, a pilot prospective study found that treatment with inhaled *Cannabis* improved quality of life in patients with long-standing CD and UC (Lahat et al., 2012). In Israel, inhaled *Cannabis* has been legally registered for palliative treatment of both CD and UC.

The limitation of the therapeutic utility of *Cannabi*s and of one of its major components, Δ^9-tetrahydrocannabinol (Δ^9-THC), is the occurrence of psychoactive effects due to the activation of brain cannabinoid CB_1 receptors

(Izzo et al., 2009**)**. Therefore, in recent years there is a growing interest into the potential therapeutic applications of non-psychotropic phytocannabinoids. One of such compounds is cannabigerol (CBG) (Fig. 1B), which was obtained in 1964 by Gaoni and Mechoulam when they separated a hexane extract of hashish on Florisil (Turner et al., 1980). Relatively few studies have sought to investigate the pharmacological actions of this compound (Izzo et al., 2009; Hill et al., 2012). CBG was shown to exert antiproliferative (Ligresti et al., 2006), antibacterial (Appendino et al., 2008) and anti-glaucoma (Colasanti et al., 1990) actions and to antagonise the anti-nausea effect of CBD (Rock et al., 2011). Potential targets of CBG actions, which are relevant for IBD, include transient receptor potential (TRP) channels (De Petrocellis et al., 2011), cyclooxygenase (COX-1 and COX-2) enzymes (Ruhaak et al., 2011), as well as cannabinoid receptors (Cascio et al., 2010). Here, we have investigated the effect of CBG in the murine model of colitis induced by dinitrobenzenesulphonic acid (DNBS).

1.3.2 Diallyl sulfide (DAS) and diallyl disulfide (DADS) (*Allium sativum*)

Garlic (*Allium sativum* L. Fam. Alliaceae), (Fig. 2A) is one of the best-researched/best-selling herbal remedies and is also commonly used as a food and a spice (Borrelli et al., 2007). Garlic has a rich history. It is mentioned in the Bible and was used by Hippocrates, Galen, Pliny the Elder, and Dioscorides. It is originated from Central Asia, but nowadays it is known only in cultivated form. The subterranean garlic bulb consists of 4-20 cloves, each enclosed within a dry, white leaf skin (Capasso et al. 2003). Traditionally, garlic has been used for the treatment of a number of ailments, including those affecting the digestive tract (Block 1985; Chiang et al., 2006). Garlic contains allyl sulfides, including diallyl sulfide (DAS) (Fig. 2B), diallyl disulfide (DADS) (Fig. 2C) and other allyl polysulfides, which are the most abundant compounds in garlic oil, accounting

(A) **(B)**

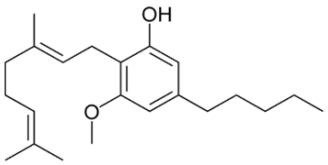

Figure 1. (A) *Cannabis sativa*; **(B)** cannabigerol

(A) **(B)**

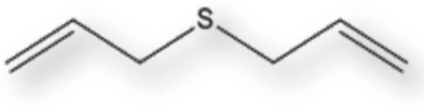

(C)

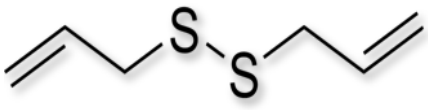

Figure 2. **(A)** *Allium sativum*; **(B)** diallyl sulfide; **(C)** diallyl disulfide

for nearly 94% of the total amount (Calvo-Gomez et al., 2004). The proportion of allyl sulfides in garlic oil consists of approximately 4.7–8% DAS and 21.9–40% DADS which depends on the extraction conditions (Sheen at al., 1991; Lawson et al., 1991). Fresh garlic cloves contain 0.2–0.5% garlic oil in the steam-distilled materials (Wang et al., 2012). DAS and DADS exert a wide number of pharmacological actions. Relevant for this study, DAS and DADS have been reported: 1) to exert antioxidant action, which is relevant in the light of the observation that free radicals play an important role in the pathogenesis of IBD and CRC (Iciek et al., 2012); 2) to act as donor of hydrogen sulfide (Gu et al., 2011), a gaseous mediator which contributes to the maintenance of gastrointestinal mucosal defense and repair (Wallace et al., 2010) and 3) to bind transient receptor potential (TRP) vanilloid type 1 (TRPV1) and transient receptor potential ankyrin type 1 (TRPA1), members of the superfamily of TRP channels which are up-regulated in the inflamed gut (Izzo et al. 2012; Holzer et al., 2011). Here, we have evaluated the effect of both DAS and DADS in the experimental model of IBD induced in the mouse by DNBS.

1.3.3 Bromelain (*Ananas comosus*)

Bromelain is a cysteine protease derived from the stem of the pineapple – named for its resemblance to the pine cone - plant, *Ananas comosus* (Fam. Bromeliaceae). *Ananas comosus* is a tropical plant with edible multiple fruit consisting of coalesced berries (Fig. 3). In the United States, bromelain is sold in health stores as a nutritional supplement to promote digestive health and as a cleansing agent to improve the texture of the skin and to promote the healing of wounds. Bromelain is also commercially available as an anti-inflammatory drug. Preclinical and/or clinical studies have reported anti-inflammatory, immunomodu-

Figure 3. *Ananas comosus*

-latory, antitumoral and wound healing actions from bromelain (Taussig et al., 1988; Orsini et al., 2006). Relevant to the present investigation, bromelain has been shown to ameliorate experimental colitis in IL-10-deficient mice and to decrease secretion of pro-inflammatory cytokines and chemokines in colon biopsies from patients with UC and CD (Hale et al., 2005; Onken et al., 2008). Although the effects of bromelain on intestinal inflammation and secretion have been extensively studied, there is a paucity of reports on the possible effect of bromelain on intestinal motility in an inflammatory process. This is an important lack of information since it is well known that motility changes play an important role in intestinal inflammation and diarrhoea. We have therefore evaluated the effect of bromelain on motility changes associated to the administration of the irritant croton oil in mice.

In recent years, studies have shown that bromelain has the capacity to modulate key pathways that support malignancy. The anti-cancer activity of bromelain consists in the direct impact on cancer cells and their micro-environment, as well as in the modulation of immune, inflammatory and haemostatic systems (Maurer, 2001; Chobotova et al., 2010). Because the actions of bromelain on colon carcinogenesis have been not investigated to date, we have evaluated the effect of this food component in a human colorectal carcinoma cell line and its potential chemopreventive effect in an animal model of colon cancer.

1.3.4 Boeravinone G (*Boerhaavia diffusa*)

Boerhaavia diffusa (Fig. 4A) is a herbaceous member of the Nyctaginaceae family which has a long history of use by indigenous and tribal people of India (Dhar et al., 1968). In particular, roots and leaves of this plant have been widely used in the folk medicine to treat several illnesses including those affecting the gastrointestinal tract. Experimental studies have demonstrated that *Boerhaavia*

diffusa preparations could be effective in the prevention and treatment of diseases, including IBD and colon cancer, in which free radicals are implicated (Kapoor et al., 1990; Pari et al., 2004). The main chemical ingredients of this plant include alkaloids, flavones and rotenoids named boeravinones (A to J) (Leyon et al., 2005). In our preliminary experiments, we found that among various boeravinones, boeravinone G (Fig. 4B) exerted a strong antioxidant effect. We have thus evaluated the effect of this boeravinone on ROS production, DNA damage and SOD activity in colorectal carcinoma cells.

(A) **(B)**

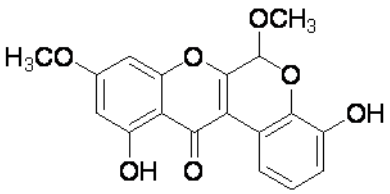

Figure 4. **(A)** *Boerhaavia diffusa* ; **(B)** boeravinone G

2.0 AIM

The aim of the present thesis is to verify the effect of a number of plant-derived compounds in experimental models of IBD and colon cancer. Compounds under study included cannabigerol, a non-psychotropic cannabinoid from Cannabis sativa, DAS and DADS, two organosulfur compounds from *Allium sativum*, bromelain, a cysteine protease from *Ananas comosus* and Boeravinone G, a rotenoid isolated from the Ayurvedic plant *Boerhaavia diffusa*. These compounds were selected because they 1) are contained in plants traditionally used for the treatment of digestive diseases, including IBD and colorectal cancer and 2) possess pharmacological properties which may predict their efficacy in intestinal inflammation and cancer.

3.0 MATERIALS AND METHODS

3.1 Drugs and reagents

CBG [purity by high-performance liquid chromatography (HPLC), 99.0%] was kindly supplied by GW Pharmaceuticals (Porton Down, Wiltshire, UK). Rimonabant (5-(p-chlorophenyl)-1-(2,4-dichlorophenyl)-4-methyl-N-piperidinopyrazole-3-carboxamide hydrochloride) and SR144528 (N-[-1S-endo-1,3,3-trimethyl-bicyclo[2.2.1]heptan-2-yl]-5-(4-chloro-3-methylphenyl)-1-(4-methyl benzyl)-pyrazole-3-carboxamide) were a kind gift from Drs MadaleineMosse` and Francis Barth (SANOFI Recherche, Montpellier, France). Allyl-sulfide (DAS), allyl-disulfide (DADS), bromelain, celecoxib, trypan blue, dinitrobenzenesulphonic acid (DNBS), azoxymethane (AOM), 3-amino-7-dimethylamino-2-methylphenazine hydrochloride [neutral red (NR) solution], dithiothreitol (DTT), fura 2-AM, MTT [3-(4,5-dimethylthiazol-2-yl)-2,5-diphenyltetrazolium bromide], croton oil, myeloperoxidase (MPO) from human leucocytes, hydrogen peroxide (H_2O_2), $FeCl_2 \cdot 4H_2O$, 2′,7′-dichlorfluorescein-diacetate (H_2DCF-DA), lipopolysaccharide (LPS, from Escherichia coli serotype O111:B4), thioglycollate medium, cadmium, 2,3-iaminonaphtalene (DAN), 2,6-di-tert-butyl-4-methylphenol (BHT), fluorescein isothiocyanate (FITC)-conjugated dextran (molecular mass 3-5 kDa), 5,5-dimethyl-1-pyrroline-N-oxide (DMPO), hydrogen peroxide (H_2O_2), $FeCl_2 \cdot 4H_2O$, trichloroacetic acid (TCA), thiobarbituric acid (TBA) and malondialdehyde (MDA) were purchased from Sigma (Milan, Italy). AM251, AM630, capsazepine, and GW9662 were obtained from Tocris Cookson (Bristol, UK).

WST-8 [2-(2-methoxy-4-nitrophenyl)-3-(4-nitrophenyl)-5-(2,4 disulfophenyl)-2H-tetrazolium, monosodium salt] cell proliferation assay kit was purchased from

Cayman Chemical Company (Germany). Monoclonal primary antibodies for $pERK_{1/2}$, ERK_2 and phospho-NF-kB p65 were obtained from Santa Cruz Laboratories (DBA S.r.l, Italy) while peroxidase-conjugated (HRP) anti-mouse IgG antibody was obtained from JacksonImmunoResearch (LiStarFish, Italy). Methyl-[^{3}H]-thymidine was purchased from PerkinElmer (Monza, Italy). Bromelain was proteolytically inactivated in the laboratories of the Department of Pharmacy, University of Naples Federico II (by Dr. Giuseppe De Rosa). N^1-3-methylbutyryl-N^4-6-aminohexanoyl-piperazine (ENMD-1068) was synthesized in the laboratories of the Department of Pharmacy, University of Naples Federico II (by Dr. Ferdinando Fiorino and Dr. Beatrice Severino). All reagents for cell culture and western blot analysis were obtained from Sigma Aldrich S.r.l. (Milan, Italy), Amersham Biosciences Inc. (UK), Bio-Rad Laboratories (USA) and Microtech S.r.l. (Naples, Italy). All chemicals and reagents employed in this study were of analytical grade. CBG was dissolved in ethanol/Tween20/saline (1:1:8; for *in vivo* experiments) or ethanol (for *in vitro* experiments). DAS and DADS were dissolved in corn oil for *in vivo* experiments or DMEM medium for in *vitro* experiments). Bromelain was dissolved in 0.9% NaCl solution for *in vivo* experiments or in DMEM for *in vitro* experiments. Celecoxib was dissolved in ethanol/Tween20/saline (1:1:8). Rimonabant and SR144528 were dissolved in dimethyl sulfoxide (DMSO). DNBS was dissolved in 50% ethanol (200 µl/mouse). ENMD-1068 was dissolved in DMEM for *in vitro* experiments or in 0.9 % NaCl solution for *in vivo* experiments. The vehicles used to dissolve CBG (60 µl/mouse *in vivo* or 0.01% ethanol *in vitro*), DAS and DADS (200µl/mouse), bromelain (60 µl/mouse) and celecoxib (60 µl/mouse) had no significant effects on the responses under study.

3.2 Animals

Male ICR mice weighting 20-22 g (for experiments on tumors and ileitis) or 30–35 g (for experiments on colitis) were purchased from Harlan Italy (San Pietro al Natisone, MI). Mice were housed in polycarbonate cages under a 12-h light/12-h dark cycle, temperature 23 ± 2° C and humidity 60%. Animals, used after 1 week of acclimation, had free access to water and food except for the 24-h period immediately preceding the administration of DNBS. All experiments complied with the Italian D.L. no. 116 of 27 January 1992 and associated guidelines in the European communities Council Directive of 24 November 1986 (86/609/ECC).

3.3 Cell culture

A human colon adenocarcinoma cell line (Caco-2), a conditionally immortalized colonic epithelial cell line (Ptk6, from a *Ptk*6 null mouse), a conditionally immortalized mouse duodenal epithelial cell line [Mode-K, by simian virus (SV)-40 large T gene transfer] and murine peritoneal macrophages were used. Mode-K and Ptk6 cells exhibit morphological and phenotypic characteristics of normal enterocytes. Caco-2 cells, purchased from the American Type Culture Collection (LGC Promochen, Italy), were cultured in Dulbecco's Modified Eagle Medium (DMEM) containing 10% Fetal Bovine Serum (FBS), 100 U/ml penicillin, 100 μg/mL streptomycin, 1 M Hepes [4-(2-Hydroxyethyl)-1-piperazineethanesulfonic acid] 2.5 %, non-essential amino acid (NEAA) 1X and 2mM L-glutamine. Caco-2 cells were used between passages 20 to 50. P*tk6* null colonic epithelial cells (used between passages 44 and 50), supplied by Dr R.H. Whitehead at the Ludwig Institute for Cancer Research (Melbourne Branch), were cultured in RPMI-1640 medium (GIBCO) containing 10% FBS, 80 U/ml penicillin and 80 μg/ml streptomycin and. Mode-K cells (used between passages 14 and 22), a gift from Dirk Haller (Chair for the Biofunctionality of Food, Departments of Food,

Nutrition and Medicine, Technical University Munich), were grown in DMEM supplemented with 2 mM L-glutamine, 10% FBS, 80 U/ml penicillin and 80 μg/ml streptomycin. Peritoneal macrophages were obtained from mice as previously described by Romano and colleagues (Romano et al., 2013). Briefly, to evoke the production of peritoneal exudates rich in macrophages, mice were injected intraperitoneally (ip) with 1 ml of 10% sterile thioglycollate medium. After 4 days, mice were killed and peritoneal macrophages were collected and seeded in appropriate plates for performing *in vitro* experiments. Peritoneal macrophages were cultured in DMEM supplemented with 10% foetal bovine serum. Caco-2, Ptk6 and Mode-K cells were routinely maintained in 75 cm^2 polystyrene flasks in an incubater at 37 °C, 95% humidity and 5% CO_2 atmosphere. The cells were trypsinized twice a week and the culture medium was replaced every 2 days. In all cell lines viability was evaluated by trypan blue staining.

The inflammatory response in peritoneal macrophages was induced by LPS from Escherichia coli serotype O111:B4 (1 μg/ml). The acute inflammatory response in macrophages required an LPS incubation time of 18 h. The oxidative stress in Ptk6 null colonic epithelial cells was induced by Fenton's reagent (H_2O_2/Fe^{2+} 2 mM, time of incubation 3 h). For reactive oxygen species (ROS), lactate dehydrogenase leakage and TBARS assay, Caco-2 were led to differentiation, (cells were used at post-confluence stage as a model of human enterocytes) while for cell vitality (neutral red assay) Caco-2 cells were used under both proliferative and differentiated state; preliminary experiments showed that a 5-7-day time of incubation was required for Caco-2 cells to undergo differentiation.

3.4 Induction of experimental colitis and pharmacological treatment

Colitis was induced in anesthetized mice by intrarectal administration (4.5-cm depth) of 150 mg/kg of DNBS (200 µl/mouse) via a lubricated polyethylene catheter (1 mm in diameter) (Hunter et al., 2005). Mice were sacrificed at 72 h post-DNBS, the abdomen was opened by a midline incision and the colon removed, isolated from surrounding tissues, opened along the antimesenteric border, rinsed, weighed and length measured (in order to determined the colon weight/colon length *ratio* used as an indirect marker of inflammation). For biochemistry analysis, tissues were kept at −80°C until use, while for histological examination tissues were fixed in 10% formaldehyde.

The dose of DNBS was selected on the basis of preliminary experiments showing a remarkable colonic damage associated to high reproducibility and low mortality for the 150 mg/kg dose. The time point of damage evaluation (i.e., 3 days after DNBS administration) was chosen because maximal DNBS-induced inflammation has been reported in mice after 3 days (Massa et al., 2004). Furthermore, previous studies have shown that 3 days after intrarectal DNBS administration in mice, the inflammatory response may be modulated by administration of cannabinoid drugs such as direct cannabinoid receptor agonists or antagonists (Borrelli et al., 2009; Massa et al., 2004).

In the preventive protocol CBG (1-30 mg/kg) was given intraperitoneally (ip) once a day for six consecutive days starting 3 days before DNBS administration, while in the curative protocol CBG (1-30 mg/kg, ip) or DAS and DADS (1-10 mg/kg, orally) was given for two consecutive days starting 24-h after DNBS administration.

3.5 Intestinal permeability

Intestinal permeability was examined using a fluorescein isothiocyanate (FITC)-labeled-dextran method, as described previously (Osanai et al., 2007). Briefly, 2 days after DNBS administration, mice were gavaged with 600 mg/kg body weight of fluorescein isothiocyanate (FITC)-conjugated dextran (molecular mass 3-5 kDa). One day later, blood was collected by cardiac puncture, and the serum was immediately analyzed for FITC-derived fluorescence using a fluorescent microplate reader with an excitation–emission wavelengths of 485–520 nm (LS55Luminescence Spectrometer, PerkinElmer Instruments). Preliminary experiments showed that FITC-dextran was stable after 24 h from its preparation. Serial-diluted FITC-dextran was used to generate a standard curve. Intestinal permeability was expressed as FITC nM found in the serum.

3.6 Upper gastrointestinal transit in the inflamed gut

Inflammation was induced as previously described (Borrelli et al., 2006; Pol et al., 1997). Briefly, two doses of croton oil (20 μl/mouse) in two consecutive days were orally administered to mice and four days after the first administration of croton oil, upper gastrointestinal transit of mice was measured. This time was selected on the basis of a previous work, (Pol et al., 1997) which reported that maximal inflammatory response occurred four days after the first treatment.

Upper gastrointestinal transit was measured in control and croton oil-treated mice by evaluating the intestinal location of rhodamine-B-labelled dextran. Animals were given fluorescent-labelled dextran (100 μl of 25 mg/ml stock solution) via a gastric tube into the stomach. Twenty minutes after administration, the animals were killed by asphyxiation with CO_2 and the entire small intestine with its content was divided into 10 equal parts as previously reported in detail (Capasso et al., 2008). Duplicate aliquots of the cleared supernatant was read in a multi-well

fluorescence plate reader (LS55 Luminescence spectrometer; Perkin Elmer Instruments, Waltham, MA, USA; excitation 530 ± 5 nm and emission 590 ± 10 nm) for quantification of the fluorescent signal in each intestinal segment. From the distribution of the fluorescent marker along the intestine, we calculated the geometric centre (GC) of small intestinal transit as follows:

GC = P(fraction of fluorescence per segment x segment number), where GC ranged from 1 (minimal motility) to 10 (maximal motility).

Bromelain (1-10 mg/kg) or vehicle (0.9% NaCl solution) was given intraperitoneally, 30 minutes before the administration of the fluorescent marker to animals. In some experiments, EDNM-1068 (4 mg/kg, dissolved in 0.9% NaCl) was given intraperitoneally 30 minutes before the administration of bromelain. The dose of EDNM-1068 was selected on the basis of previous works (Kelso et al., 2006). In another set of experiments, bromelain (100–500 mg/kg) was given orally 1 hour before the administration of the fluorescent marker.

3.7 Experimental colon carcinogenesis and pharmacological treatment

Mice were randomly divided into the following 4 groups (10 animals/group): Group 1 (control) was treated with vehicles; group 2 was treated with azoxymethane (AOM) plus the vehicle used to dissolve bromelain; group 3 was treated with AOM plus bromelain (1 mg/kg) and group 4 was treated with AOM plus celecoxib (10 mg/kg). AOM (40 mg/kg in total, ip) was administered, at the single dose of 10 mg/kg, at the beginning of the first, second, third and fourth week. Bromelain and celecoxib were given (ip) every day for the whole duration of the experiment starting one week before the first administration of AOM. The doses of bromelain and celecoxib were selected on the basis of previous published work dealing with the effects of these drugs in subchronic or chronic experiments (Beuth et al., 2005; Rahman et al. 2012). All animals were euthanized by

asphyxiation with CO_2 3 months after the first injection of AOM. Based on our laboratory experience, this time (at the dose of AOM used) was associated with the occurrence of a significant number of ACF, polyps and tumours (Aviello et al., 2012). For aberrant crypt *foci* (ACF), polyps and tumours determination, the colons were rapidly removed after sacrifice, washed with saline, opened longitudinally, laid flat on a polystyrene board and fixed with 10% buffered formaldehyde solution before staining with 0.2% methylene blue in saline. Colons were examined as previously reported (Aviello et al., 2012) using a light microscope at 20X magnification (Leica Microsystems, Milan Italy).

3.8 Histology and immunohistochemistry

Histological and immunochemistry evaluations, performed 3 days after DNBS administration, was assessed on a segment of 1 cm of colon located 4 cm above the anal canal. After fixation for 24 h in saline 10% formaldehyde, samples were dehydrated in graded ethanol and embedded in paraffin. Thereafter, 5-μm sections were deparaffinized with xylene, stained with hematoxylin–eosin, and observed in a DM 4000 B Leica microscope (Leica Microsystems, Milan, Italy). In the CBG experiments, microscopic scoring were performed using a modified version of the scoring system reported by D'Argenio and colleagues (D'argenio et al., 2006). Briefly, colon was scored considering (1) the submucosal infiltration (0, none; 1, mild; 2–3, moderate; 4–5 severe), (2) the crypt abscesses (0, none, 1–2 rare; 3–5, diffuse) and (3) the mucosal erosion (0, absent; 1, focus; 2-3, extended until the middle of the visible surface; 4-5, extended until the entire visible surface). For immunohistochemical detection of Ki-67 (after CBG treatment), paraffin-embedded slides were immersed in a Tris/ethylenediaminetetraacetic acid buffer (pH 9.0), were heated in a decloaking chamber at 125°C for 3 min and were cooled at room temperature for 20 min. After adding 3% hydrogen peroxide,

sections were incubated for 10 min. After washing the sections with Tris-buffered saline Tween-20 (pH 7.6), they were stained with rabbit monoclonal antibody to Ki-67 (Ventana Medical systems, Tucson, Arizona). Briefly, each tissue section was incubated with primary antibody to Ki-67 (1:100) for 30 min at room temperature. The slides were washed three times with Tris-buffered saline Tween-20 and were incubated with secondary antibody for 30 min. After, the slides were reacted with streptavidin for 20 min and the reaction was visualized by 3,3'-diaminobenzidine tetrahydrochloride for 5 min. Finaly, the slides were counterstained with Mayer's hematoxylin. The intensity and localization of immunoreactivities against the primary antibody used were examined on all sections with a microscope (Leica Microsystems, Milan, Italy). In DAS and DADS experiments, microscopic analysis were scored considering (i) the leucocyte infiltration (0-3=mucosal, 0-2=submucosal, 0-1=muscolaris), (ii) ulcerations (0-2) and (iii) crypt loss in intestinal architecture (0-4). For immunostaining assays, colons were cut into 5-µm sections and exposed to antibodies for interferon-γ-induced protein 10 (IP-10) chemochine detection. On colonic sections (5-µm sections deparaffinized) of animals treated with DAS and DADS (10 mg/kg) the expression of IP 10 was evaluated. Following deparaffinization, the slides containing colonic sections were washed in 1X PBS for three times. Subsequently blocking was performed with a specific blocking buffer (serum of the animal corresponding to secondary antibody) for 60 minutes at room temperature. Then the slides were incubated with primary antibody anti-IP 10 (dilution 1:20) overnight at 4°C. After 24 hours three more washes in 1X PBS were carried out and slides were incubated for 1-2hours with secondary antibodies conjugated to fluorochromes (DAPI 1:200= blueandALEXA1:1000=

green). Finally, after cover-glasses application on slides, IP-10 expression was examined using a fluorescence-microscope (Leica Microsystems, Germany).

3.9 Myeloperoxidase (MPO) activity

Myeloperoxidase (MPO) activity was determined as previously described (Goldblum et al., 1985). Full-thickness colons were homogenized in an appropriate lysis buffer [0.5% hexadeciltrimethylammonium bromide (HTAB) in MOPS 10 Mm] in ratio 50 mg tissue /1 ml MOPS. The samples were then centrifuged for 20 minutes at 15,000 x g at 4 °C. An aliquot of the supernatant was then incubated with sodium phosphate buffer (NaPP, pH 5.5) e tetra-methyl-benzidine 16 mM. After 5 minutes, H_2O_2 (9.8 M) in NaPP was added and the reaction stopped adding acetic acid. The rate of exchange in absorbance was measured by a spectrophotometer at 650 nm. Different dilutions of human MPO enzyme of known concentration were used to obtain a standard curve. MPO activity was expressed as units (U)/ml.

3.10 Superoxide dismutase (SOD)

A modified version of the Kuthan and colleagues method was used to detect superoxide dismutase (SOD) activity (Kuthan et al., 1986). For *ex vivo* experiments full-thickness colons from control and DNBS-treated mice (treated or not with CBG 30 mg/kg) were homogenized in PBS 1X. Homogenates were centrifuged at 25.000×g for 15 min at 4°C. Extraction of Cu-Zn SOD was obtained treating the cytosolic lysates with ethanol (1:1) and chloroform (1:0.6) at 25°C for 15 min. After centrifugation (15.000 x g, 15 min, 4°C), 125 µl of the surnatant was incubated (for 20 min) with 613 µl of a reaction mixture containing 0.12 mM xanthine, 48 mM Na_2CO_3, 0.094 mM ethylendiaminetetracetic acid (EDTA), 60 mg/l BSA, 0.03 mM nitro blue tetrazolium (NBT) and 0.006 U/ml xanthine oxidase. Finally, $CuCl_2$ (0.8 mM) was added to stop the reaction.

Absorbance readings at 560 nm were recorded using a Beckman DU62 spectrophotometer. Superoxide radical scavenging capacity of CBG (30 mg/kg) at the end of 30 min were expressed as ng SOD/mg tissues contained in the lysates. For *in vitro* experiments, Caco-2 cytosolic extracts were prepared as previously described (Aviello et al., 2010). Briefly, after boeravinone G (0.1-1 ng/ml) incubation for 24 hours followed by a treatment with H_2O_2/Fe^{2+} 1 mM for 3 hours, the medium was removed and cells were washed with ice cold PBS. The cells were collected by scraping for 10 min at 4°C with lysis buffer [50mM Tris-HCl pH=7.4, 0.25 % sodium deoxycholate, 150mM NaCl, 1mM EGTA, 1mM NaF, 1 % NP-40, 1mM PMSF, 1mM Na_3VO_4 containing complete protease inhibitor cocktail (Roche Diagnostics, Mannheim, Germany)]. After centrifugation at 16,200 x g for 15 min at 4°C, the supernatants were collected and protein concentration was determined by Bradford method (Bradford et al., 1976). Cytosolic lysates were used for the evaluation of SOD activity. Cytosolic lysates were incubated at 25 °C for 20 min with a reaction mixture containing 1.2 mM xanthine, 0.03 mM nitro blue tetrazolium (NBT), 0.26 U/mL xanthine oxidase. Similarly to the *ex vivo* SOD detection protocol, absorbance readings at 560 nm were recorded using a Beckman DU62 spectrophotometer. Superoxide radical-scavenging capacity of boeravinone G (0.1-1 ng/ml) at the end of 30 min was expressed as ng SOD/mg proteins contained in the cell lysates.

3.11 Immunoblotting

For *ex vivo* experiments, full-thickness colons were homogenized in lysis buffer (1:2, w/v) containing 0.5 M β-glycerophosphate, 20 mM $MgCl_2$, 10 mM ethylene glycol tetraacetic acid, and supplemented with 100 mM DTT and protease/phosphatase inhibitors (100 mM dimethylsulfonyl fluoride, 2 mg/ml apronitin, 2 mM leupeptin, and 10 mM Na_3VO_4). Homogenates were centrifuged

at 600 × g for 5 min at 4°C; the supernatants were collected and centrifuged at 16,200 × g for 10 min at 4°C. For *in vitro* experiments, Caco-2 cytosolic lysates treated with bromelain and boeravinone G were obtained as previously described (Aviello et al., 2010). Briefly, after bromelain (0.1-10 μg/ml) or after boeravinone G (0.1-1 ng/ml) incubation for 24 hours, the medium was removed and cells were washed with ice cold PBS. The cells were collected by scraping for 10 min at 4°C with lysis buffer [50mM Tris-HCl pH=7.4, 0.25 % sodium deoxycholate, 150mM NaCl, 1mM EGTA, 1mM NaF, 1 % NP-40, 1mM PMSF, 1mM Na_3VO_4 containing complete protease inhibitor cocktail (Roche Diagnostics, Mannheim, Germany)]. After centrifugation at 16,200 x g for 15 min at 4°C, the supernatants were collected. Protein concentration was determined by Bio-Rad Protein Assay (Bio-Rad, Milan, Italy), using the Bradford method. Lysate aliquots containing 50 μg of proteins both from colons and Caco-2 cells (treated with bromelain and boeravinone G) were subjected to electrophoresis on a sodium dodecyl sulphate (SDS) 10% polyacrylamide gel and electrophoretically transferred onto a nitrocellulose transfer membrane (Protran, Schleicher&Schuell, Germany). Proteins were visualized on the filters by reversible staining with Ponceau-S solution (Sigma) and de-stained in PBS containing 0.1% Tween 20. All antibodies were used at 1:1000 dilution in milk buffer (5% non-fat dry milk in PBS/Tween 0.1 %). The immunoblots of homogenates from colons were incubated with mouse polyclonal antibodies for cyclooxigenase type 2 (COX-2) (BD Bioscience, Belgium) and inducible nitric oxide synthase (iNOS) (Cayman Chemical, USA), while the immunoblots of homogenates from ileum were incubated with a mouse polyclonal antibody for protease-activated receptors type 2 (PAR-2, epitope specificity within amino acids 37-50) (Santa Cruz Biotechnology, Inc.). The lysates from Caco-2 were incubated at 4 °C with mouse monoclonal antibodies for

$pERK_{1/2}$, ERK_2 (Santa Cruz, DBA S.r.l, Italy), phosho-Akt and rabbit polyclonal antibody for Akt and phospho-NF-kB p65 (Cell Signaling from Euroclone, Milan, Italy). Subsequently, the membranes were incubated for 1 hour at room temperature with 1:2000-diluition of anti-mouse or anti-rabbit IgG-Horseradish peroxidase-conjugated secondary antibody (Amersham Biosciences, UK). After washing in PBS/Tween 0.1%, the membranes were analyzed by enhanced chemiluminescence's (ECL; Amersham Biosciences (UK). The signal was visualized using ImageQuant 400 equipped with software ImageQuant Capture (GE Healthcare, Milan, Italy) and analysed using Quantity One Software version 4.6.3. The membranes were probed with an anti β-actin antibody to normalize the results, which were expressed as a *ratio* of densitometric analysis of COX-2/β-actin, iNOS/β-actin and PAR-2/β-actin bands. The effect of bromelain and boeravinone on the MAP kinase and phosphoinositide 3-kinase activation was expressed as *ratio* of densitometric analysis of $pERK_{1/2}$/total ERK bands and pAkt/Akt and phospho-NF-kB p65/β-actin bands, respectively.

3.12 Enzyme-linked immunosorbent assay

Interleukin-1β (IL-1β), interleukin-10 (IL-10) and interferon-gamma (IFN-γ) levels in homogenates obtained from full-thickness colonic tissues and IL-6, IP-10 and IFN-γ levels in supernatants obtained from Mode-K cells were quantified using commercial ELISA kits (Tema Ricerca, S.r.L. Italy; R&D Systems Germany, respectively) according to the manufacturer's instructions.

3.13 Cytotoxicity assay

Cytotoxicity assays were performed using the NR, MTT and WST-8 assays. For NR assay (Aviello et al., 2011), cells were seeded in a 96-well plate [murine macrophages at the density of 1×10^5 cells/ well, Caco-2 at a density of $1x10^4$ cells/well (under both proliferative and differentiated state), P*tk6* null colonic

epithelial cells at a density of $3x10^4$ cells/well] and treated with the compounds considered. After 24-h the cells were washed and 200 µl NR dye solution (50 µg/ml in DMEM) were added to each well for 3 h at 37°C. After washing in PBS, 100 µl of 1% acetic acid were added and the absorbency was measured at a wavelength (λ) of 540 nm using a multiwell reader (Perkin-Elmer Instruments). Treatments were compared with 20 % DMSO and the results are expressed as percentage of cell viability. In the MTT assay, as described by Mosmann and colleagues (1983), cell respiration was assessed by the mitochondrial dependent reduction of MTT to formazan. Caco-2 cells ($1x10^4$ cells/well in a 96-well plate in a proliferating state) after treatement with the compounds considered, were incubated with the MTT solution (0.25 mg/ml) for 1 h at 37 °C.The supernatant was removed after treatment and the formed formazan crystals were dissolved in DMSO (100 µl/well) at room temperature for 10 min. The absorbance was read at the wavelength of 490 nm in a multiwell plate reader (Bio-Rad, Model 550). The mean absorbance, taken from cells grown in the absence of the extracts (vehicle alone), was taken as 100% cell survival (control). The number of viable cells was also measured using a WST-8 assay (NacalaiTesque, Kyoto, Japan). After 24 hours treatment of Mode-K cells (seeded at the density of $1x10^5$ cells/well in a 24 –well plate) with DAS and DADS, 100 microliters of WST-8 solution was added into each well and the cells were incubated for 2 h. The absorbance was measured at a test wavelength of 600 nm using a microplate reader (Benchmark, Bio-Rad Laboratories, CA). Cell cytotoxicity was evaluated as the ratio of the absorbance of the sample to that of the control. CBG was used at the concentration between 0.001 and 10 µM. DAS and DADS were used at the concentration between 10 and 100 µg/ml, while interferon-γ at the 50 ng/ml concentration. Bromelain was used

at the concentration between 1 and 10 μg/ml. Boeravinone G was used at the concentration between 0.1 and 1 ng/ml.

3.14 Lactate dehydrogenase (LDH) leakage assay

The injury to Caco-2 cells was quantitatively assessed through the measurement of lactate dehydrogenase (LDH) levels. Caco-2 cells were seeded in 6-well plates at the density of 3.0 $x10^6$ and led to differentiation. Differentiated cells were treated with vehicle (DMSO 0.1 % v/v) or boeravinone G (0.1-1 ng/ml) for 24 h. An aliquot of the medium was removed from the culture plates and then analyzed for LDH leakage into the culture media by using a commercial kit (Sigma Diagnostics). The total LDH activity was determined after cells were scraped and thoroughly disrupted by Ultra Turax for 30 seconds. The percentage of LDH leakage was calculated to determine membrane integrity. The LDH leakage was expressed as a percentage of the total activity: (activity in the medium)/(activity in the medium + activity of the cells) x 100.

3.15 Nitrites measurement

Nitrites, stable metabolites of nitric monoxide (NO), were measured in macrophages and Mode-K medium as previously described (Aviello et al., 2011). Mouse peritoneal macrophages (5×10^5 cells per well seeded in a 24-well plate) were incubated with CBG (0.001–1 μM) for 30 min and subsequently with LPS (1 μg/ml) for 18 h. Mode-K cells (1×10^5 cells per well seeded in a 24-well plate) were incubated with DAS and DADS (50 μg/ml) in the presence of IFN-γ (50 ng/ml) for 24h. After reduction of nitrates to nitrites by cadmium, cell supernatants were incubated with DAN (50 μg/ml) for 7 min. After stopping the reaction with 2.8 N NaOH, nitrite levels were measured using a fluorescent microplate reader (LS55Luminescence Spectrometer, PerkinElmer Instruments, excitation–emission wavelengths of 365–450 nm). In a subsequent set of

experiments, rimonabant 1 μM, CB_1 receptor antagonist) and SR144528 (1 μM, CB_2 receptor antagonist) were incubated 30 min before CBG (1 μM).

3.16 Quantitative (real-time) RT-PCR analysis

Peritoneal macrophages (treated or not with CBG 30 min before LPS) were collected in RNA later (Invitrogen, Carlsbad, CA, USA) and homogenized in 1.0 ml of Trizol® (Invitrogen). Total RNA was extracted according to the manufacturer's recommendations and further purified and DNA digested by the Micro RNA purification system (Invitrogen). Total RNA eluted from spin cartridge wasUV-quantified by a Bio-Photometer® (Eppendorf, Santa Clara, CA, USA), and purity of RNA samples was evaluated by the RNA-6000-Nano® microchip assay using a 2100 Bioanalyzer® equipped with a 2100 Expert Software® (Agilent, Santa Clara, CA, USA) following the manufacturer's instructions.

For all samples tested, the RNA integrity number was greater than 8 relative to a 0–10 scale. One microgram of total RNA, as evaluated by the 2100 Bioanalyzer, was reverse transcribed in cDNA by the SuperScript III SuperMix (Invitrogen).

The reaction mixture was incubated in a termocycler iCycler-iQ5® (Bio-Rad, Hercules, CA, USA) for a 5 min at 60°C step, followed by a rapid chilling for 2 min at 4°C. The protocol was stopped at this step and the reverse transcriptase was added to the samples, except the negative controls (–RT). The incubation was resumed with two thermal steps: 10 min at 25°C followed by 40 min at 50°C. Finally, the reaction was terminated by heating at 95°C for 10 min. Quantitative realtime PCR was performed by an iCycler-iQ5® in a 20mL reaction mixture containing 1 X SYBR green supermix (Bio-Rad), 10 ng of cDNA (calculated on the basis of the retro-transcribed RNA) and 330 nM for each primer. Primer sequences and optimum annealing temperature (TaOpt) were designed by the

AlleleID software (PremierBiosoft). The amplification profile consisted of an initial denaturation of 2 min at 94°C and 40 cycles of 30 s at 94°C, annealing for 30 s at TaOpt and elongation for 45 s at 68°C. Fluorescence data were collected during the elongation step. A final melt-curve data analysis was also included in the thermal protocol. Assays were performed in quadruplicate (maximum Ct of replicate samples <0.5), and a standard curve from consecutive fivefold dilutions (100 to 0.16 ng) of a cDNA pool representative of all samples was included for PCR efficiency determination. Relative normalized expression was evaluated as previously described (De Petrocellis et al., 2012).

Real Time-PCR method was also used to quantifyt IP-10 mRNA on Mode-K cells treated with DAS and DADS at concentration of 50 μg/ml. RNA from Mode-K cells was extracted using Trizol Reagent (Invitrogen, Karlsruhe, Germany) according to the manufacturer's instructions. Extracted RNA was solved in 20 µl water containing 0.1% diethyl-pyrocarbonate. RNA concentration and purity (A_{260}/A_{280} *ratio*) was determined by spectrophotometric analysis (ND-1000 spectrophotometer, NanoDrop Technologies, Willigton, USA). Reverse transcription was performed using 1 µg total RNA. Real-time PCR was performed using 1 µl cDNA in a Light CyclerTM system (Roche Diagnostics, Mannheim, Germany) as previously described (Ruiz et al., 2005). The amplified product was detected by the presence of a ALEXA green fluorescent signal. Melting curve analysis was used to document amplicon specificity and crossing points (Cp) were determined. Relative induction of gene mRNA expression was calculated according to the $2^{-\Delta\Delta C}$ (Pfaffl et al., 2001) method and normalized to the expression of GAPDH (glyceraldehyde 3-phosphate dehydrogenase). Data were expressed as fold change against untreated cells.

3.17 Measurement of $[Ca^{2+}]_i$ in Caco-2 cells

Intracellular calcium measurement was performed using a modified method adapted from the procedure described by Jacob and colleagues (Jacob et al., 2005). Briefly, after washing in PBS (Phosphate Buffered Saline), Caco-2 cells were trypsinized with 0.25 % trypsin-EDTA at 37°C for 5 min, centrifuged at 1000 x g for 3 min, and then re-suspended at the concentration of 55000 cell/ml in HEPES buffer solution (HBS) (composition in mM: NaCl 125, KCl 4, $CaCl_2$ 2, L-Glutamine 4, Glucose 10, Hepes 30) containing Fura-2AM (10 μM) and ENMD 1068 (5 mM). After 30 min, some cells were treated with bromelain (1 μg/ml) for 20 min. After these treatments, cells were centrifuged at 1000 x g for 2 min, and then re-suspended in calcium-free HBS. Intracellular calcium levels were measured using a fluorescent microplate reader (LS55 Luminescence Spectrometer, Perkin-Elmer Instruments, excitation-emission wavelengths of 343/485 nm). The results are expressed as 343/485 nm ratio.The treatments were carried out in triplicate and four independent experiments were performed.

3.18 ^{3}H-thymidine incorporation assay

Cell proliferation was evaluated in colorectal carcinoma cell line Caco-2 using the ^{3}H-thymidine incorporation as previously described (Aviello et al., 2010). Briefly, Caco-2 cells were seeded in 24-well plates at a density of $1.0x10^{4}$ in DMEM supplemented with 10 % FBS and grown for 24 h. The resulting monolayers were washed three times with 200 μl of phosphate buffered saline (PBS) and then 200 μl of serum-free DMEM was added to each well. After 24 h of serum starvation, the cells were washed three times with PBS and incubated with DMEM supplemented with 10 % FBS containing bromelain or inactivated bromelain (1-10 μg/ml) in presence of ^{3}H-thymidine (1 μCi/well) for 24 h. Cells were scraped in 1 M NaOH and collected in plastic miniature vials (PerkinElmer) filled up with liquid for scintillation counting (UltimaGold® PerkinElmer). Treatments were

compared with 300 μM spermine. Cell proliferation was expressed as count *per* minute on μg of protein (CPM/μg protein) of incorporating ^{3}H-thymidine cells. The treatments were carried out in triplicate and three independent experiments were performed. The protein content was quantified using the Bradford method.

3.19 Intracellular reactive oxygen species (ROS) measurement

The generation of intracellular reactive oxygen species (ROS) was estimated using the fluorescence probe 2′,7′-dichlorfluorescein-diacetate (H2DCF-DA) (Borrelli et al., 2009). For the experiments, cells were plated in 96-multiwell black plates (Corning, USA) at the density of 3×10^{4} cells/well and 1×10^{4} cells/well for P*tk*6 and Caco-2 cells, respectively. P*tk6* null colonic epithelial cells were incubated for 24 h at 37°C with CBG (0.1-10 μM) while confluent Caco-2 cell monolayers were incubated for 24 h at 37 °C with bromelain (1-10 μg/ml) or boerhavinone G (0.1-1 ng/ml). After washing, cells were incubated for 1 h with 200 μl of 100 μM H_2DCF-DA in HBSS containing 1% FBS. Finally, cells were rinsed and incubated with the Fenton's reagent (H_2O_2/Fe^{2+} 2 mM) for 3 h at 37°C. The DCF fluorescence intensity was detected using a fluorescent microplate reader (excitation 485 nm and emission 538 nm; Perkin-Elmer Instruments). The intracellular ROS levels were expressed as fluorescence intensity (picogreen).

3.20 Thiobarbituric acid reactive substances (TBARS) assay

Lipid peroxidation products [thiobarbituric acid reactive substances (TBARS) also known as malondialdehyde-equivalents (MDA-equivalents)] from Caco-2 cells were measured by the thiobarbituric acid colorimetric assay (Canadanovic et al., 2005). Briefly, Caco-2 cells were seeded in 6-well plates at the density of 3.0×10^{6} and led to differentiation. Differentiated cells were treated with boeravinone G (0.1-1 ng/ml corresponding to 0.28-2.8 nM) for 24 h and then washed with PBS and incubated with the Fenton's reagent (H_2O_2/Fe^{2+} 1 mM) for 3 h at 37 °C. The 1

mM concentration was selected on the basis of our preliminary experiments, which showed submaximal effects of H_2O_2/Fe^{2+} in this assay (pmol MDA/mg protein: control 182.1±17.90, H_2O_2/Fe^{2+} 0.25 mM 182.6±20.68, H_2O_2/Fe^{2+} 0.5 mM 298.5±17.62, H_2O_2/Fe^{2+} 1 mM 628.5±34.58, H_2O_2/Fe^{2+} 2 mM 985.5±62.5, H_2O_2/Fe^{2+} 4 mM 1039±62.3; n=8. EC_{50}: 0.96±0.07 mM, E_{max}: 1052±50.37 %).After incubation, the cells were washed and scraped in ice cold PBS. The cells were lysed by six cycles of freezing and thawing in PBS and then centrifuged at 16200 x g for 10 min at 4°C. Trichloroacetic acid (TCA, 10% w/v) was added to the cellular lysate and, after centrifugation at 16200 x g for 10 min, 0.67% (w/v) thiobarbituric acid (TBA) was added to the supernatant and the mixture was heated at 80 °C for 30 min. After cooling, MDA-equivalents formation was recorded at the wavelength of 532 nm, using a Beckman DU62 spectrophotometer. A standard curve of MDA was used to quantify the levels of MDA-equivalents formed during the experiments, and the results are presented as μmol of MDA-equivalents/mg of cellular protein previously determined by the Bradford method (Bradford et al., 1976).

3.21 DNA damage assay (Comet assay)

The presence of DNA fragmentation was examined by single cell gel electrophoresis (Comet assay), as previously described (Aviello et al., 2010). Briefly, Caco-2 cells were seeded in the 25 cm^2 flasks at a density of $4x10^5$ cells and incubated with boeravinone G (0.1-1 ng /ml) at 37°C for 24 h. After incubation the cells were treated with H_2O_2 (75μM) for 5 min on ice and then centrifuged at 1000 x g for 5 min. This concentration of H_2O_2 produced a submaximal damage of DNA (data not shown). The supernatant was discarded and the pellet was mixed with 85 μl of 0.85% low melting point agarose (LMA) in PBS. Cells were added to previously prepared gels of 1% normal agarose (NMA).

The gels on frosted slides were maintained in lysis solution (2.5 M NaCl, 100 mM Na_2EDTA, 10 mM Tris and 1% Triton X-100, pH 10) at 4 °C for 1 h, and then electrophoresed in an appropriate buffer (300 mM NaOH, 1 mM Na_2EDTA, pH>12) at 26 V, 300 mA for 20 min. After running, the gels were neutralized in 0.4 M Tris–HCl, pH 7.5 (3 × 5 min washes) and stained with 20 μl of ethidium bromide (2 μg/ml) before scoring. Images were analyzed using a fluorescence microscope (Nikon) interfaced with a computer. DNA damage was analyzed and quantified by measuring the percent of fluorescence intensity in the tail (tail intensity) through the Komet 5.0 image analysis software (Kinetic Imaging). Each treatment was carried out in duplicate, and 100 random selected comets from two microscope slides were analyzed.

3.22 Statistical analysis

Data were expressed as the mean±standard error (SE mean) of n experiments. To determine statistical significance, Student's t test was used for comparing a single treatment mean with a control mean, and an one-way analysis of variance followed by a Tukey–Kramer multiple comparisons test was used for analysis of multiple treatment means. Values of $p<0.05$ were considered significant.

4.0 RESULTS

4.1 Cannabigerol (CBG) and intestinal inflammation: *in vivo* and *ex vivo* studies

4.1.1 Dinitrobenzene sulfonic acid (DNBS) model of colitis

4.1.1.1 Colon weight/colon length *ratio*

DNBS administration caused a significant increase in colon weight/colon length *ratio*, a simple and reliable marker of intestinal inflammation/damage (Gálvez et al., 2000), (Fig. 5A and 5B). CBG (1-30 mg/kg, *ip*) given before (preventive protocol, Fig. 5A) or after (curative protocol, Fig. 5B) the inflammatory insult, significantly reduced the effects of DNBS on colon weight/colon length *ratio*. Significant protection was achieved starting from the 1 mg/kg (preventive protocol) and 5 mg/kg (curative protocol) doses. In order to confirm the anti-inflammatory curative activity of CBG, we measured intestinal permeability and performed histological analysis, immunohistochemistry and, MPO and SOD activities on colonic tissues. The selected CBG dose was 30 mg/kg.

4.1.1.2 Histological analysis

Histological evaluations of colonic mucosa of healthy control animals showed normal appearance with intact epithelium (Fig. 6A). In the DNBS group, colons showed tissue injury which was mainly characterized by necrosis involving the full thickness of the mucosa, infiltrations of granulocytes into the mucosa/submucosa and oedema of submucosa (Fig. 6B). CBG (30 mg/kg, *ip*, given after the inflammatory insult) reduced the signs of colon injury (microscopic score: control, 0.50±0.22; DNBS, $9.0\pm0.45^{\#}$; CBG 30 mg/kg, 6.0±0.45*, n=4, $^{\#}p<0.001$ *vs* control and *p<0.01 *vs* DNBS alone). In the colon of

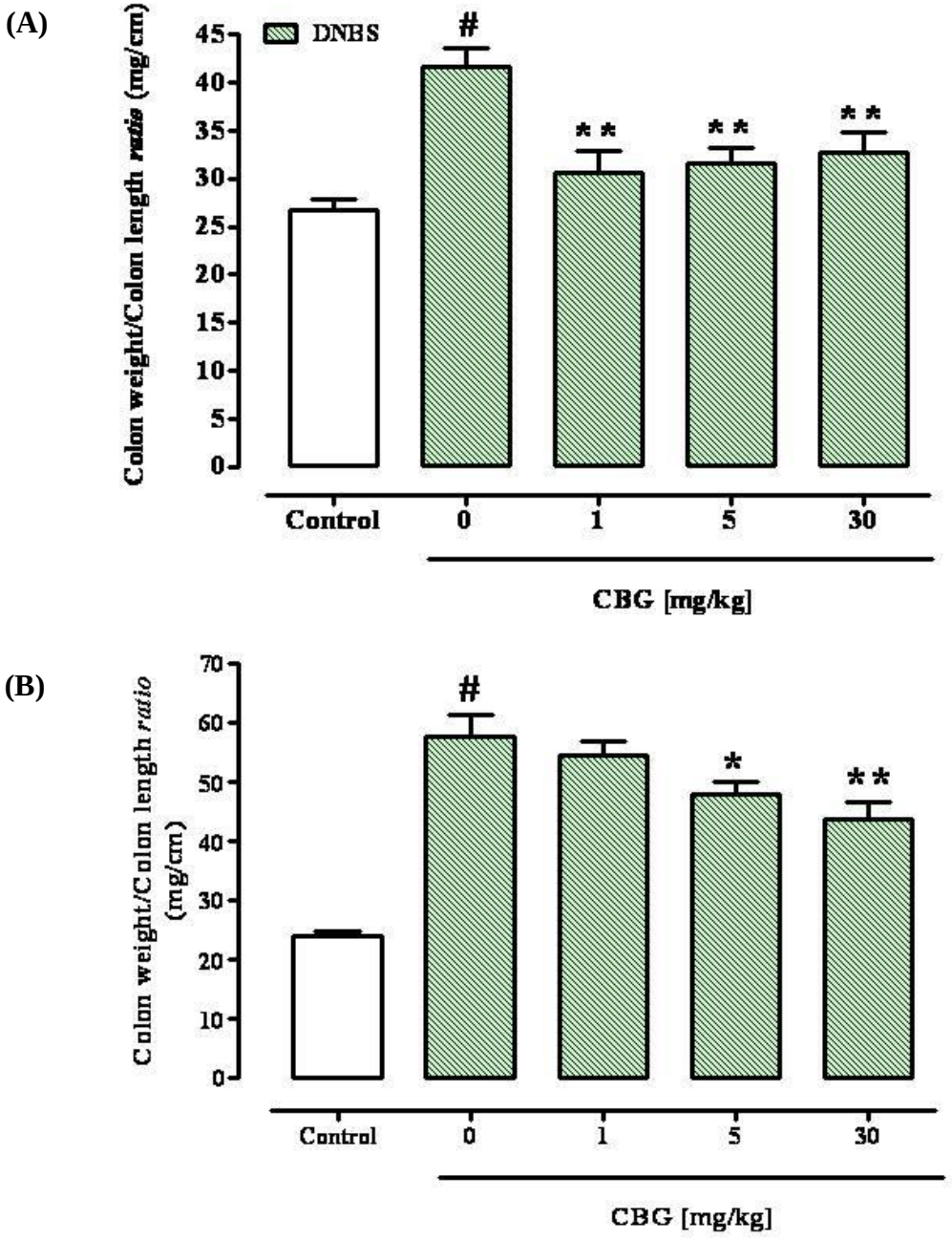

Figure 5. Dinitrobenzene sulfonic acid (DNBS)-induced colitis in mice. Colon weight/length *ratio* of colons from untreated and DNBS-treated mice in the presence or absence of cannabigerol (CBG). Tissues were analyzed 3 days after vehicle or DNBS (150 mg/kg, intrarectally) administration. CBG (1-30 mg/kg) was administered (ip) once a day for six consecutive days starting 3 days before DNBS (preventive protocol, A) or for two consecutive days starting 24-h after the inflammatory insult (curative protocol, B). Bars are mean ± SEM of 12-15 mice for each experimental group. $^{\#}p<0.001$ *vs* control, $^{*}p<0.05$ and $^{**}p<0.01$ *vs* DNBS alone.

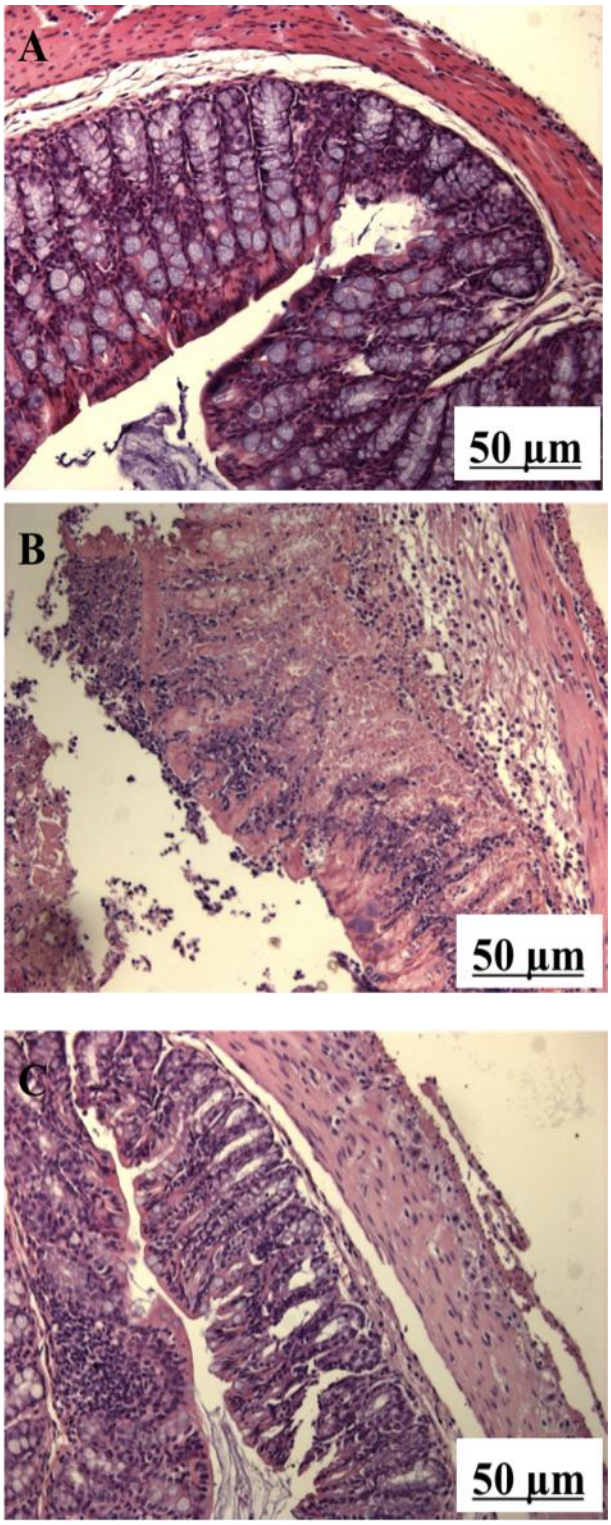

Figure 6. Histological evaluations of inflamed and non-inflamed colons: effect of cannabigerol (30 mg/kg, ip). No histological modification was observed in the mucosa and submucosa of control mice (A); mucosal injury induced by dinitrobenzene sulfonic acid administration (B); treatment with CBG reduced colon injury by stimulating regeneration of the glands (C). Histological analysis was performed 3 days after dinitrobenzene sulfonic acid administration. CBG (30 mg/kg) was administered (ip) for two consecutive days starting 24-h after the inflammatory insult (curative protocol). Original magnification 200X. The figure is representative of 4 experiments.

CBG (30 mg/kg)-treated animals, the glands were regenerating, the oedema in submucosa was reduced, and the erosion area was superficial (Fig. 6C).

4.1.1.3 Immunohistochemical detection of Ki-67

The curative action of CBG was further confirmed by immunohistochemistry. In normal colonic mucosa, the predominant area of cell proliferation is localized to the lower of the crypts as revealed by Ki-67 distribution (Fig. 7A). In the colon from DNBS-treated mice, total necrosis with Ki-67 immunoreactivity on inflammatory cells and in a few remaining surface elements was observed (Fig. 7B). CBG (30 mg/kg, ip, given after the inflammatory insult) partially counteracted the effect of DNBS on cell proliferation, its mitotic activity being restricted to the lower half of the mucosa (i.e. the mature superficial cells were not in a proliferative state) (Fig. 7C).

4.1.1.4 Intestinal permeability

FITC-conjugated dextran presence (an index of membrane integrity) was not detected in the serum of healthy control animals. The administration of DNBS induced FITC-conjugated dextran appearance in the serum. CBG treatment (30 mg/kg) completely abolished DNBS-induced increased intestinal permeability (Fig. 8).

4.1.1.5 Myeloperoxidase (MPO) activity

DNBS-induced colitis was associated with significantly increased neutrophilic infiltration, as evaluated by MPO (Fig. 9). CBG, given after the inflammatory insult, at the dose of 30 mg/kg (curative protocol), counteracted DNBS-induced increase in MPO activity (Fig. 9).

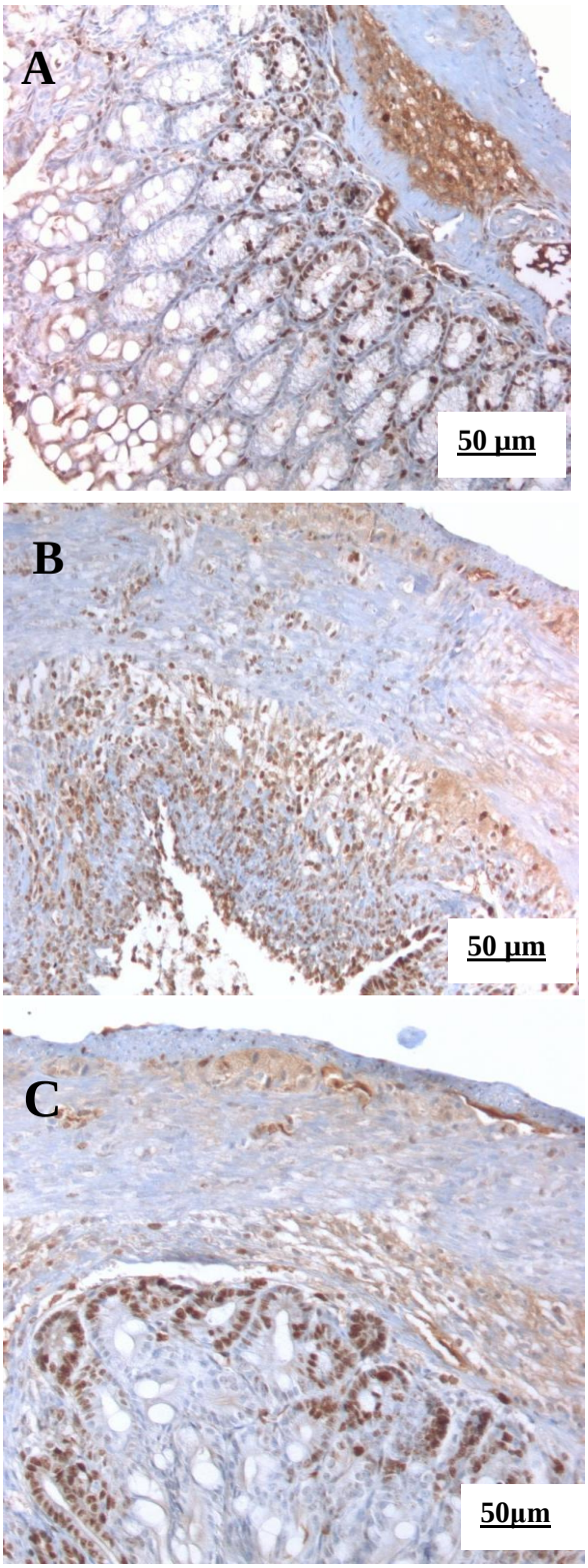

Figure 7. Different patterns of Ki-67 immunoreactivity in the colonic mucosa of control mice (A), dinitrobenzene sulfonic acid -treated mice (B) and mice treated with dinitrobenzene sulfonic acid plus cannabigerol (C). (A) Ki-67 immunopositive cells were localised to the lower part of the crypts. (B) Ki-67 immunopositive cells were observed on inflammatory cells. (C) Ki-67 immunopositive cells were observed only in the expanded basal zone. Cannabigerol (30 mg/kg) was administered (ip) for two consecutive days starting 24-h after the inflammatory insult (curative protocol). The figure is representative of 4 experiments.

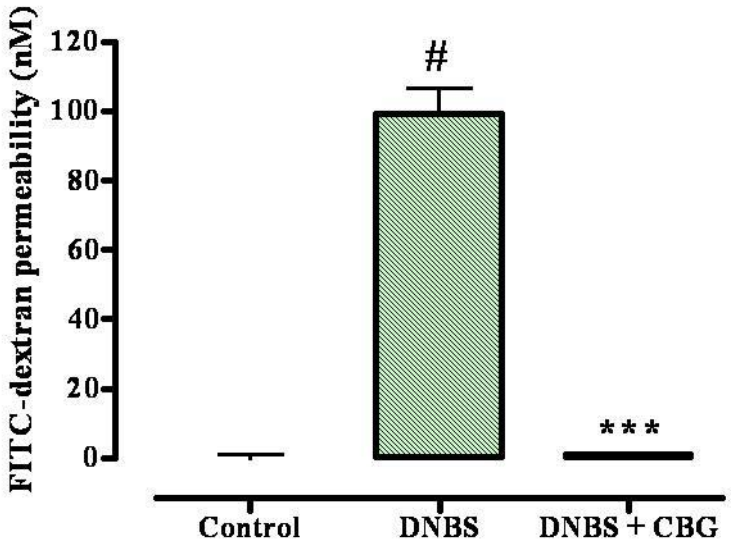

Figure 8. Effect on intestinal permeability in the colonic mucosa of control mice, dinitrobenzene sulfonic acid (DNBS)-treated mice and mice treated with DNBS plus cannabigerol (CBG). CBG (30 mg/kg) was administered (ip) for two consecutive days starting 24-h after the inflammatory insult (curative protocol). $^{\#}p<0.001$ *vs* control and $^{***}p<0.001$ *vs* DNBS alone; n=5 mice.

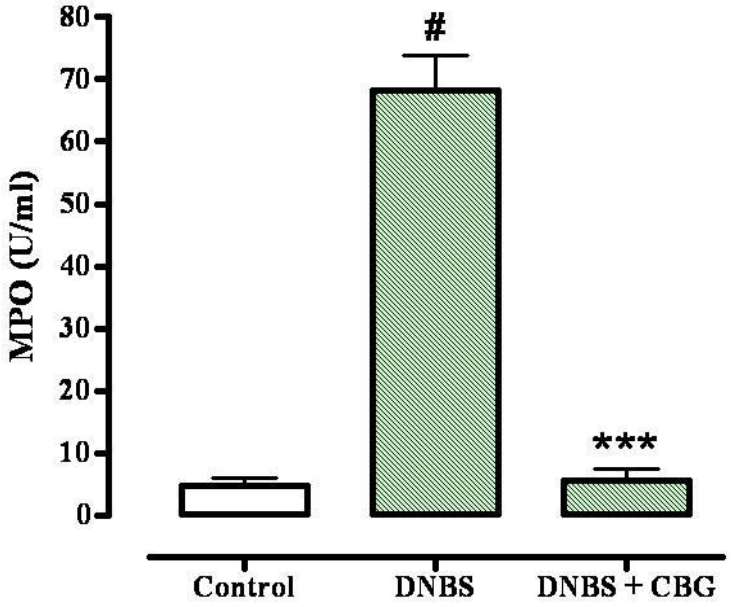

Figure 9. Inhibitory effect of cannabigerol (CBG) on myeloperoxidase (MPO, a marker of intestinal inflammation) activity in dinitrobenzene sulfonic acid (DNBS)-induced colitis in mice. Tissues were analysed 3 days after vehicle or DNBS (150 mg/kg, intrarectally) administration. CBG (30 mg/kg) was administered (ip) for two consecutive days starting 24-h after the inflammatory insult (curative protocol). Bars are mean ± SEM of 5 mice for each experimental group. $^{\#}p<0.001$ *vs* control and $^{***}p<0.001$ *vs* DNBS alone.

4.1.1.6 Inducible nitric oxide synthase (iNOS) and cycloxygenase-2 (COX-2) expression

Densitometric analysis indicated a significant increase in the expression of both iNOS and COX-2 in the inflamed colons (Fig. 10). CBG (30 mg/kg, *ip*, curative protocol) reduced iNOS (Fig. 10A), but not COX-2 (Fig. 10B) over-expression induced by DNBS.

4.1.1.7 Interleukin-1β (IL-1β), interleukin-10 (IL-10) and interferon-γ (IFN-γ) levels

The levels of IL-1β and IFN- γ were significantly increased by DNBS (Fig. 11A and 11B). By contrast, IL-10 production significantly decreased in the colon from DNBS-treated mice (Fig. 11C). Treatment with CBG (30 mg/kg, ip, curative protocol) counteracted the changes in IL-1β, IL-10 and IFN- γ levels observed in the inflamed colons (Fig. 11A, 11B and 11C).

4.1.1.8 Superoxide dismutase (SOD) activity

DNBS produced a significant decrease in SOD activity. CBG, at the dose of 30 mg/kg (curative protocol), counteracted DNBS-induced reduction in SOD activity (Fig. 12).

4.2 Cannabigerol (CBG) and intestinal inflammation: *in vitro* studies

4.2.1 Studies in macrophages

4.2.1.1 Nitrites measurement in macrophages

LPS (1 μg/ml for 18 h) administration caused a significant increase in nitrite production (Fig. 13A). A pre-treatment with CBG (0.001-1 μM, 30 min before LPS) caused a significant reduction in nitrite production (Fig. 13A). The inhibitory effect of CBG (1 μM) on nitrite production in LPS-treated macrophages was accompanied by decrease of iNOS protein with no significant changes in its transcriptional levels (i.e. of iNOS mRNA) (Fig. 13B and 13C). CBG (up to 1

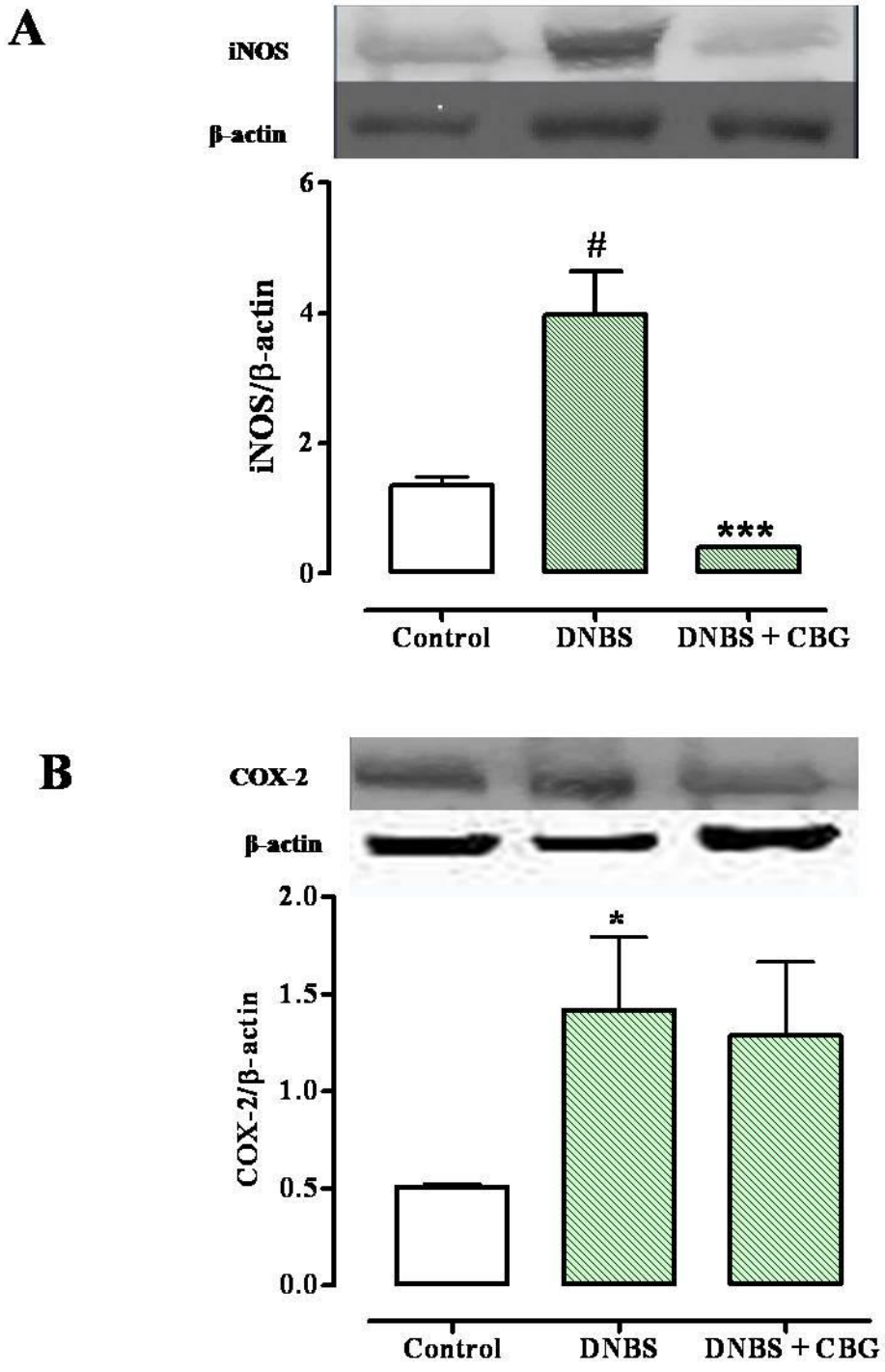

Figure 10. Inducible nitric oxide synthase (iNOS) (A) and cyclooxygenase-2 (COX-2) (B) expression in colonic tissues of animals treated or not with dinitrobenzene sulfonic acid (DNBS): effect of cannabigerol (CBG). Measurements were performed 3 days after DNBS (150 mg/kg, intrarectally) administration. CBG (30 mg/kg) was administered (ip) for two consecutive days starting 24-h after the inflammatory insult (curative protocol). Results are means ± SEM of 3-4 experiments. $^{*}p<0.05$ and $^{\#}p<0.001$ *vs* control; $^{***}p<0.001$ *vs* DNBS alone.

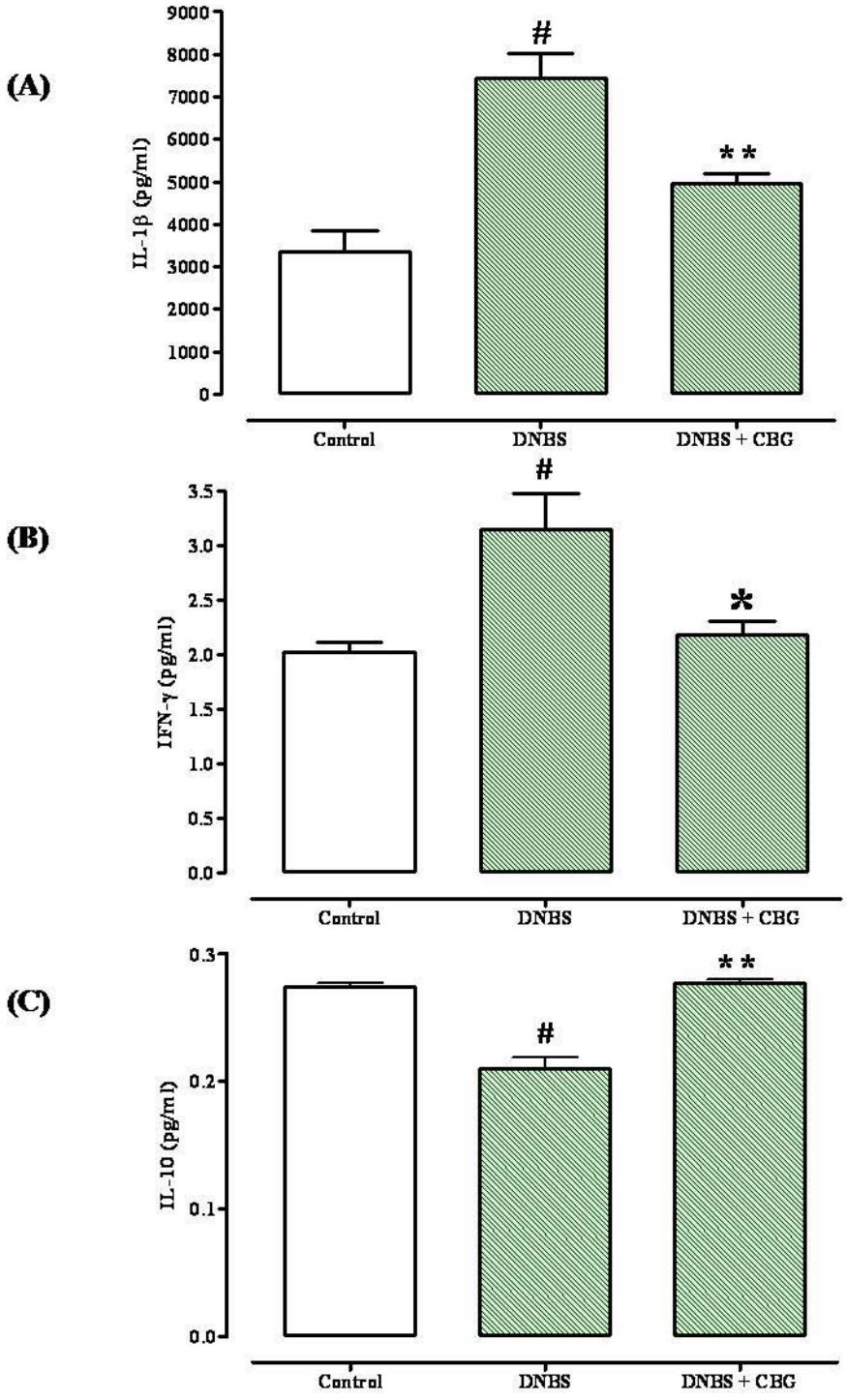

Figure 11. Effect of cannabigerol (CBG) on interleukin-1β (IL-1β) (A), interferon-γ (IFN-γ) (B) and interleukin-10 (IL-10) (C) levels in mouse colons treated with dinitrobenzene sulfonic acid (DNBS). Measurements were performed 3 days after DNBS (150 mg/kg, intrarectally) administration. CBG (30 mg/kg) was administered (ip) for two consecutive days starting 24-h after the inflammatory insult (curative protocol). Results (expressed as picograms per ml of proteic extract) are mean ± SEM of 3-4 experiments. $^{\#}p<0.01$-0.001 *vs* control, $^{*}p<0.05$ and $^{**}p<0.01$ *vs* DNBS alone.

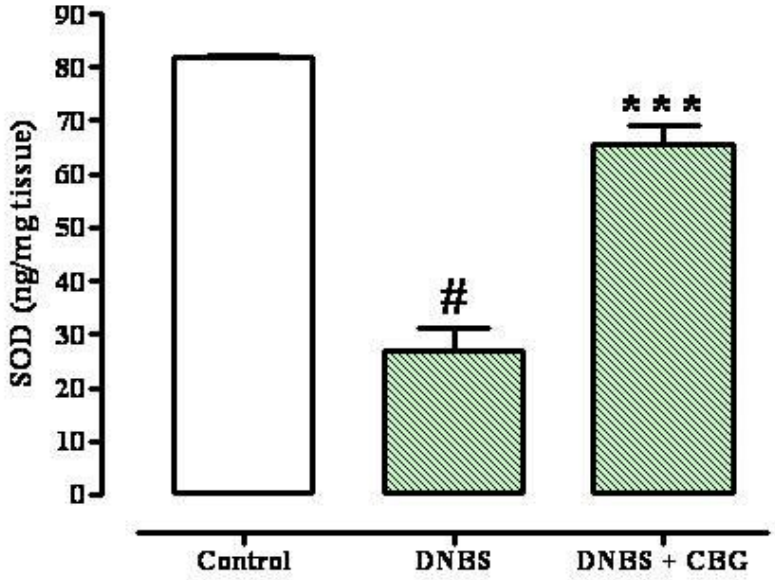

Figure 12. Cannabigerol (CBG) counteracted superoxide dismutase (SOD, an enzyme that catalyzes the conversion of superoxide into hydrogen peroxide and oxygen) activity in dinitrobenzene sulfonic acid (DNBS)-induced colitis in mice. Tissues were analysed 3 days after vehicle or DNBS (150 mg/kg, intrarectally) administration. CBG (30 mg/kg) was administered (ip) for two consecutive days starting 24-h after the inflammatory insult (curative protocol). Bars are mean ± SEM of 5 mice for each experimental group. $^{\#}p<0.001$ *vs* control and $^{***}p<0.001$ *vs* DNBS alone.

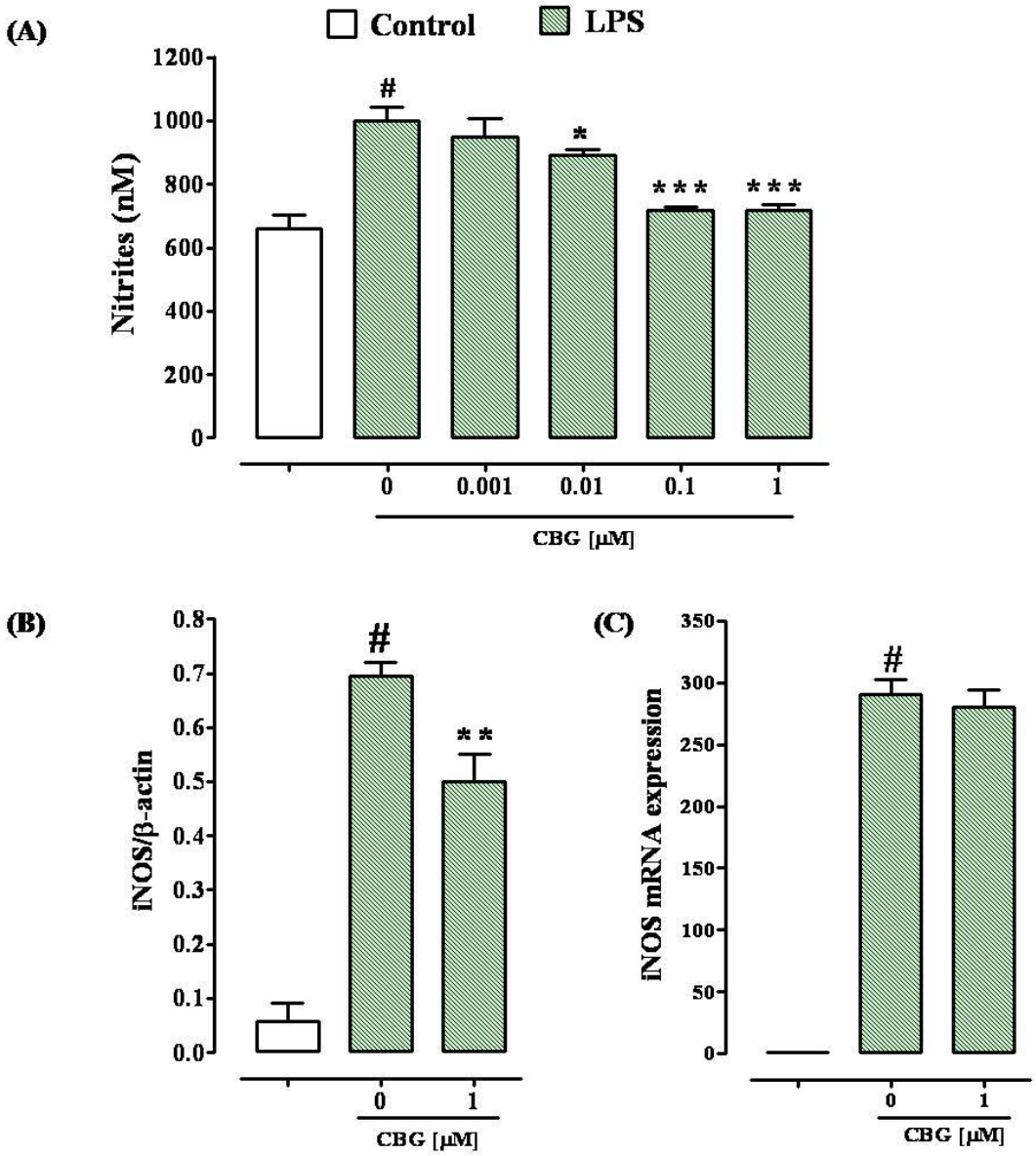

Figure 13. Effect of cannabigerol (CBG) on nitrite levels (A) in the cell medium of murine peritoneal macrophages incubated with lipopolysaccharide (LPS, 1 μg/ml) for 18 h. CBG (0.001–1 μM) was added to the cell media 30 min before LPS challenge. Results, expressed as nitrite concentration (nM), are mean±SEM of four experiments (in triplicates). Figures 13B and 13C show the effect of CBG (1 μM) on inducible nitric oxide synthase (iNOS) expression in cell lysates, evaluated by western blot analysis (B, n=5) or RT-PCR (C, n=4), respectively. $^{\#}p<0.001$ *vs* control; $^{*}p<0.05$, $^{**}p<0.01$ and $^{***}p<0.001$ *vs* LPS alone.

μM) had no significant cytotoxic effect on peritoneal macrophages after a 24-h exposure (data not shown). Moreover CBG, at concentrations used, did not modify *per se* basal nitrite levels in peritoneal macrophages (data not shown).

Because CBG can inhibit endocannabinoid metabolism and hence indirectly activate cannabinoid receptors (De Petrocellis et al., 2011), in another set of experiments we verified if CBG effect on nitrite production was sensitive to selective CB_1 and CB_2 receptor antagonists. We found that rimonabant (0.1 μM, CB_1 receptor antagonist) did not modify the inhibitory effect of CBG (1 μM) (Fig. 14A). By contrast, SR144528 (0.1 μM, CB_2 receptor antagonist) enhanced the inhibitory effect of CBG (1 μM) on nitrite production (Fig. 14B).

4.2.1.2 CB_1 and CB_2 mRNA expression in macrophages

A challenge with LPS (1 μg/ml for 18 h) caused up-regulation of CB_1 receptors and down-regulation of CB_2 receptors (Fig. 15A and 15B). CBG (1 μM) did not modify cannabinoid CB_1 and CB_2 receptors mRNA expression both in control and in LPS-treated macrophages (Fig. 15A and 15B).

4.2.2 Reactive oxygen species (ROS) production in intestinal epithelial cells

The exposure of P*tk6* null colonic epithelial cells to H_2O_2/Fe^{2+} (2 mM) produced a significant increase in ROS formation (Fig. 16). A pre-treatment for 24 h with CBG (0.1-10 μM) reduced ROS formation as measured by the inhibition of DCF fluorescence intensity. The effect was significant starting from the concentration of 1 μM (Fig. 16). CBG (up to 10 μM) had no significant cytotoxic effect on colonic epithelial cells after a 24-h exposure (data not shown).

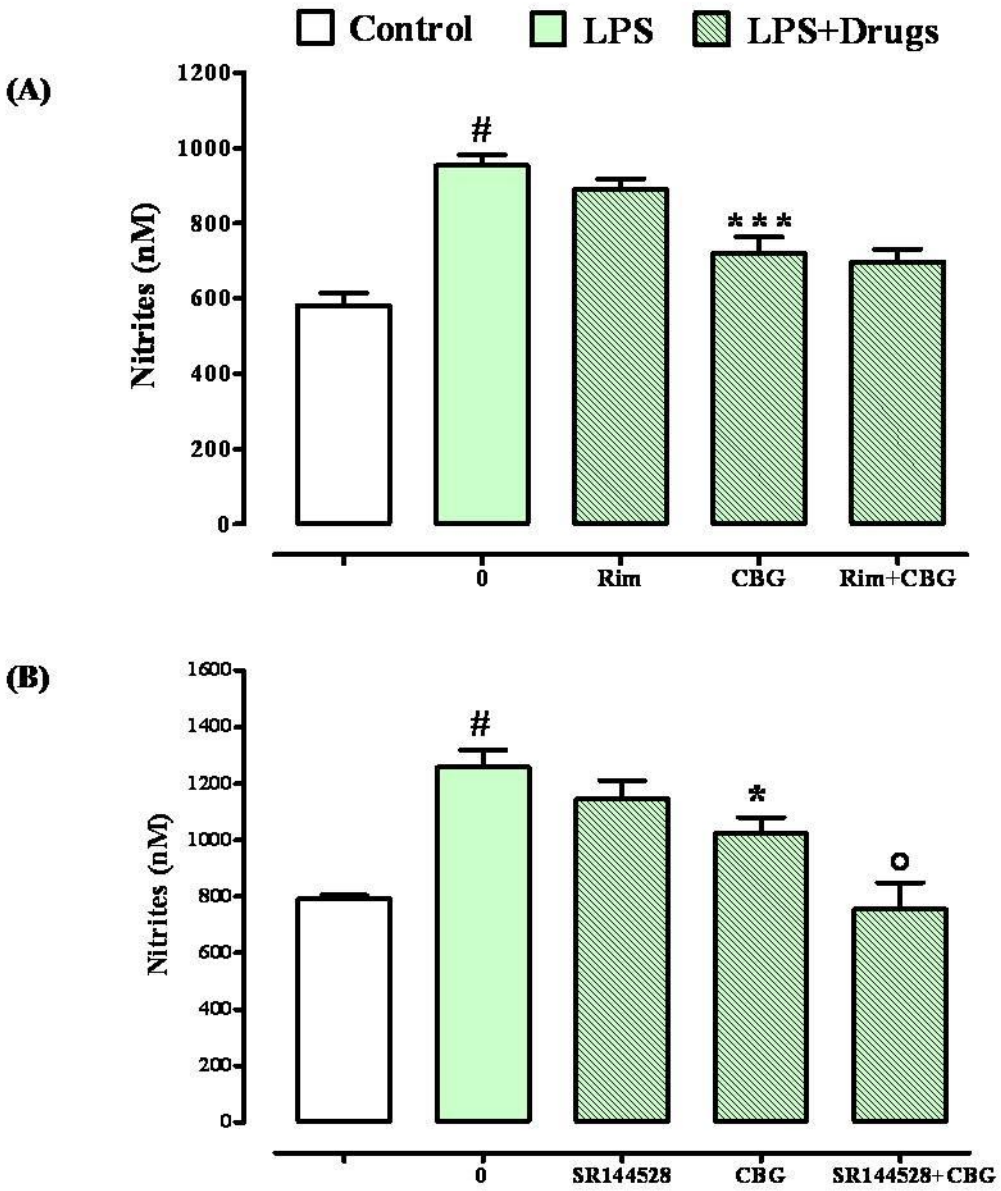

Figure 14. Effect of cannabigerol (CBG, 1 μM) alone or in presence of the cannabinoid CB_1 receptor antagonist rimonabant (Rim, 0.1 μM) (A) or the cannabinoid CB_2 receptor antagonist SR144528 (0.1 μM) (B) on nitrite levels in the cell medium of murine peritoneal macrophages incubated with lipopolysaccharide (LPS, 1 μg/ml) for 18 h. The antagonists were added to the cell media 30 min before CBG exposure. LPS was incubated 30 min after CBG. Results are means±SEM of three experiments (in triplicates). $^{\#}p<0.001$ *vs* control; $^{*}p<0.05$ and $^{***}p<0.001$ *vs* LPS alone; $^{\circ}p<0.001$ *vs* LPS+CBG.

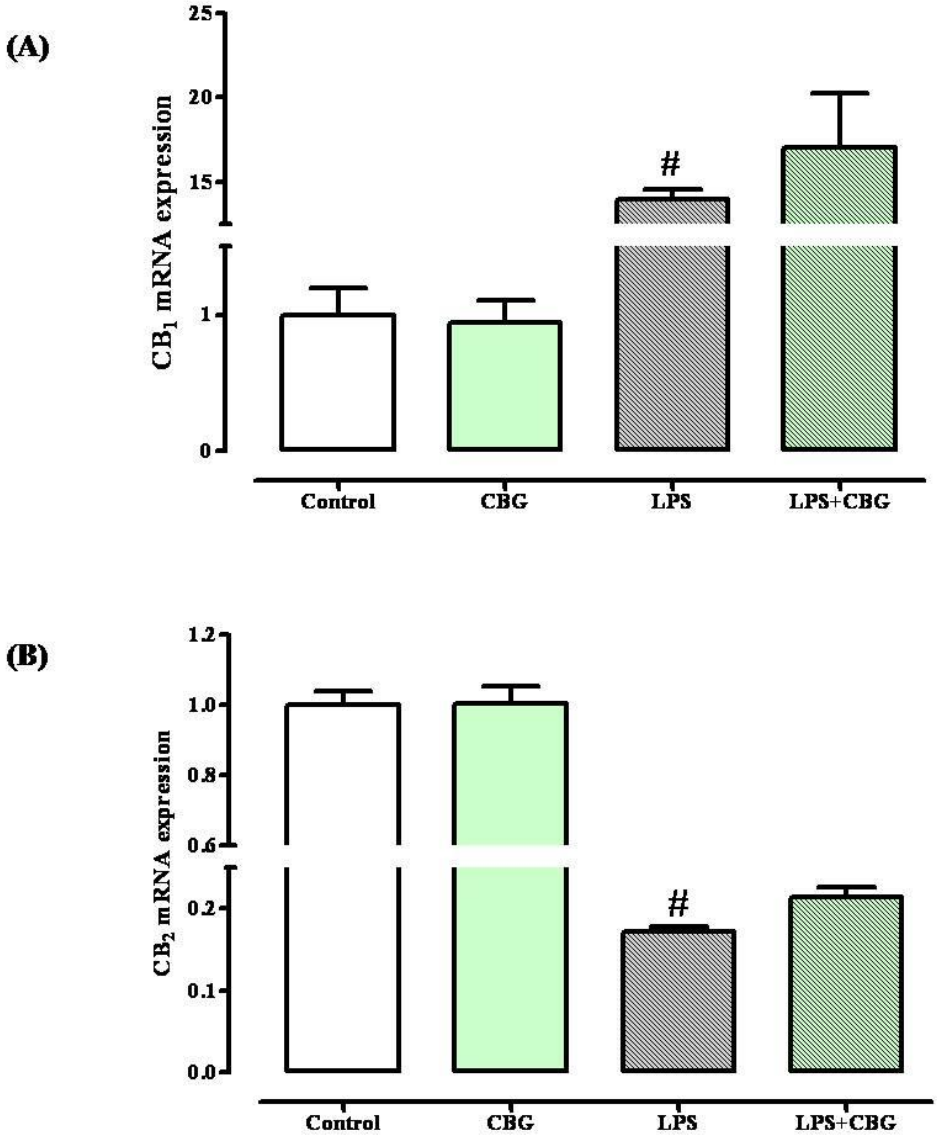

Figure 15. Relative mRNA expression of cannabinoid CB_1 receptor (A) and cannabinoid CB_2 receptor (B) in cell lysates from macrophages incubated or not with lipopolysaccharide (LPS, 1 μg/ml) for 18 h. Cannabigerol (CBG, 1 μM) was added alone to the cell media or 30 min before LPS challenge. Data were analyzed by GENEX software for group wise comparisons and statistical analysis. Results are means±SEM of four experiments. $^{\#}p<0.001$ *vs* control.

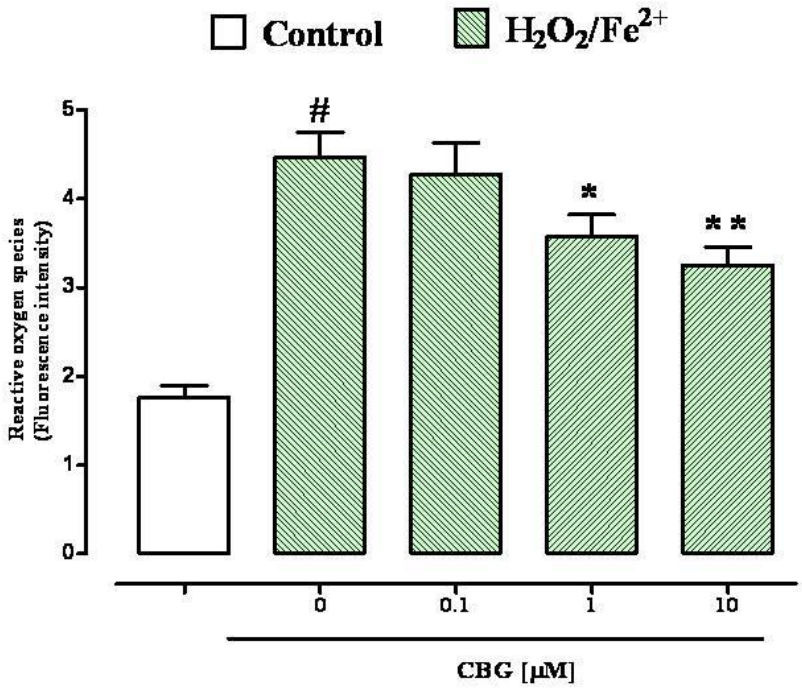

Figure 16. Reactive oxygen species (ROS) production produced by Fenton's reagent (2 mM H_2O_2/Fe^{2+}) in P*tk6* null colonic epithelial cells after 24-h exposure to cannabigerol (CBG, 0.1-10 µM). Results are mean ± SEM of five experiments. $^{\#}p<0.001$ *vs* control, $^{*}p<0.05$ and $^{**}p<0.01$ *vs* H_2O_2/Fe^{2+}alone.

4.3 Diallyl sulfide (DAS)/diallyl disulfide (DADS) and intestinal inflammation: *in vivo* and *ex vivo* studies

4.3.1 Dinitrobenzene sulfonic acid (DNBS) model of colitis

4.3.1.1 Animal body weight and colon weight/colon length *ratio*

Three days after intracolonic administration of DNBS (150 mg/kg, intrarectally), a significant body weight loss was observed (Fig. 17). The treatment of animals with DAS and DADS, at the doses of 1–10 mg/kg (orally), significantly reduced DNBS-induced effects on body weight (Fig. 17).

DNBS administration caused a significant increase in colon weight/colon length *ratio* (Fig. 18) which is suggestive of intestinal inflammation/damage. DAS and DADS (1 and 10 mg/kg) significantly reduced the increase in colon weight/colon length *ratio* induced by DNBS (Fig. 18).

4.3.1.2 Histological analysis

No histological modification was observed in control mice (Fig. 19A). Microscopic damage induced by DNBS administration was characterized by leucocyte infiltration (into mucosa, submucosa and *muscolaris*), crypts loss and ulceration (Fig. 19B). A treatment with DAS and DADS (both at the 10 mg/kg dose) significantly reduced the histological damage (Fig. 19C and 19D).

4.3.1.3 Immunohistochemical detection of interferon-γ induced protein 10 (IP-10)

The curative action of diallyl sulfide (DAS) and diallyl disulfide (DADS) was further confirmed by immunohistochemistry. Immunostaining showed that colonic inflammation induced by DNBS increased IP-10 levels, compared to control animals. DAS and DADS at dose of 10 mg/kg decreased DNBS-induced up-regulation of IP-10 levels (Fig. 20).

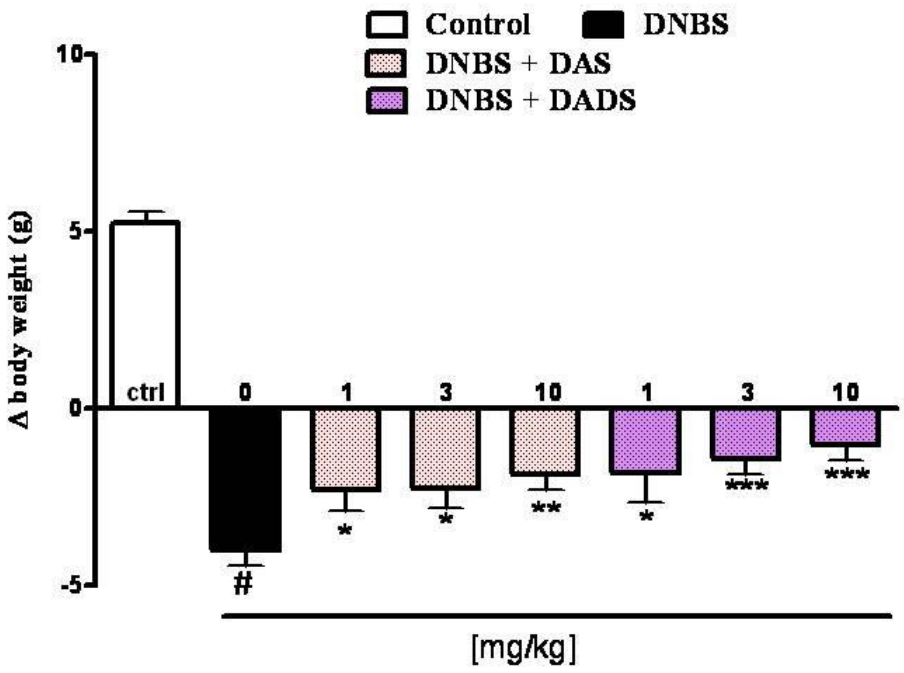

Figure 17. Dinitrobenzene sulfonic acid (DNBS)-induced colitis in mice. Effect of diallyl sulfide (DAS) and diallyl disulfide (DADS) (1–10 mg/kg, orally) on body weight variation induced by DNBS, (150 mg/kg, intrarectally). Changes in mice body weight were monitoring every day for the whole duration of the experiment (starting from colitis induction). Bars are mean ± SEM of 8-10 mice for each experimental group. $^{\#}p<0.001$ *vs* Ctrl; $^{*}p<0.05$, $^{**}p<0.01$ and $^{***}p<0.001$ *vs* DNBS alone.

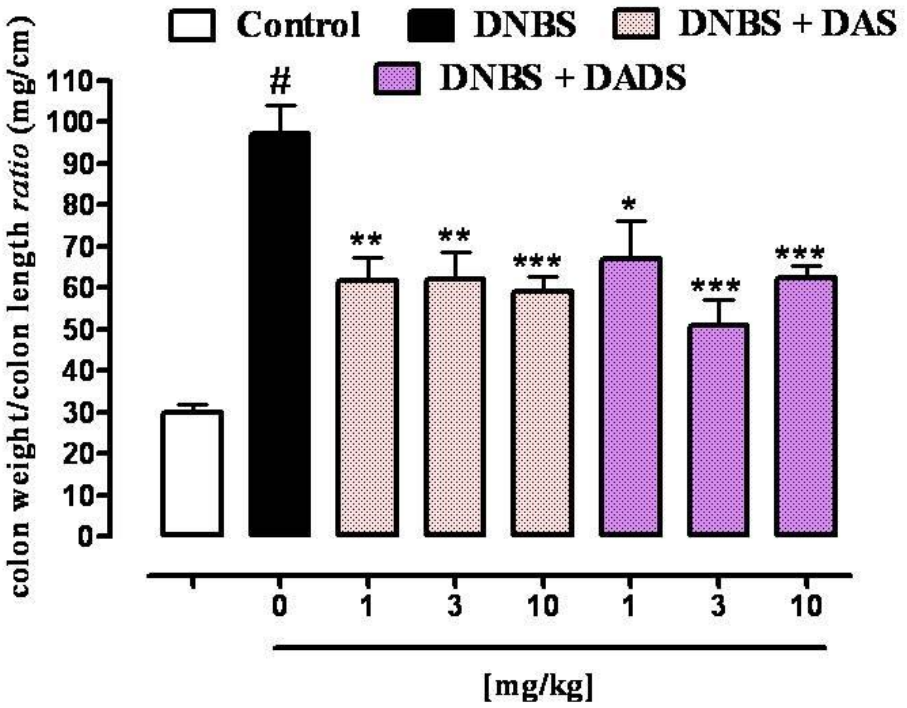

Figure 18. Dinitrobenzene sulfonic acid (DNBS)-induced colitis in mice. Colon weight/colon length *ratio* of colons from untreated and DNBS-treated mice in the presence or absence of diallyl sulfide (DAS) or diallyl disulfide (DADS) (1-10 mg/kg, orally). Tissues were analyzed 3 days after vehicle or DNBS (150 mg/kg, intrarectally) administration. DAS and DADS were administrated orally once a day for two consecutive days starting 24-h after the inflammatory insult. Bars are mean ± SEM of 8-10 mice for each experimental group $^{\#}p<0.001$ *vs* control; $^{**}p<0.01$ and $^{***}p<0.001$ *vs* DNBS alone.

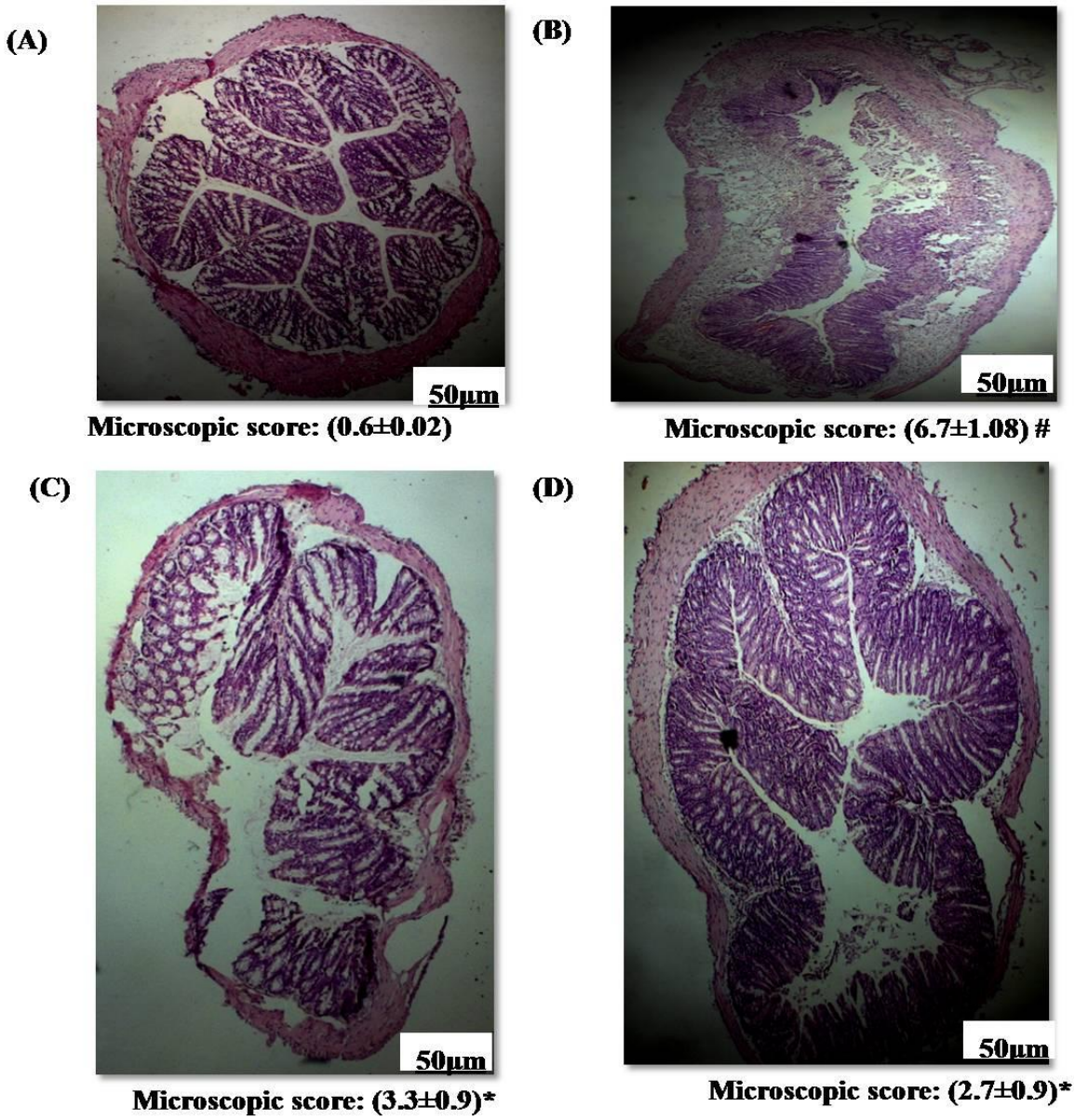

Figure 19. Histological evaluations of inflamed and non-inflamed colons: effect of diallyl sulfide (DAS) and diallyl disulfide (DADS) (10 mg/kg, orally). No histological modification was observed in the *mucosa* and *submucosa* of control mice (A); mucosal injury induced by dinitrobenzene sulfonic acid (DNBS) (B); DNBS plus DAS (C); DNBS plus DADS (D). DAS and DADS were administrated orally once a day for two consecutive days starting 24-h after the inflammatory insult. Histological analysis was performed 3 days after DNBS administration. Original magnification 200X. The figure is representative of 6 experiments. $^{\#}p<0.001$ *vs* control, $^{*}p<0.05$ *vs* DNBS alone.

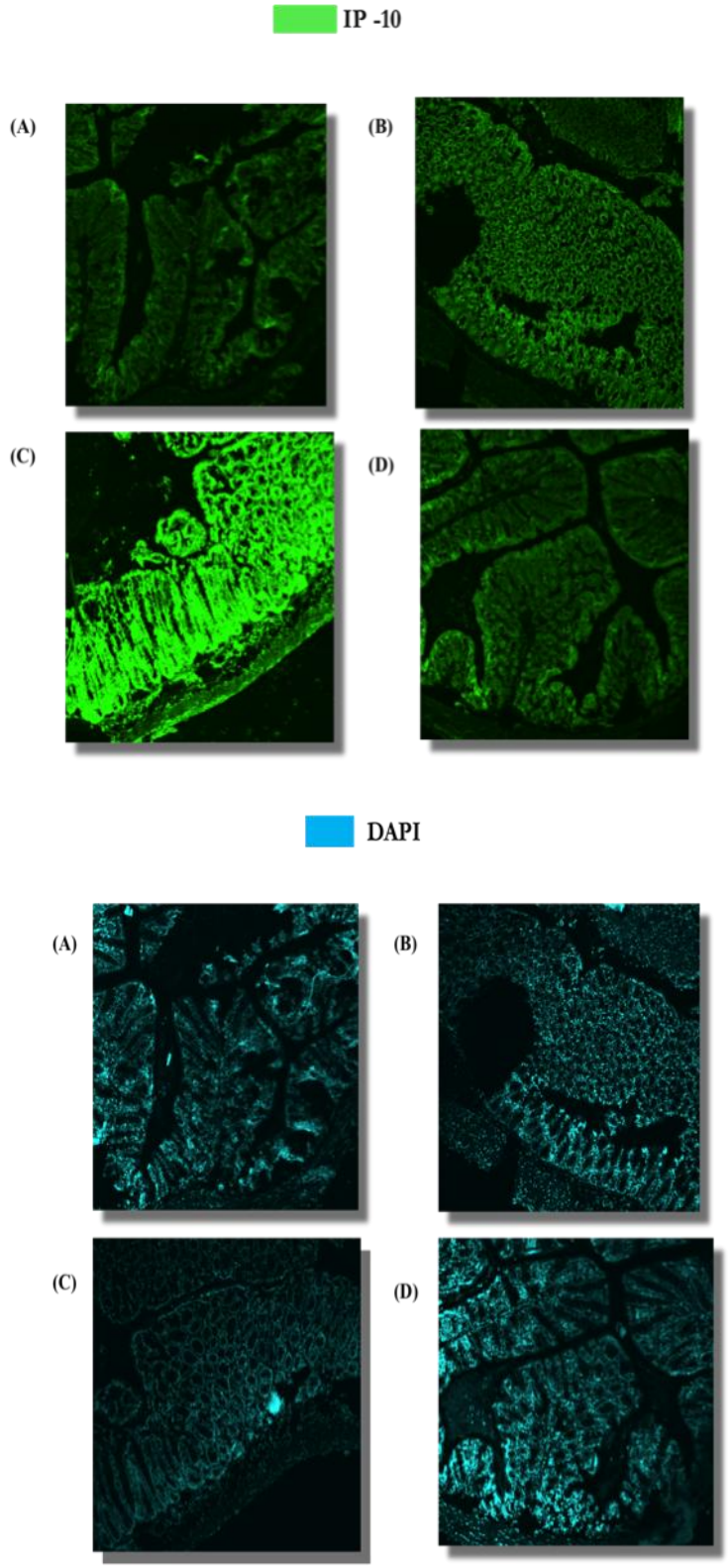

Figure 20. Interferon-γ induced protein 10 (IP-10) levels (green) in colonic mucosa of mice untreated (A); treated with: dinitrobenzene sulfonic acid (DNBS) (B); diallyl sulfide plus DNBS (C); diallyl disulfide plus DNBS (D). Diallyl sulfide and diallyl disulfide were administrated orally once a day for two consecutive days starting 24-h after the inflammatory insult. Immunohistological analysis was performed 3 days after DNBS administration. DAPI (blue) is index of intracellular nuclei orientation. The figure is representative of 4 experiments.

4.4 Diallyl sulfide (DAS) and diallyl disulfide (DADS) in intestinal inflammation: *in vitro* studies

4.4.1 Experiments in murine intestinal epithelial (Mode-K) cells

4.4.1.1 Diallyl sulfide (DAS) and diallyl disulfide (DADS): cytotoxicity in Mode-K cells

The effect of DAS and DADS on cell viability, using the WST-8 assay, was evaluated in the Mode-K cell line. DAS and DADS alone, or in combination with IFN-γ (50 ng/ml) did not affect Mode-K cell viability after 24-h exposure (% of cell viability ± SEM in Mode-K cells: control 99.73 ± 2.041; DAS 5µg/ml 93.72 ± 3.88; DAS 10 µg/ml 96.17±3.83; DAS 20 µg/ml 93.37±6.17; DAS 30 µg/ml 108.03±8.35; DAS 50 µg/ml 99.45±6.20; DAS 75µg/ml 92.50±6.98; DAS 100 µg/ml 95.56 ± 4.02; DMSO (20 % v/v), used as positive control, significantly (p< 0.001) reduced Mode-K cell viability: (% of cell viability ± SEM: control 99.73 ± 2.041; DMSO 8.77 ± 1.126; n=3. Control 100.05 ± 3.55; DADS 5µg/ml 118.89 ± 4.69; DADS 10 µg/ml 98.84±8.78; DADS 20 µg/ml 100.82±8.5; DADS 30 µg/ml 115.68±9.79; DADS 50 µg/ml 105.99±11.77; DADS 75 µg/ml 90.28±8.18; DADS 100 µg/ml 97.88±10.91; DMSO (20 % v/v) significantly (p<0.001) reduced Mode-K cell viability: (% of cell viability ± SEM: control 100.05 ± 3.55; DMSO 9.2± 0.88; n=3. Control 90.25 ± 1.51; IFN-γ (50 ng/ml) 84.5 ±2.66; DAS 50 µg/ml plus IFN-γ (50 ng/ml) 86.12±1.41; DADS 50 µg/ml plus IFN-γ (50 ng/ml) 96.18±2.57; n=3).

4.4.1.2 Diallyl sulfide (DAS) and diallyl disulfide (DADS): interferon-γ induced protein 10 (IP-10) and interleukin-6 (IL-6) levels in Mode-K cells.

The treatment with IFN-γ (50 µg/ml) induced a significant increase in IP-10 levels in Mode-K cells (Fig. 21A and 21B). DADS, but not DAS, at the

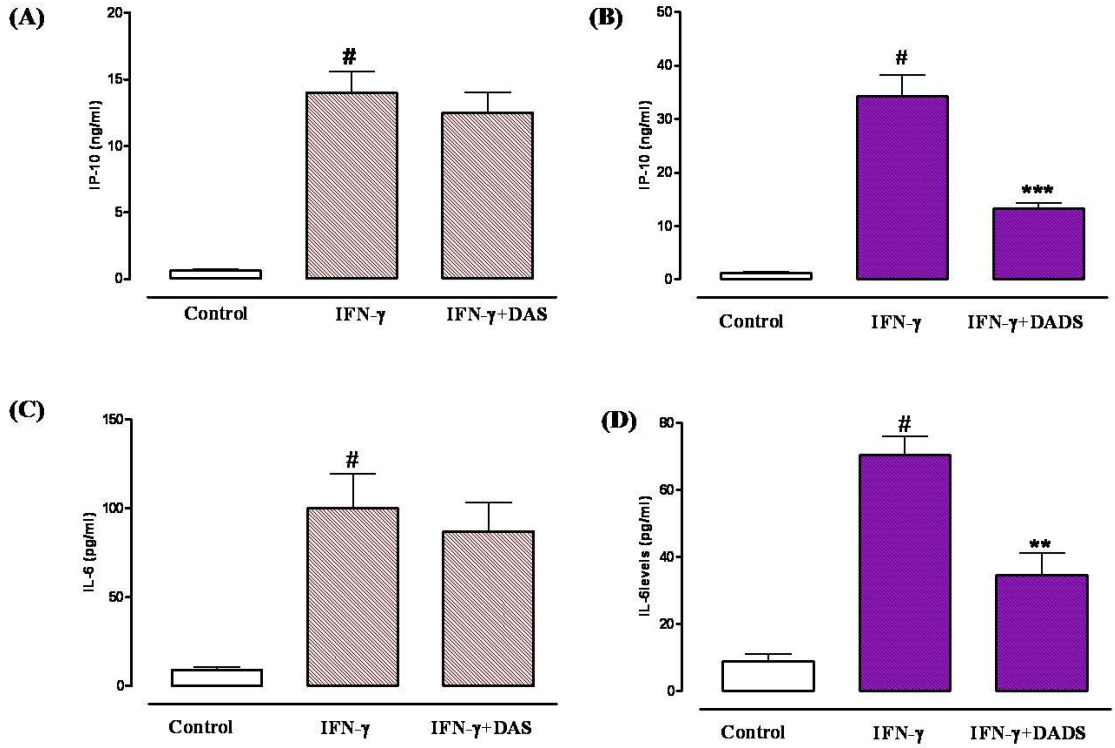

Figure 21. Effect of diallyl sulfide (DAS) and diallyl disulfide (DADS) (50 μg/ml) on interferon-γ induced protein 10 (IP-10) (A, B) and interleukin-6 (IL-6) (C, D) levels in the cell medium of Mode-K cells incubated with interferon-γ (IFN-γ, 50 ng/ml) for 24 h. Results (expressed as nanograms or picograms per ml of proteic extract) are mean ± SEM of 3-4 experiments. $^{\#}p<0.01$-0.001 *vs* control, $^{**}p<0.01$ and $^{***}p<0.001$ *vs* IFN-γ alone.

concentration of 50 μg/ml, reduced significantly IP 10 levels increased by IFN-γ (Fig. 24A and 24B). Similarly, DADS (50 μg/ml), but not DAS, was able to reduce significantly IFN-γ-induced IL-6 levels production (Fig. 21C and 21D). DAS and DADS (50 μg/ml) did not modify *per se* basal levels of IP-10 and IL-6 in Mode-K cells (data not shown).

4.4.1.3 Interferon-γ induced protein 10 (IP-10) mRNA expression in Mode-K cells

DADS (50 μg/ml), but not DAS (50 μg/ml), reduced the expression of IP-10 mRNA induced by IFN-γ in Mode-K cells (Fig. 22).

4.4.1.4 Nitrites measurement in Mode-K cells

IFN-γ (50 ng/ml for 24 h) administration caused a significant increase in nitrite production (Fig. 23). A treatment with DAS (50 μg/ml), but not with DADS (50 μg/ml) caused a significant reduction in nitrite production. DAS and DADS (50 μg/ml) did not modify *per se* basal nitrite levels in Mode-K cells (data not shown).

4.5 Bromelain and intestinal inflammation

4.5.1 Upper gastrointestinal transit in the inflamed gut

Bromelain, administered intraperitoneally, at the dose ranging from 1 to 10 mg/kg, reduced significantly and in a dose-dependent manner the intestinal transit, both in control mice and in animals with the experimental inflammation induced by croton oil (Fig. 24A and 24B). By contrast, bromelain, given orally (100-500 mg/kg) was inactive in control animals (GC: control 5.0 ± 0.26; bromelain 100 mg/kg 4.9 ± 0.12; bromelain 250 mg/kg 5.2 ± 0.24; bromelain 500 mg/kg 4.8 ± 0.18; n=10-12 animals for each experimental group), but it reversed the increase in motility induced by croton oil (Fig. 25). The inhibitory effect of bromelain (500 mg/kg orally) was reverted by the PAR-2 receptor antagonist ENMD-1068 (4

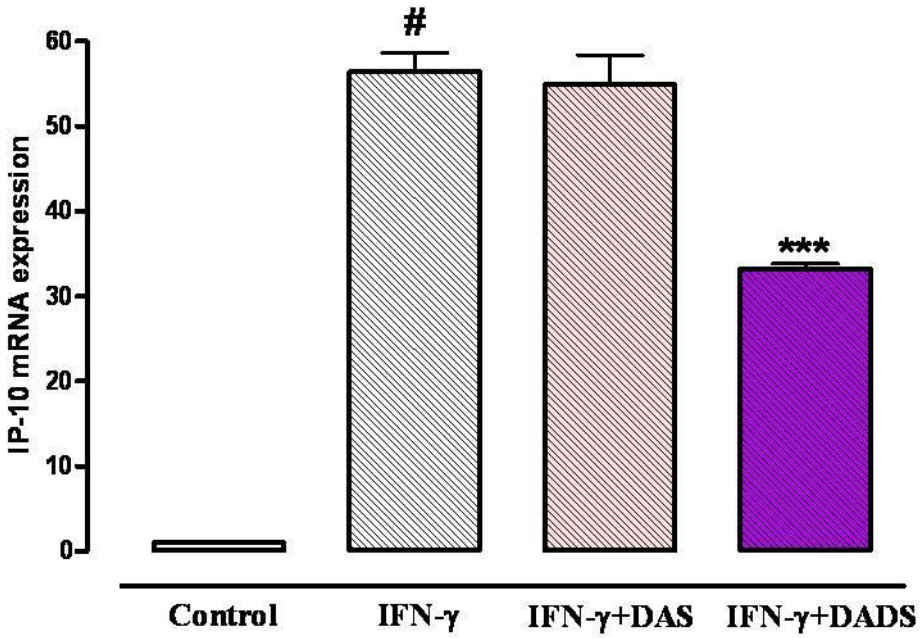

Figure 22. Effect of diallyl sulfide (DAS) and diallyl disulfide (DADS) (50 μg/ml) on the relative mRNA expression of interferon-γ induced protein 10 (IP-10) in cell lysates from Mode-K cells incubated with interferon-γ (IFN-γ, 50 ng/ml) for 24 h. Results are means±SEM of 3 experiments. $^{\#}p<0.001$ *vs* control, $^{***}p<0.001$ *vs* IFN-γ alone.

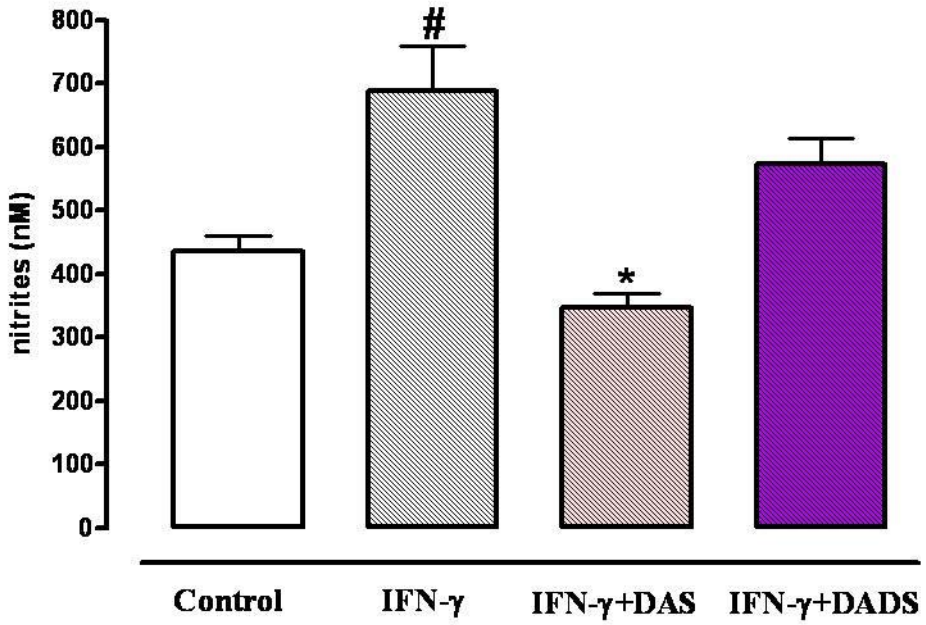

Figure 23. Effect of diallyl sulfide (DAS) and diallyl disulfide (DADS) (50 μg/ml) on nitrite levels in the cell medium of Mode-K cells incubated with interferon- γ (IFN-γ, 50 ng/ml) for 24 h. Results are means±SEM of three experiments (in triplicates). $^{\#}p<0.001$ *vs* control; $^{*}p<0.05$ *vs* IFN-γ alone.

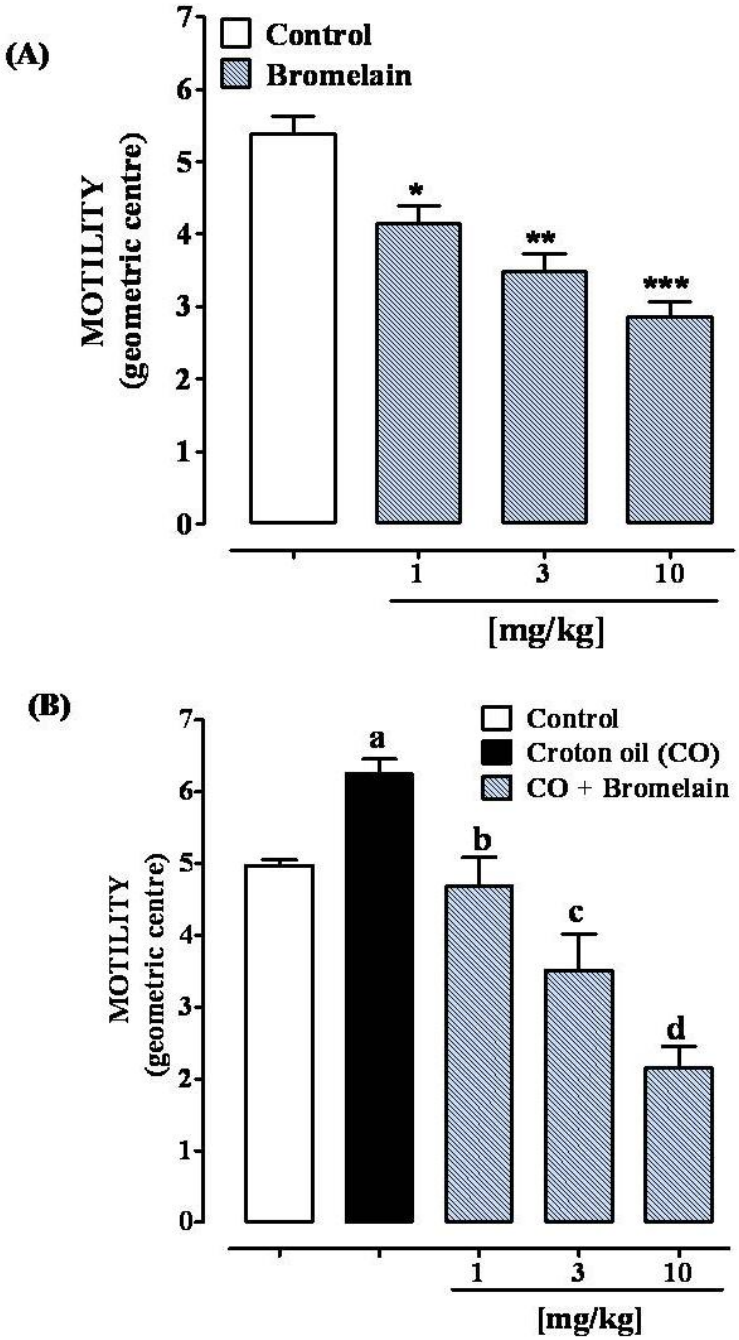

Figure 24. Effect of intraperitoneally injected bromelain (1–10 mg/kg) on intestinal transit in physiological (A) and (B) inflammatory conditions [croton oil (CO)-treated mice]. Transit was expressed as the geometric center of the distribution of a fluorescent marker along the small intestine (see Materials and Methods section). Bars represent the mean ± SEM of 10–12 animals for each experimental group. $^{*}p < 0.05$; ** $p< 0.01$ and *** $p< 0.001$ *vs* control. ^{a} $p< 0.01$ *vs* control; $^{b}p< 0.05$, $^{c}p< 0.01$ and $^{d}p< 0.001$ *vs* CO alone.

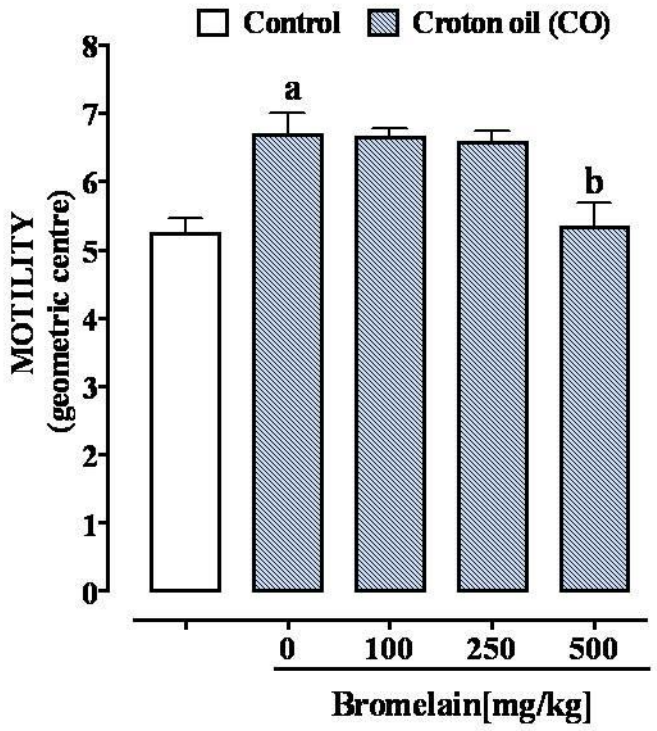

Figure 25. Effect of orally administered bromelain (100–500 mg/kg) on intestinal transit in croton oil (CO)-treated mice. Transit was expressed as the geometric center of the distribution of a fluorescent marker along the small intestine (see Materials and Methods section). Bars represent the mean ± SEM of 10–12 animals. [a]$p < 0.01$ *vs* control; [b]$p < 0.05$ *vs* CO alone.

mg/kg, ip) [GC: control 5.2 ± 0.22; croton oil 6.7 ± 0.33[a]; croton oil + bromelain 5.3 ± 0.35[b]; croton oil + bromelain + ENMD-1068 8.1 ± 0.18[c]. [a]p< 0.01 vs control, [b]p< 0.05 *vs* CO, and [c]p<0.001 vs croton oil + bromelain; n=8 mice for each experimental group]. ENMD-1068 alone did not significantly affect transit in croton oil-treated mice (data not shown).

4.5.2 Protease-activated receptor type 2 (PAR-2) expression in the inflamed intestine

Western blot analysis revealed the expression of PAR-2 in ileal tissues of healthy and croton oil-treated animals (Fig. 26). However, the densitometric analysis indicated a significant decrease in the expression of PAR-2 in the inflamed gut (Fig. 26).

4.5.3 Effect of bromelain on intracellular calcium levels in Caco-2 cells

Bromelain (1 μg/ml) ($p<0.01$) increased $[Ca^{2+}]_i$ in Caco-2 cells and this effect was significantly ($p<0.05$) reduced by the PAR-2 antagonist ENMD-1068 (5 mM) (Fig. 27). Bromelain and ENMD-1068, at the concentrations used in this assay, did not affect cell viability in Caco-2 cells (data not shown).

4.6 Bromelain and colon carcinogenesis *in vivo*

The carcinogenic agent AOM given alone induced the appearance of ACF, polyps and tumours (Fig. 28). Bromelain (1 mg/kg) significantly reduced the total number of ACF/mouse, the number of ACF with four or more crypts (Fig. 28A and 28B) and the number of tumors/mouse, and completely prevented the formation of polyps (Fig. 28C and 28D). Celecoxib (10 mg/kg), used as a reference drug, was also able to reduce the total number of ACF/mouse, the number of ACF with four or more crypts, the number of tumours and the number of polyps (Fig. 28A, 28B, 28C and 28D).

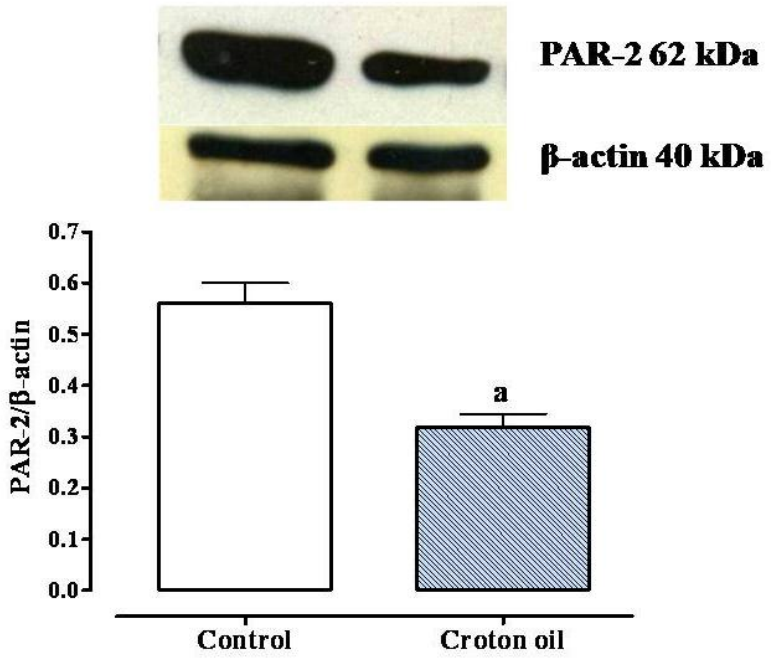

Figure 26. Protease-activated receptor type 2 **(**PAR-2) expression in ileum of control (vehicle) and croton oil (40 µl/mouse)-treated mice (see Materials and Methods for details). Bars represent the mean ± SEM of three experiments. [a]$p < 0.05$ *vs* control.

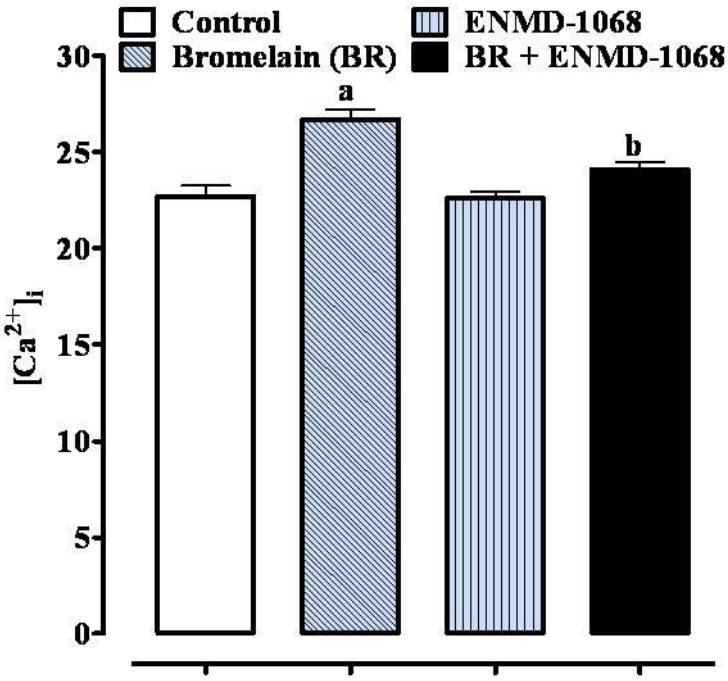

Figure 27. Effect of bromelain (BR) (1 μg/ ml) alone and in the presence of ENMD-1068 (5 mmol L^{-1}) on intracellular calcium concentration ($[Ca^{2+}]_i$) in Caco-2 cells. Bars represent the mean ± SEM of four experiments. [a]$p< 0.01$ *vs* control; [b]$p< 0.05$ *vs* BR.

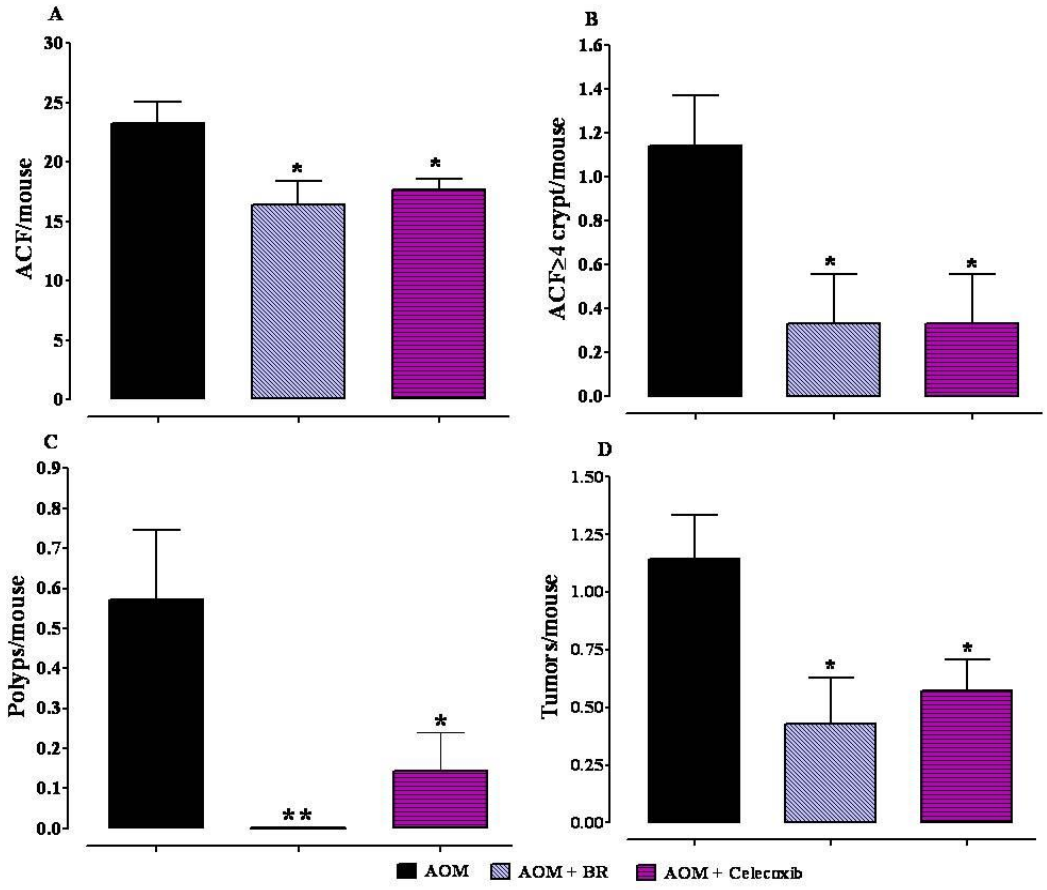

Figure 28. Effect of Bromelain (BR, 1 mg/kg) on the formation of aberrant crypt foci (ACF, A), ACF with four or more crypts (B), polyps (C) and tumours (D) induced by the carcinogenic substance azoxymethane (AOM) in the mouse colon. AOM (40 mg/kg in total, intraperitoneally) was administered, at the single dose of 10 mg/kg, at the beginning of the first, second, third and fourth week. BR was administered (intraperitoneally) three times a week for the whole duration of the experiment (starting from 1 week before the first administration of AOM). Data represent mean ± SEM of 10 animals $^{*}p<0.05$ and $^{**}p<0.01$ *vs* AOM alone.

4.7 Bromelain and colon carcinogenesis in colorectal carcinoma (Caco-2) cells

4.7.1 Cytotoxicity assay

The exposure of non-differentiated and differentiated Caco-2 cells to bromelain (BR), at the concentration ranging from 0.1 to 10 µM, did not affect cell viability after 24-h exposure (% of cell viability ± SEM in non-differentiated Caco-2 cells: control 100.9 ± 1.3; BR 0.1 µM 98.6 ± 2.3; BR 0.3 µM 94.93 ± 3.5; BR 1 µM 99.2 ± 4.2; BR 3 µM 100.0 ± 2.7; BR 10 µM 102.1 ± 4.1; n=3. % of cell viability ± SEM in differentiated Caco-2 cells: control 101.4 ± 1.3; BR 0.1 µM 100.1 ± 0.5; BR 0.3 µM 99.8 ± 1.7; BR 1 µM 101.0 ± 2.5; BR 3 µM 100.8 ± 2.0; BR 10 µM 102.9 ± 1.7; n=3.). DMSO (20 % v/v), used as positive control, significantly ($p<0.001$) reduced Caco-2 cell viability (% of cell viability ± SEM in not differentiated Caco-2 cells: control 100.9 ± 1.3; DMSO 34.5 ± 4.3; n=3. % of cell viability ± SEM in differentiated Caco-2 cells: control 101.4 ± 1.3; DMSO 28.3 ± 2.5; n=3).

4.7.2 Cell proliferation

Both bromelain and proteolytically inactive bromelain, significantly and in concentration depended manner, reduced the ^{3}H-thymidine incorporation in proliferating Caco-2 cells (Fig. 29A and 29B). The anti-proliferative effect was significant starting from the 3 µg/ml and 1 µg/ml concentration for bromelain and inactivated bromelain, respectively (Fig. 29A and 29B).

4.7.3 MAP kinase and phospho-Akt expression

The possible molecular mechanism of bromelain on cell proliferation was investigated by studying its effect on the mitogen-activated protein kinases (MAPK) and phosphoinositide 3-kinase (PI3K)/Akt signalling pathways. The MAPK pathway involves two closely related kinases, known as extracellular-

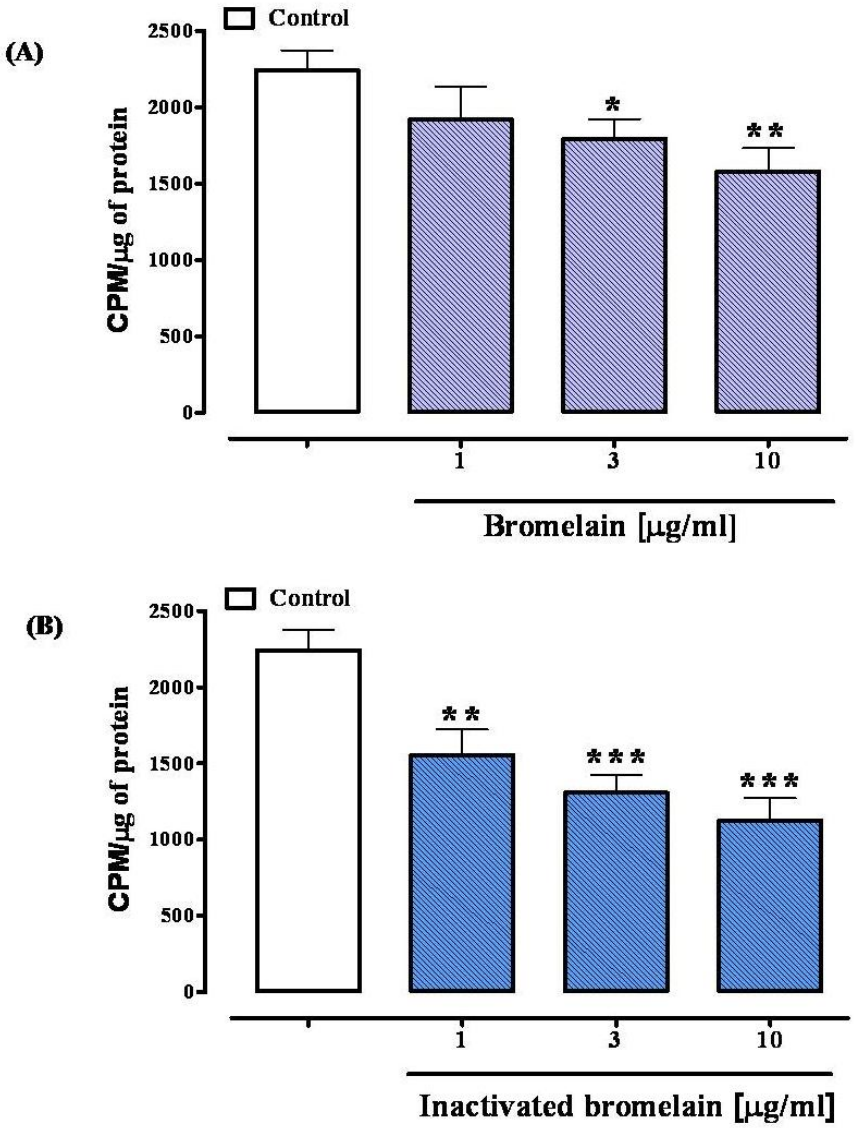

Figure 29. Antiproliferative effect of bromelain (1-10 µg/ml) (A) and inactivated bromelain (1-10 µg/ml) (B) in colorectal carcinoma (Caco-2) cells. Each bar represents the mean ± S.E.M. of three independent experiments. $^{*}p<0.05$, $^{**}p<0.01$ and $^{***}p<0.001$ *vs* control.

signal-related kinase 1 (ERK1, p44) and 2 (ERK2, p42) that come from dimerization of total cytosolic ERK. Bromelain (1-10 μg/ml) significantly and in concentration depended manner reduced the expression of phosphorylated ERK_1 ($pERK_1$) and ERK_2 ($pERK_2$) (Fig. 30A and 30B). The effect was significant starting from the 3 μg/ml concentration. Similarly, the expression of phosphoinositide 3-kinase was significantly reduced by bromelain (1-10 μg/ml) (Fig. 31).

4.7.4 Intracellular ROS levels

Hydrogen peroxide in the presence of iron (II) ions (Fenton's reagent, 2 mM), induced an oxidative stress in Caco-2 cells, resulting in an increased production of intracellular ROS (Fig. 32). Pre-incubation of Caco-2 cells for 24 hours with bromelain (1-10 μg/ml) reduced the production of cytosolic ROS levels induced by 2 mM H_2O_2/Fe^{2+} (Fig. 32). The effect was significant at the concentration of 10 μg/ml (Fig. 32).

4.8 Boeravinone G: antioxidant and genoprotective activities in Caco-2 cells

4.8.1 Cytotoxicity assay

Boeravinone G (0.1-1 ng/ml) did not affect Caco-2 cell survival (% cell survival: control 100±0, boeravinone G 0.1 ng/ml 97.2±4.21, boeravinone G 0.3 ng/ml 100.3±2.62, boeravinone G 1 ng/ml 99.7±3.69, n=6) nor it produce any increase in the release of LDH from Caco-2 cell line (% LDH leakage: control 11.5±0.51, boeravinone G 0.1 ng/ml 9.8±0.39, boeravinone G 0.3 ng/ml 10.4±0.46, boeravinone G 1 ng/ml 10.8±0.55, n=6).

4.8.2 Lipid peroxidation

Boeravinone G (0.1-1 ng/ml) significantly and in a concentration-related manner reduced H_2O_2/Fe^{2+} 1mM-induced TBARS formation in Caco-2 cells (Fig. 33).

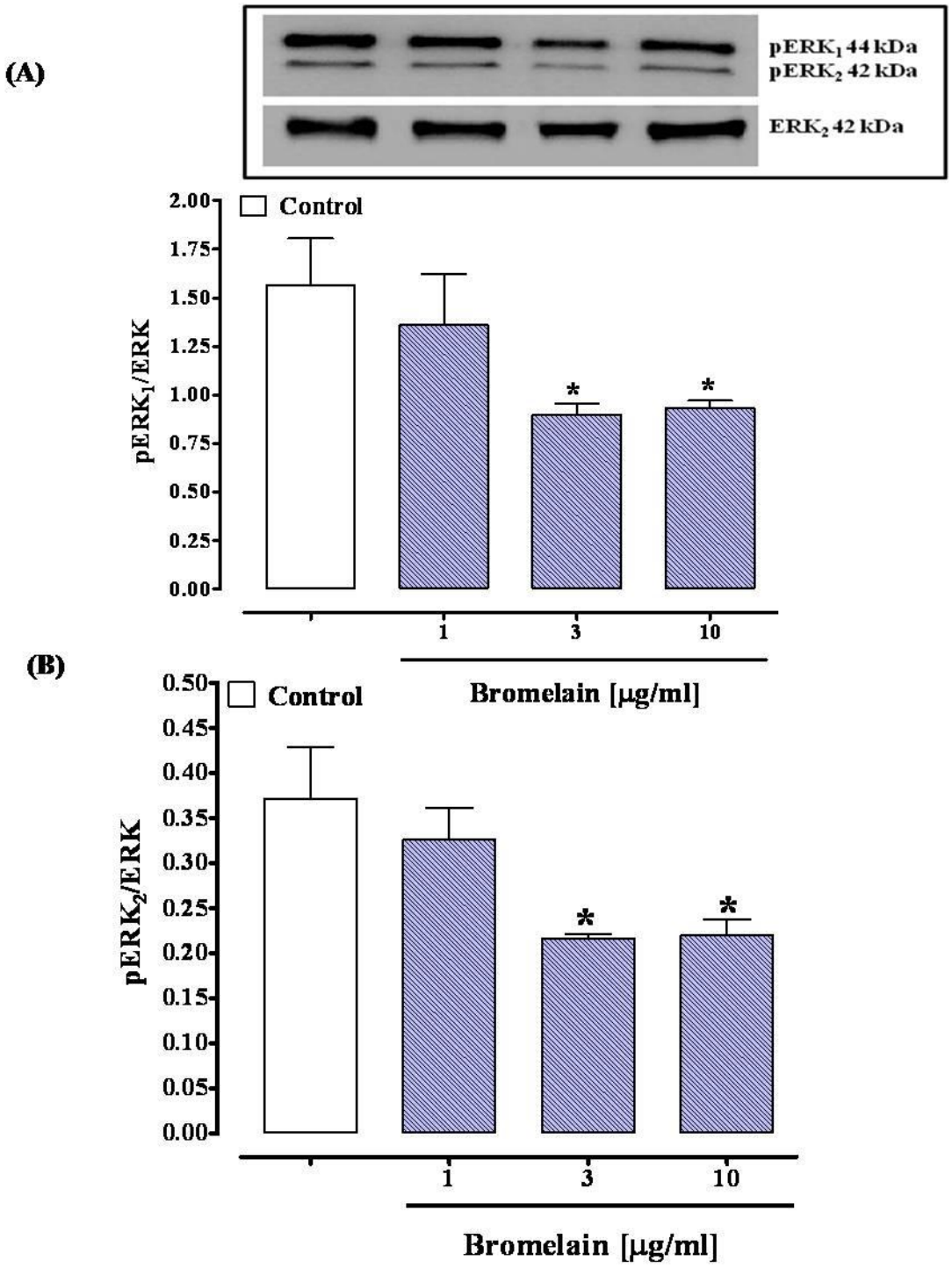

Figure 30. Phosphorylated ERK1 ($pERK_1$) (A) and ERK2 ($pERK_2$) (B) expression (MAP-kinase activation) in Caco-2 cells after 24 hours of bromelain (1-10 µg/ml) incubation. The insert shows a representative example of Western blot analysis. $^{*}p< 0.001$ versus control, n=3, mean ± S.E.M.

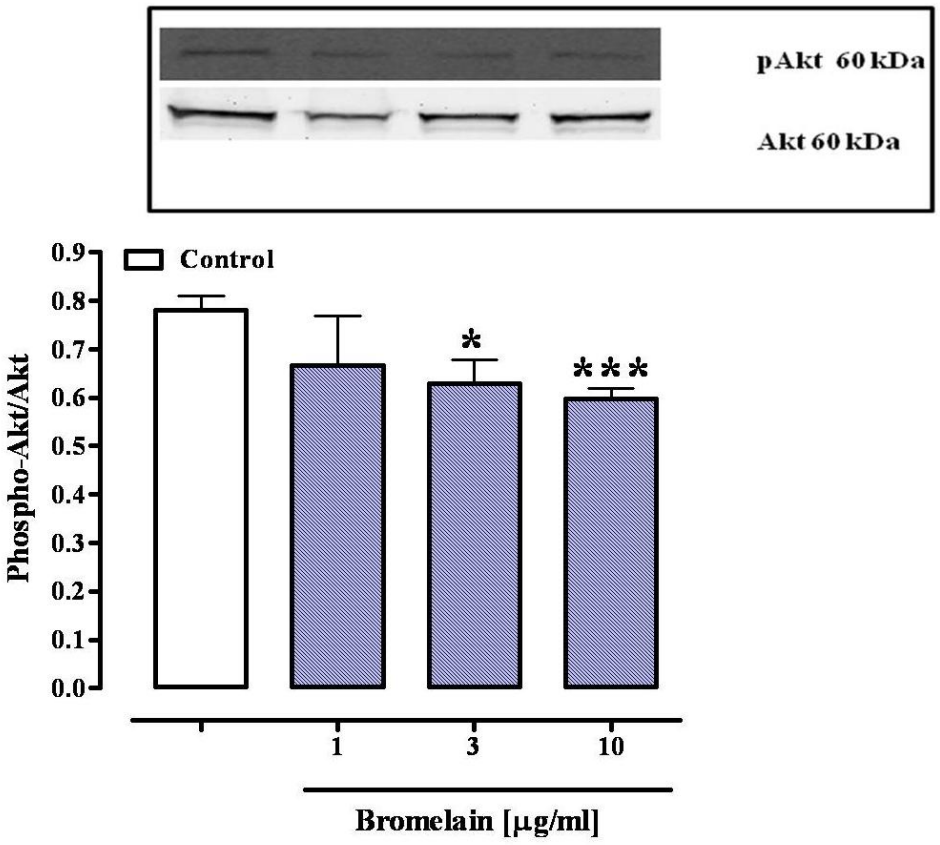

Figure 31. Phospho-Akt expression after 24 hours exposure with bromelain (1-10 μg/ml) in colorectal carcinoma (Caco-2) cells. The insert shows a representative example of Western blot analysis. *p< 0.05 and ***p<0.001 versus control, n=3, mean ± S.E.M.

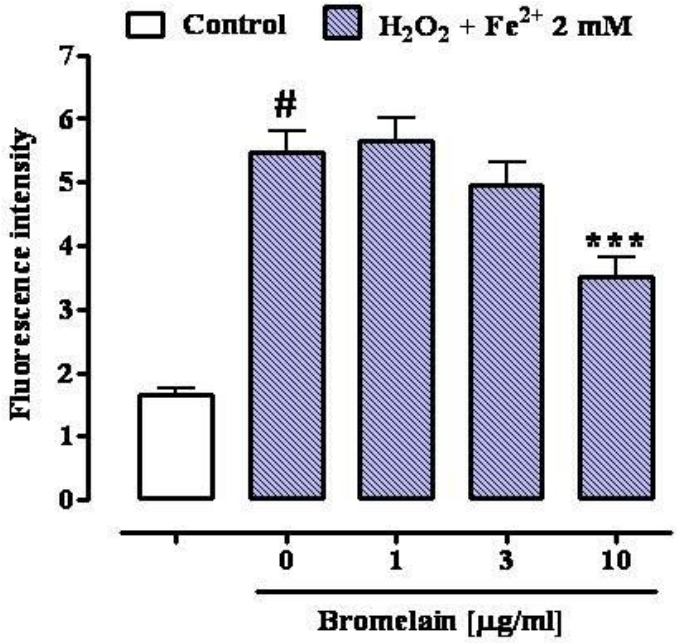

Figure 32. Effect of bromelain (1-10 µg/ml) on Fenton's reagent (H_2O_2/Fe^{2+} 2 mM)-induced reactive species (ROS) production in colorectal carcinoma (Caco-2) cells. Effect observed in differentiated Caco-2 cells after 24-hours bromelain exposure. Data represent mean ± S.E.M. of 6 experiments. $^{\#}p<0.001$ *vs* control; ***$p<0.001$ *vs* H_2O_2/Fe^{2+} alone.

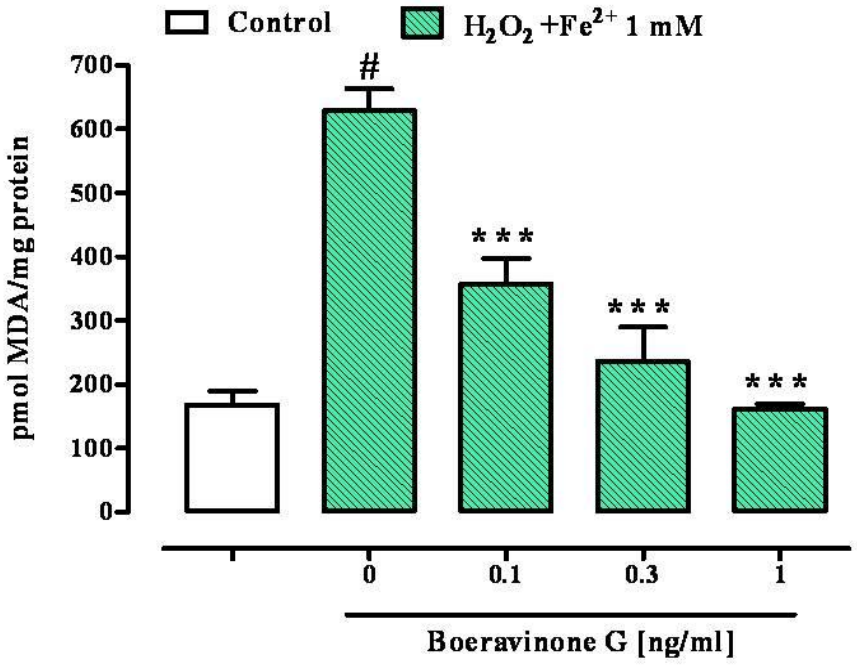

Figure 33. Effect of boeravinone G (0.1–1 ng/ml) on Fenton's reagent (H_2O_2/Fe^{2+} 1 mM)-induced malondialdehyde-equivalents (MDA-equivalents) production. Effect observed in differentiated Caco-2 cells after 24-hour boeravinone G exposure. Data represent mean ± SEM of 6 experiments. $^{\#}p<0.001$ *vs* control and $^{***}p<0.001$ *vs* H_2O_2/Fe^{2+} alone.

Boeravinone G given alone (i.e. in absence of H_2O_2/Fe^{2+} treatment), at all concentrations used, did not modify the TBARS levels (pmol MDA/mg protein: control 168.5±21.35, boeravinone G 0.1 ng/ml 175.8±13.54, boeravinone G 0.3 ng/ml 173.3±17.21, boeravinone G 1 ng/ml 171.8±14.16; n=6)

4.8.3 Intracellular ROS

Boeravinone G (0.1-1 ng/ml), concentration-dependently, reduced the formation of ROS induced by H_2O_2/Fe^{2+} 2mM in Caco-2 cells (Fig. 34). Boeravinone G (0.1-1 ng/ml), given alone (i.e. in absence of H_2O_2/Fe^{2+} treatment), did not affect the formation of ROS (Fluorescence intensity: control 2.45±0.09, boeravinone G 0.1 ng/ml 2.45±0.14, boeravinone G 0.3 ng/ml 2.36±0.17, boeravinone G 1 ng/ml 2.42±0. 09; n=6).

4.8.4 DNA damage (Comet assay)

Exposure of the Caco-2 cells to H_2O_2 (75 μM) produced a significant DNA damage (Fig. 35), expressed as comet tail intensity. Boeravinone G (0.1-1 ng/ml) significantly and in a concentration dependent manner reduced the DNA damage induced by H_2O_2 (Fig. 35). Consistent with the TBARS assay, a significant inhibitory effect was achieved for the 0.1-1 ng/ml boeravinone G concentrations. Boeravinone G (0.1-1 ng/ml) did not produce DNA damage detected by the Comet assay in Caco-2 cells not treated with H_2O_2 (% tail intensity: control 5.37±0.26, boeravinone G 0.1 ng/ml 5.29±0.19, boeravinone G 0.3 ng/ml 5.21±0.22, boeravinone G 1 ng/ml 5.32±0.25; n=4). These results are suggestive of a lack of genotoxic effect.

4.8.5 Superoxide dismutase (SOD) activity

Boeravinone G (0.1-1 ng/ml), used alone (i.e. in absence of H_2O_2/Fe^{2+} treatment), did not modify the activity of SOD in Caco-2 cells [SOD activity (ng/mg protein): control 17.7±0.64, boeravinone G 0.1 ng/ml 18.02±0.90, boeravinone G 0.3 ng/ml

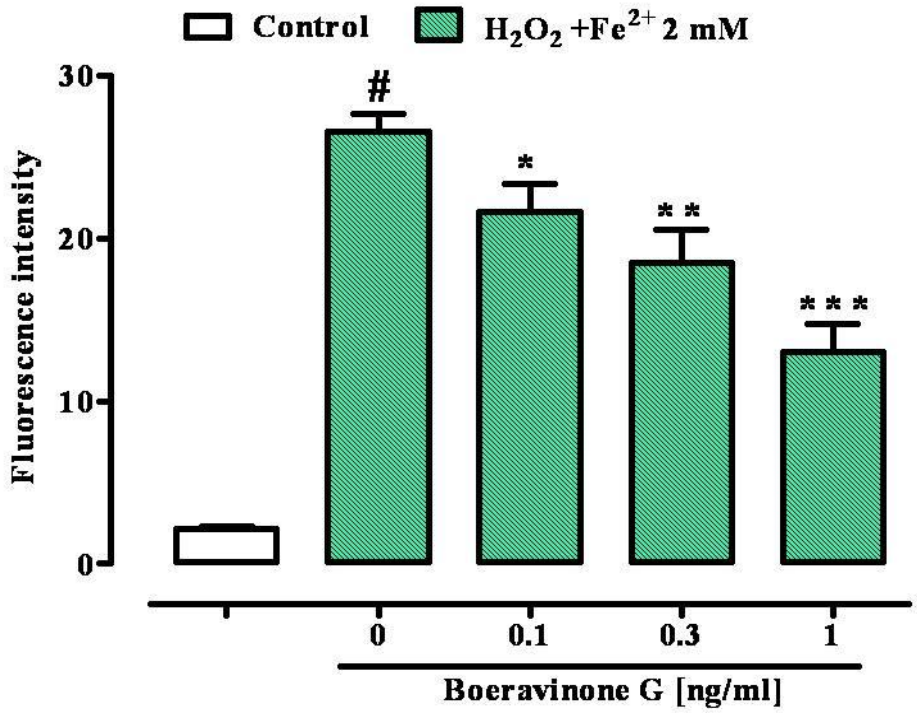

Figure 34. Effect of boeravinone G (0.1–1 ng/ml) on Fenton's reagent (H_2O_2/Fe^{2+} 2 mM)-induced reactive species (ROS) production. Effect observed in differentiated Caco-2 cells after 24-hour boeravinone G exposure. Data represent mean ± SEM of 6 experiments. $^{\#}p<0.001$ *vs* control (vehicle); $^{*}p<0.05$, $^{**}p<0.01$ and $^{***}p<0.001$ *vs* H_2O_2/Fe^{2+} alone.

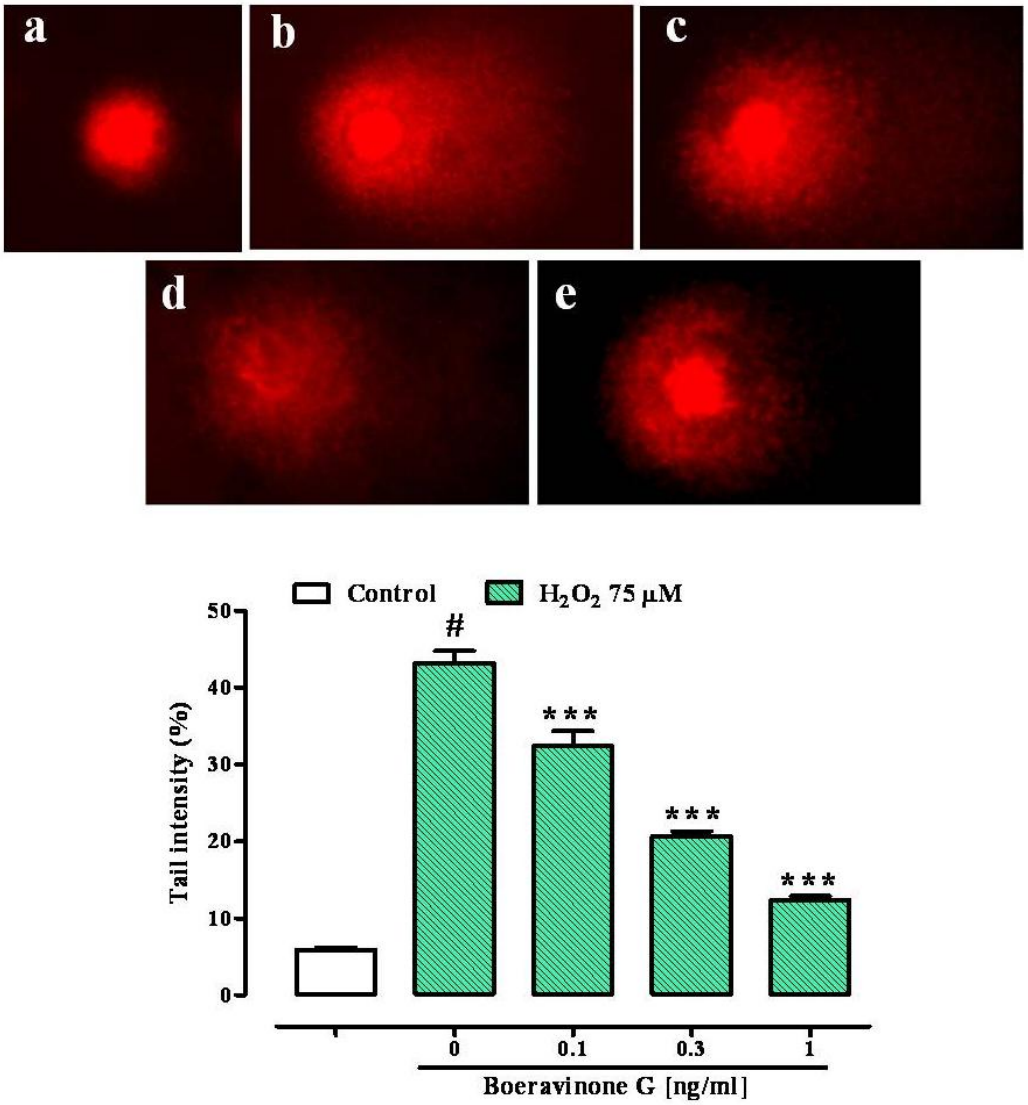

Figure 35. Effect of boeravinone G (BG, 0.1–1 ng/ml) on DNA damage. DNA damage (tail intensity) was detected by the Comet assay in Caco-2 cells exposed to 75 µM H_2O_2 for 5 min in absence or presence of boeravinone G. a = control; b = H_2O_2 75 µM; c = H_2O_2 75 µM+BG 0.1 ng/ml; d = H_2O_2 75 µM+BG 0.3 ng/ml; e = H_2O_2 75 µM+BG 1 ng/ml. Data represent mean ± SEM of 4 experiments. $^{\#}p<0.001$ *vs* control and $^{***}p<0.001$ *vs* H_2O_2 alone.

17.86±0.96, boeravinone G 1 ng/ml 17.2±0.79; n=6]. However, twenty four hours exposure of Caco-2 cells to H_2O_2/Fe^{2+} (1mM) produced a significant decrease in SOD activity which was concentration-dependently counteracted by boeravinone G (Fig. 36). Interestingly, at the 1 ng/ml concentration of boeravinone G, SOD was significantly increased compared to control.

4.8.6 Phosphorylated ERK_1 ($pERK_{1/2}$) and phospho- nuclear-factor kappa B (NF-kB) p65 expressions

Fenton's reagent (H_2O_2/Fe^{2+} 1 mM) elicited a significant increase in the levels of phosphorylated ERK1 (pERK1), ERK2 (pERK2) and NF-kB p65 (Fig. 37 and 38). Boeravinone G (at 0.3 and 1 ng/ml) significantly reduced the levels of pERK1 and phospho-NF-kB p65 (Fig. 37A). Surprisingly, at the lower concentration of boheravinone G tested (i.e., 0.1 ng/ml), an increased level of both pERK1 and phospho-NF-kB p65 was observed (Fig. 37A and 38). By contrast, boeravinone G, at all the concentration evaluated (0.1-1 ng/ml), did not affect H_2O_2/Fe^{2+}-induced $pERK_2$ up-regulation (Fig. 37B).

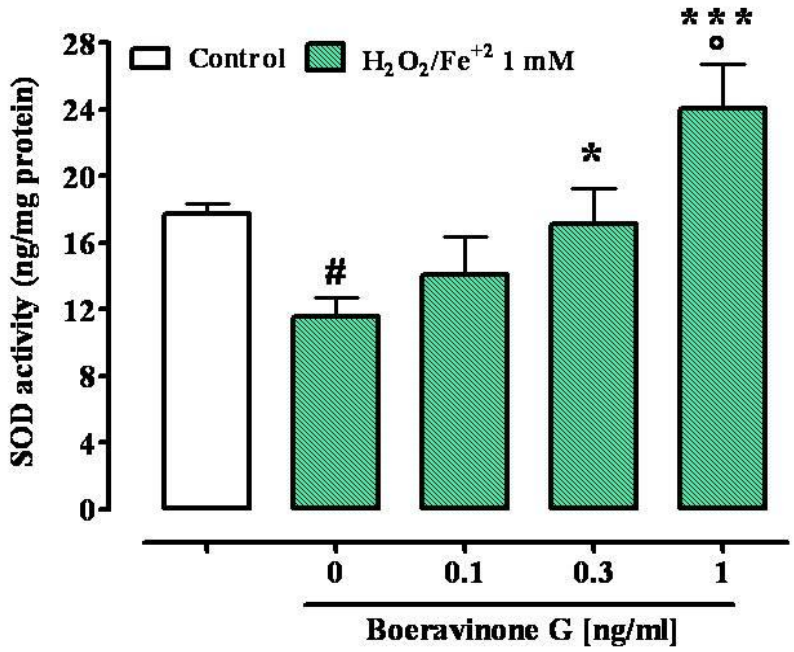

Figure 36. Effect of boeravinone G (0.1–1 ng/ml) on superoxide dismutase (SOD) activity. SOD activity was evaluated in Caco-2 cells exposed to Fenton's reagent (H_2O_2/Fe^{2+} 1 mM) without or with boeravinone G (0.1–1 ng/ml). Data represent mean ± SEM of 4 experiments. $^{\#}p<0.001$ *vs* control (vehicle); $^{*}p<0.05$ and $^{***}p<0.001$ *vs* H_2O_2/Fe^{2+} alone; $^{\circ}p<0.05$ *vs* control.

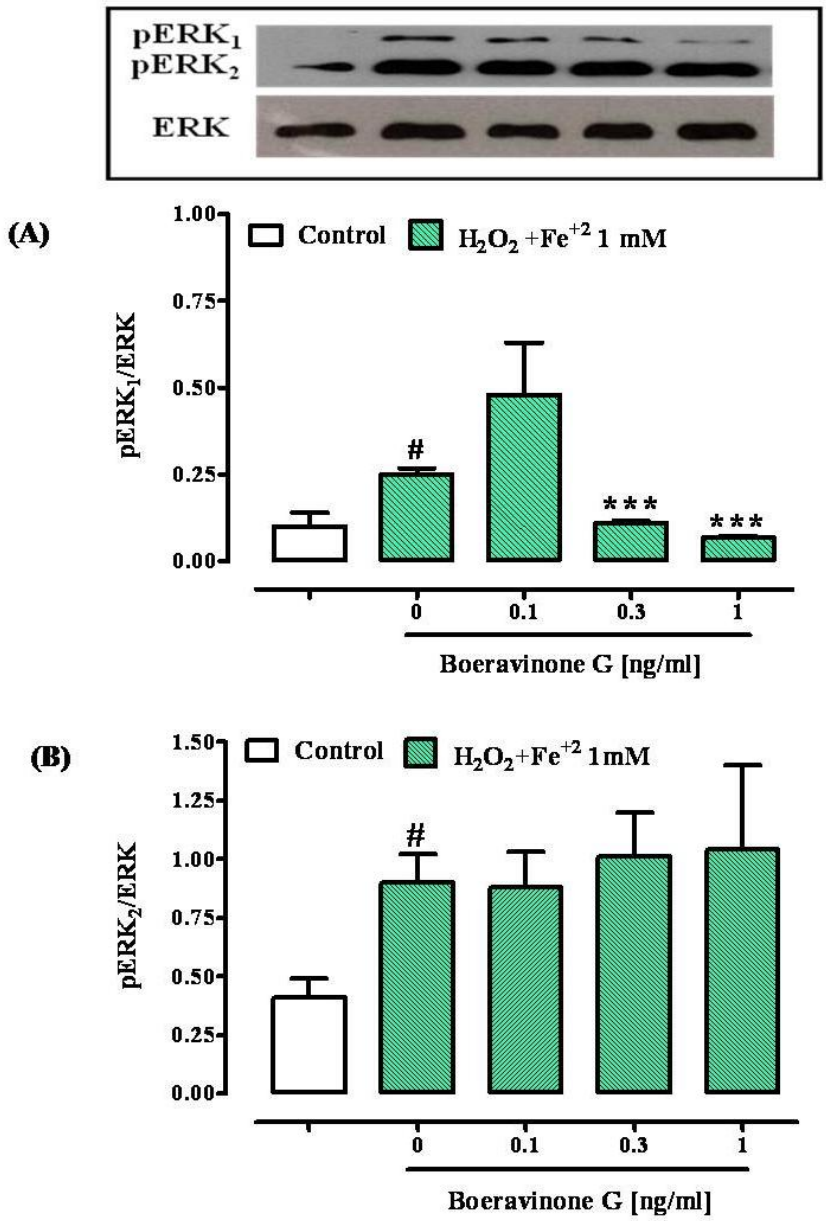

Figure 37. Effect of boeravinone G (0.1–1 ng/ml) on $pERK_1$ (A) and $pERK_2$ (B) expression**.** Quantitative analysis and representative western blot analysis of $pERK_1$ and $pERK_2$ in Caco-2 cells exposed to Fenton's reagent (H_2O_2/Fe^{2+} 1 mM) without or with boeravinone G (0.1–1 ng/ml). The results were normalized with anti-ERK_2 ($pERK_{1/2}/ERK_2$). $^{\#}p<0.01$ *vs* control; ***$p<0.001$ *vs* H_2O_2/Fe^{2+} alone

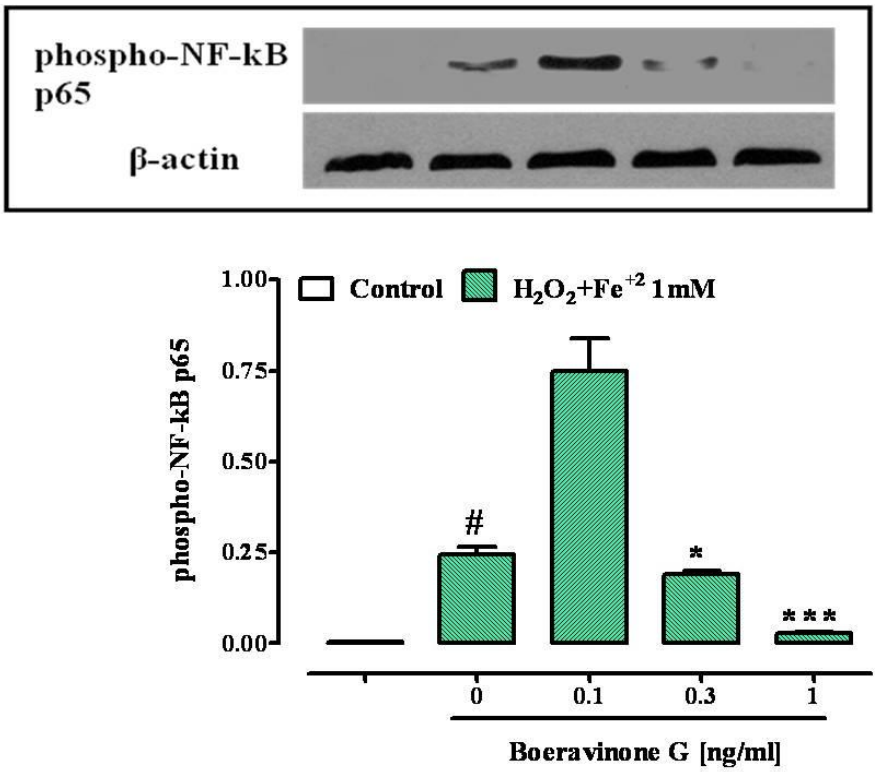

Figure 38. Effect of boeravinone G (0.1–1 ng/ml) on phospho-NF-kB p65 expression. Quantitative analysis and representative western blot analysis of phospho-NF-kB p65 in Caco-2 cells exposed to Fenton's reagent (H_2O_2/Fe^{2+} 1 mM) without or with boeravinone G (0.1–1 ng/ml). The results were normalized with anti-βactin antibodies. $^{\#}p<0.001$ *vs* control; $^{*}p<0.05$ and $^{***}p<0.001$ *vs* H_2O_2/Fe^{2+} alone.

5.0 DISCUSSION

Inflammatory bowel disease and colorectal cancer are widespread diseases which affect millions of persons worldwide. Despite the progress in pharmacotherapy, preventive measures and cures are still unsatisfactory. Thus, there is an urgent need for safe and effective therapeutics. In the present study we have evaluated a number of compounds in experimental models of IBD and CRC. These include cannabigerol, a non-psychotropic cannabinoid from *Cannabis sativa*, DAS and DADS, two organosulfur compounds from *Allium sativum*, bromelain, a cysteine protease from *Ananas comosus* and Boeravinone G, a rotenoid isolated from the Ayurvedic plant *Boerhaavia diffusa*. A detailed discussion of the results obtained for each compound is reported below.

5.1 Cannabigerol

Anecdotal and scientific evidence suggests that *Cannabis* use may relieve the symptoms of patients with IBD (Naftali et al., 2011; Lahat at al., 2012; Leyon et al., 2005). The effects of Δ^9-THC and CBD, i.e. the best studied among *Cannabis* ingredients, on experimental models of IBD has been previously documented (Borrelli et al., 2009; Jamontt et al. 2010). We have here demonstrated that CBG exerts preventive and curative effects in the DNBS model of colitis. *In vitro*, CBG attenuates both nitrite production in macrophages and ROS production in intestinal epithelial cells.

We have found that CBG reduced colon weight/colon length *ratio* of the inflamed colonic tissue, which is considered a reliable and sensitive indicator of the severity and extent of the inflammatory response (Gálvez al., 2000). CBG was effective when given both before and after the inflammatory insult, suggesting a preventive and a curative (therapeutic) beneficial effect. Significant protective effects were achieved starting from the 1 mg/kg dose (preventive protocol) and 5

mg/kg (curative protocol). Maximal efficacy was achieved with the 1 mg/kg dose and the 30 mg/kg dose in the preventive and in the curative protocol, respectively. Because the main goal in IBD is to cure rather than to prevent, we performed further studies (histological analysis, immunoistochemistry, neutrophil infiltration, intestinal membrane integrity as well as cytokines and enzymes assay) by evaluating the effect of CBG (given after the inflammatory insult., i.e. as a curative treatment) and at the most effective dose of 30 mg/kg. Thus, histological examination showed that CBG 30 mg/kg reduced the signs of colon injury; specifically, in the colon of CBG-treated animals, the glands were regenerating, the oedema in submucosa was reduced and the infiltration of granulocytes into the mucosa and submucosa was reduced. The curative effect of CBG was further demonstrated by its capacity to abrogated the increase in intestinal permeability induced by DNBS treatment. Furthermore, immunohistochemical analysis demonstrated that CBG limited the colonic diffusion of Ki-67, a useful marker for the evaluation of dysplasia in ulcerative colitis (Andersen et al., 1998).We also measured some cytokines which are known to be involved in IBD (Madsen et al., 2002), namely IL-10 (an anti-inflammatory cytokine) as well as IL-1β and IFN-γ (two pro-inflammatory cytokines) (Strober et al., 2011; Barbara et al., 2000; Ito et al., 2006) We found that CBG counteracted the colonic variations of the three cytokines induced by DNBS, thus suggesting the possible involvement of these molecules in CBG-mediated intestinal anti-inflammatory effects. Finally, we demonstrated that CBG counteracted the increase in the expression of iNOS (induced by DNBS), a key enzymes involved in the pathogenesis of IBD (Kolios et al., 2004). Because we have shown that CBG inhibits iNOS expression in the inflamed intestine and considering that activated macrophages, which express

iNOS, play a major role in IBD (Palmer et al., 1988), we evaluated the effect of CBG on nitric oxide production in these cells.

Stimulation of murine macrophages by LPS results in the increased expression of iNOS, enzyme which catalyses the formation of large amounts of NO from the aminoacid L-arginine (Moncada et al., 1997). CBG reduced the expression of iNOS and the levels of nitrites, the stable metabolites of NO, with a maximal inhibitory effect achieved at the 0.1 and 1 μM concentrations. These concentrations can be easily reached in the plasma after *in vivo* administration of the phytocannabinoid, since it has been demonstrated that ip administration of CBG (120 mg/kg) yields a peak plasma value of 373 μM (Deiana et al., 2012). Because CBG is a weak cannabinoid (CB_1 and CB_2) receptors partial agonist and also inhibits the reuptake of endocannabinoids (Cascio et al., 2010; De Petrocellis et al., 2011; Pollastro et al., 2011), we investigated the possible role of these receptors by evaluating: 1) the effect of selective CB_1 and CB_2 receptor antagonists on CBG-induced inhibition of nitrite production induced by LPS, and 2) possible alterations in cannabinoid receptors mRNA produced by CBG in LPS-challenged macrophages. Surprisingly, we observed that the inhibitory effect of CBG was further increased by a selective CB_2 receptor antagonist (i.e. SR144528), at concentrations that, however, were inactive per se. These results, whilst demonstrating that exogenous activation of CB_2 reduces NO formation in macrophages, negate the possibility that CBG acts via this mechanism, and instead suggest that an endogenous CB_2 tone may exist, which may couple negatively to the CBG signalling pathway and counteract CBG inhibition of nitrite production. Also, we cannot rule out the possibility the CBG and the CB_2 receptor antagonist SR144528, which exerts anti-inflammatory effects in some experimental conditions (Pollastro et al., 2011) may act in an additive/synergistic

way to reduce nitrite production. When we verified if CBG changed the expression of CB_1 and CB_2 receptors, as it is the case for the phytocannabinoid cannabichromene (Izzo et al., 2012), we found that CBG did not modify the effect of LPS on cannabinoid receptors.

Finally, we explored the possibility that CBG could protect the intestinal mucosa by reducing oxidative stress. The impairment of antioxidant defence of intestinal epithelial cells leading to oxidative stress is a critical event in the development of inflammation in the gut (Xavier et al., 2007). We measured SOD activity, an important antioxidant defence in the gut (Watterlot et al., 2010) and ROS production, a major tissue-destructive force contributing significantly to the pathogenesis of IBD (Kruidenier et al., 2002). We found here that CBG restored the decreased SOD activity induced by DNBS administration in colonic tissues as well as reduced ROS production induced by Fenton's reagent in mouse intestinal epithelial cells.

In summary, our study demonstrated that CBG exerts beneficial actions in the DNBS model of colitis in mice. The effect of CBG was associated to modulation of intestinal cytokine levels and down-regulation of intestinal iNOS expression. Studies on peritoneal macrophages suggest that CBG inhibits iNOS-derived nitric oxide production. Also, CBG protects intestinal epithelial cells exposed to oxidative stress. Both the antioxidant action and the inhibitory action on iNOS-derived NO production might contribute to the protective action of CBG observed *in vivo.*

5.2 Bromelain

We have here evaluated the effect of bromelain in a model of intestinal dysfunction associated to intestinal inflammation as well as in an experimental model of colon cancer. Previous investigators have shown that bromelain

decreases colonic inflammation in experimental models of colitis and decreases the secretion of pro-inflammatory cytokines and chemokines in human colon biopsies obtained from patients with IBD (Onken et al., 2008; Hale et al., 2005). Since the effect, of bromelain on intestinal inflammation are well-established, we investigated here its effect on motility in a mouse model of intestinal inflammation. We used the irritant compound croton oil, which has been extensively studied to induce hypermotility associated to inflammation in mice (Borrelli et al., 2006; Capasso et al., 2001; Pol et al., 1997). We found that bromelain was more potent in reducing transit in the model of intestinal inflammation induced by croton oil than in healthy animals. Also, bromelain was more active after ip than after oral administration. This is not surprising since bromelain is a proteolytic enzyme that is mostly destroyed by gastric acid. We also found that the inhibitory effect of bromelain on intestinal transit, was reverted by ENMD-1068, a PAR-2 receptor antagonist. It is very unlikely that the higher potency of bromelain in the inflamed gut is due to PAR-2 hyper-expression because we found, in accordance to other studies (Sato et al., 2006), a down-regulation of such receptor in the inflamed intestine. Further studies are needed to verify if the decreased PAR-2 protein expression is due to proteolysis or to changes in mRNA expression. Because the effect of bromelain *in vivo* was counteracted by a PAR-2 antagonist, we investigated the possibility that this cysteine protease might directly activate such receptors. Because activation of PAR-2 results in an increase in $[Ca^{2+}]_i$, we performed further experiments in order to evaluated the effect of bromelain on $[Ca^{2+}]_i$. We found that bromelain increased $[Ca^{2+}]$ in Caco-2 cells (one of the assays to evaluate PAR-2 activation) and this effect was reduced by the selective PAR-2 antagonist ENMD-1068. Collectively, such results suggest that bromelina activates PAR-2. In support to

these conclusions, others have recently shown that bromelain, as well as other cysteine proteases such as ficin and papain, activates PAR-2 receptors as determined by [Ca^{2+}] mobilization in HeLa cells (Reddy et al., 2010).

Next, we investigated the effect of bromelain in experimental colon carcinogenesis. Several animal and human studies indicates that bromelain might have some anticancer activity (Maurer et al., 2001; Pavan al., 2012), but its possible chemopreventive action against gastrointestinal tumours has been not explored to date. Because previous investigators have shown the efficacy of IP-administered bromelain in experimental cancer (Beuth et al., 2005; Chobotova et al. 2010) and because most proteins administered orally without enteric protection are hydrolysed by gastric acid and/or proteinases, we have used the ip route of administration. We have here shown that bromelain (1 mg/kg) prevented the formation of preneoplastic lesions, polyps and tumours induced in the mouse colon by the administration of the carcinogenic agent AOM. The 1 mg/kg bromelain dose in mice is about 30-40 fold lower than the documented lethal dose of bromelain after ip administration (Maurer et al., 2001)

In order to investigate bromelain mode of action, we performed experiments in colorectal carcinoma Caco-2 cells. Previous investigators have shown that bromelain exerted antiproliferative effects in different tumour cell lines, including gastric carcinoma cells, glioblastoma cells, ovarian cancer cells and breast cancer cells (Maurer et al., 2001; Pavant al., 2012). In the present study we have shown that bromelain, at non-cytotoxic concentrations, reduced cell proliferation in Caco-2 cells. Because the proteolytic action has been supposed to be responsible of many of its pharmacological activities (Maurer et al., 2001; Pavant al., 2012), we analyzed the effect of inactivated bromelain on Caco-2 cell proliferation. We found that the antiproliferative action of bromelain was not related to its

proteolytic activity, since proteolytically inactive bromelain also exerted antiproliferative actions.

In order to further investigate the action of bromelain, we analyzed two pathways which are essential in the regulation of tumoural cell growth, i.e. phosphoinositide 3-kinase (PI3K)/Akt and MAP kinase pathways (Weigelt et al. 2012; Efferth et al., 2012). Our results showed that bromelain down-regulated Akt, ERK_1 and ERK_2 phosphorylation in Caco-2 cells suggesting a possible involvement of such pathways in the bromelain action. Specifically, bromelain seems to promote apoptotic cell death in tumoural cells and to reduce cell proliferation of tumoural cells by inhibiting AKT and $ERK_{1/2}$ phosphorylation, respectively. Our results are in agreement with previous observations which reported an inhibitory effect of bromelain on the activity of cell survival regulators such as Akt and ERK (Kalra et al., 2008; Mynott et al., 1999).

We also evaluated the effect of bromelain on oxidative stress, which represent a critical event in the development of gastrointestinal tumours (Birben et al., 2012).

In conclusion, we have shown that bromelain inhibits intestinal hypermotility due to an inflammatory stimulus as well as exerts chemopreventive actions against colon carcinogenesis *in vivo* and antiproliferative actions in colorectal carcinoma cells. The effect of bromelain on intestinal motility could be due to its ability to activate PAR-2, as revealed by its ability to increase $[Ca^{2+}]i$ – in a PAR-2 antagonist-sensitive manner – in intestinal epithelial cells. The antitumoural action of bromelain could be related to inhibition of tumoural cell proliferation as well as to stimulation of apoptotic processes by blocking the MAP kinase and (PI3K)/Akt signaling.

5.3 Diallyl sulfide (DAS) and diallyl disulfide (DADS)

DAS and DADS, two garlic-derived organosulfur compounds have been previously reported to exert anti-inflammatory effects (Lee et al., 2009; Kalayarasan et al., 2009; Woo et al., 2007). Moreover, DADS has been reported to prevent the intestinal damage induced by endotoxin in rats (Chiang et al., 2006). Here, we report that DAS and DADS exert curative effects in the DNBS model of colitis and also reduce the levels of cytokines and chemokines induced by IFN-γ in isolated intestinal epithelial cells.

We have found that DAS and DADS, administered orally after the administration of the inflammatory stimulus, reduced the decrease in body weight associated to DNBS administration, thus suggesting a beneficial effect of these compounds on the overall mice health. The curative effects of DAS and DADS was further demonstrated by their ability to reduce colon weight/colon length *ratio* of the inflamed colonic tissue, a simple and reliable indicator of intestinal inflammation. Significant effects were achieved starting from the 1 mg/kg dose for both compounds. Notably, the doses of DAS and DADS able to exert curative effects (1 mg/kg corresponding to 0.007 mmol/kg) is lower than the dose previously shown to prevent the intestinal damage induced by endotoxin (0.025 mmol/kg) (Chiang et al., 2006). Because the most effective dose of DAS and DADS was the 10 mg/kg dose, we performed histological and immunohistochemical analyses using colons of mice treated with the 10 mg/kg dose. Histological examination showed that both DAS and DADS reduced the signs of colon injury; specifically, in the colon of DAS- or DADS- treated animals, the glands were regenerating and the oedema in mucosa and submucosa was reduced. A further demonstration of the beneficial effect of DAS and DADS comes from the immunohistochemical analysis, which showed a reduced colonic diffusion of IP-10 (a member of the CXC chemokine family) in the inflamed gut of animals treated with DAS or

DADS. It has been reported that the expression of IP-10 is elevated in patients with ulcerative colitis, suggesting its possible use as a marker for ulcerative colitis severity (Banks et al., 2003). Furthermore, the importance of IP-10 as a pro-inflammatory mediator in IBD has been also demonstrated by experimental studies reporting the ability of anti-IP-10 antibodies to decrease inflammation in several experimental models of colitis (Hyun et al., 2005; Suzuki et al., 2007).

In order to further investigate the effect of DAS and DADS on intestinal inflammation, we performed some experiments in intestinal epithelial (Mode-K) cells activated by IFN-γ. Intestinal epithelial cells are crucial for maintaining intestinal homeostasis (Artis, 2008) and failure to control inflammatory processes at the epithelial cell level may critically contribute to ulcerative colitis pathogenesis. Intestinal epithelial cells react on bacterial as well as immune-derived pro-inflammatory signals by secreting cytokines and chemokines like IL-6 and IP-10 to activate and attract Th1-immune cells and phagocytic cells to the site of infection (Hoermannsperger et al., 2009). We have observed that stimulation of Mode-K cells with IFN-γ resulted in increased levels of IP-10 and IL-6. DADS (but not DAS), at the concentration of 50 μM, reduced the levels of IP10 and IL-6. The inhibitory effect of DADS on IFN-γ-induced IP-10 levels was associated to down-regulation of IP-10 mRNA. The lack of efficacy of DAS to reduce IP10 and IL-6 levels remain to be investigated. By contrast, DAS (but not DADS) was able to reduce IFN-γ-stimulated nitrite production. The lack of effect of DADS on nitrite production is in accordance with other studies reporting no significant effect of DADS on endotoxin-induced nitrite levels in the rat intestinal mucosa (Chiang et al., 2006).

In conclusion, we have shown that orally-administered garlic-derived DAS or DADS exerts therapeutic actions in the DNBS model of IBD, as revealed by

macroscopic evaluation, histology and immunohistochemistry. In intestinal epithelial cells, DADS reduced IP-10 and IL-6 levels, while DAS inhibited IFN-γ-stimulated nitrite production.

5.4 Boeravinone G

We have found that boeravinone G, among a number of rotenoids extracted from *Boerhaavia diffusa,* possesses remarkable antioxidant properties in intestinal epithelial cells. These results are potentially relevant because free radicals have been implicated in the aetiology of various human gastrointestinal disorders such as IBD and CRC (Willcox et al., 2004; Sachidanandam, 2005; Dryden et al., 2005; Bickers and Athar, 2006; Rahman et al. 2006). Further, we showed that boeravinone G protected the DNA from an oxidative insult, which is of interest because DNA damage is a crucial step in carcinogenesis and oxidatively-derived DNA lesions have been observed in many tumours (Hart et al., 2012).

Using the Caco-2 cell line and H_2O_2 as a free radical generator, we evaluated the effect of boeravinone G on lipid peroxidation (assessed as MDA-equivalents) and ROS production. Lipid peroxidation is a complex process occurring in biological membranes that contain oxidation-susceptible polyunsaturated fatty acids, and leading to the production of lipid hydroperoxides and their metabolites (Ramasarma, 2012). The cytosolic levels of malondialdehyde and its reactive equivalents are adequate indicators of lipid peroxidation. In the present study, we have demonstrated that boeravinone G reduced the TBARS levels and ROS formation generated by the Fenton's reagent. Importantly, the antioxidant activity of boeravinone G occurred at nanomolar concentrations, while other well known antioxidant compounds, such as vitamins C and E exert antioxidant activity in the micromolar range (Esterbauer and Cheeseman, 1990; Rego, 1999). We also

evaluated the potential genoprotective effect of boeravinone G on ROS-induced DNA damage. It is well known that ROS damages DNA, which appears to represent the major target involved in mutagenesis, carcinogenesis and aging cell responses (Anderson and Phillips, 1999; Nakabeppu et al., 2006). DNA damage, induced by using H_2O_2, was evaluated by the Comet assay, which is a very sensitive method for the evaluation of genotoxic/genoprotective effects (Karihtala et al., 2007). Our experiments showed that boeravinone G was able to reduce H_2O_2-induced DNA damage. We thus hypothesise that the protective action of boeravinone G, assessed by the TBARS and the ROS assays (see above), could be related to its ability to protect DNA from an oxidative insult .

In order to investigate the potential targets involved in the boeravinone G antioxidant/genoprotective action, we have analyzed the effect of this plant ingredient on an antioxidant defence enzyme (SOD) and on two signal transduction pathways (MAP kinase and NF-kB) that play a pivotal role in the oxidative stress-induced gastrointestinal disorders (Collins et al. 2004; Kim et al., 2005). SOD is one of the most effective intracellular enzymatic antioxidants and it acts catalyzing the dismutation of superoxide into oxygen and hydrogen peroxide. According to previous work (Valko et al., 2006; Liu et al., 2005), we have shown a significant decrease in SOD activity in intestinal epithelial cells treated with H_2O_2/Fe^{2+}. Boeravinone G counteracted the decreased SOD activity thus suggesting a stimulatory effect of this compound on the defence mechanisms of the cells.

When the generation of ROS exceeds the capability of the cellular defence systems, several signalling protein kinases and transcription regulatory factors are activated (Collins et al. 2004; Kim et al., 2005; Goldstone et al., 2006). Indeed, oxidative stress leads to activation of extracellular-signal-related kinases (ERKs)

(Conde de la Rosa et al., 2006; Aikawa et al., 1997), which are members of the mitogen-activated protein kinase (MAPK) family, and nuclear factor kB (NF-kB) (Kulich et al., 2003). We have observed that boeravinone G, at the concentrations of 0.3 and 1 ng/ml, counteracted the increased ERK phosphorylation induced by H_2O_2/Fe^{2+}-exposure. Surprisingly, the effect of boeravinone G on the ERK phosphorilation was significant only for the 44-kDa isoform $pERK_1$ (and not for the $pERK_2$ isoform) suggesting a selectivity of action. A differential role for the two kinases in cell signalling has been previously documented (Kefaloyianni et al., 2006). The down-regulation in ERK phosphorylation after boeravinone G exposure is consistent with the observed effect of this compound on SOD activity. Indeed, it is well known the strictly correlation existing between Cu-Zn SOD enhancement and ERKs phosphorilation inhibition (Vantaggiato et al., 2006). Similarly, we have found an increase in phosphorylated NF-kB p65 levels in differentiated Caco-2 cells during the oxidative stress and such increase was counteracted by boeravinone G, thus suggesting an involvement of this pathway in the boeravinone G antioxidant activity.

Since boeravinones belong to the chemical class of rotenoids, widely used as botanical insecticides and generally characterized by high toxicity (Shi et al., 2004), we carried out additional experiments to ensure that boeravinone G, at the concentrations used in our experiments, did not exert any toxic effects. Cytotoxicity was assessed quantitatively by both MTT and LDH assays. We observed no decrease in the cell viability and no increase of LDH release when Caco-2 cells were incubated in the presence of boeravinone G. Moreover, the lack of boeravinone G toxicity has also been demonstrated by the Comet assay since the rotenoid, administered alone (i.e. in absence of damage induced by H_2O_2) did

not affect DNA integrity. Collectively, these results suggest that boeravinone G was neither cytotoxic nor genotoxic in Caco-2 cells.

In conclusion, we have shown that boeravinone G exerts potent antioxidant/genoprotective actions. The genoprotective effect of boeravinone G was associated to up-regulation of $pERK_1$ and NF-kB levels. In the light of the importance of antioxidant/genoprotective activity in the treatment or prevention of gut disorders, such as IBD and colon cancer, these results can be regarded as the initial step for a future *in vivo* evaluation using well-established animal models of IBD and CRC.

6.0 CONCLUSIONS

Plants have a long history of use in the treatment of gastrointestinal diseases, including IBD and CRC. Our study further supports the concept that the plant kingdom may by a source of novel compounds with potential therapeutic activity in such widespread diseases. Specifically, we have shown that:

1. Cannabigerol (CBG), a non psychotropic cannabinoid extracted from the marijuana plant *Cannabis sativa*, exerts therapeutic actions in the model of murine colitis induced by DNBS. The effect of CBG was associated to modulation of intestinal cytokine levels and down-regulation of intestinal iNOS expression, the latter result confirmed in isolated peritoneal macrophages. Also, CBG protects intestinal epithelial cells exposed to oxidative stress. Both the inhibitory action on iNOS and its antioxidant action might contribute to the protective action of CBG.

2. Diallyl sulfide (DAS) and diallyl disulfide (DADS), from *Allium sativum*, exert beneficial actions in the DNBS model of IBD. Both compounds reduced inflammation and damage, as revealed by gross evaluation, histology and immunohistochemistry. In intestinal epithelial cells, DADS reduced IP-10 and IL-

6 levels, while DAS inhibited IFN-γ-stimulated nitrite production. Such activities may help to explain the protective action of these garlic derived ingredients in experimental IBD.

3. Bromelain, a cysteine protease derived from the stem of pineapple (*Ananas comosus*), normalises intestinal hypermotility in the inflamed gut and exerts chemopreventive actions in an experimental model of colon carcinogenesis. The effect of bromelain on intestinal motility could be due to its ability to activate the PAR-2. On the other hand, its antitumoural action could be related to the stimulation of apoptotic processes via blockade of MAP kinase and (PI3K)/Akt signaling.

4. Boeravinone G, a rotenoid isolated from the Ayurvedic plant *Boerhaavia diffusa*, exerts potent antioxidant and genoprotective actions. The genoprotective effect of boeravinone G was associated to up-regulation of $pERK_1$ and NF-kB expression. These promising *in vitro* results will be confirmed *in vivo* in experimental models of IBD and colon carcinogenesis.

Overall, our study not only unravel new interesting pharmacologically active plant compounds for specific gastrointestinal diseases, but opens the possibility to translate such preclinical results to possible future clinical trials.

7.0 REFERENCES

Aikawa R, Komuro I, Yamazaki T, Zou Y, Kudoh S, Tanaka M, Shiojima I, Hiroi Y, Yazaki Y. Oxidative stress activates extracellular signal-regulated kinases through Src and Ras in cultured cardiac myocytes of neonatal rats. J Clin Invest. 1997;100:1813-1821.

Alhouayek M, Muccioli GG. The endocannabinoid system in inflammatory bowel diseases: from pathophysiology to therapeutic opportunity. Trends Mol Med. 2012;18:615-625.

Andersen SN, Rognum TO, Bakka A, Clausen OP. Ki-67: a useful marker for the evaluation of dysplasia in ulcerative colitis. Mol Pathol. 1998;51:327-332.

Anderson D, Phillips BJ. Comparative in vitro and in vivo effects of antioxidants. Food Chem Toxicol. 1999;37:1015-1025.

Appendino G, Gibbons S, Giana A, Pagani A, Grassi G, Stavri M, Smith E, Rahman MM. Antibacterial cannabinoids from Cannabis sativa: a structure-activity study. J Nat Prod. 2008;71:1427-1430.

Artis D. Epithelial-cell recognition of commensal bacteria and maintenance of immune homeostasis in the gut. Nat Rev Immunol. 2008;8:411–420.

Aviello G, Borrelli F, Guida F, Romano B, Lewellyn K, De Chiaro M, Luongo L, Zjawiony JK, Maione S, Izzo AA, Capasso R. Ultrapotent effects of salvinorin A, a hallucinogenic compound from Salvia divinorum, on LPS-stimulated murine macrophages and its anti-inflammatory action in vivo. J Mol Med (Berl). 2011;89:891-902.

Aviello G, Romano B, Borrelli F, Capasso R, Gallo L, Piscitelli F, Di Marzo V, Izzo AA. Chemopreventive effect of the non-psychotropic phytocannabinoid cannabidiol on experimental colon cancer. J Mol Med (Berl). 2012;90:925-934.

Aviello G, Rowland I, Gill CI, Acquaviva AM, Capasso F, et al. Antiproliferative effect of rhein, an anthraquinone isolated from Cassia species, on Caco-2 human adenocarcinoma cells. J Cell Mol Med. 2010;14:2006–2014.

Banks C, Bateman A, Payne R, Johnson P, Sheron N. Chemokine expression in IBD. Mucosal chemokine expression is unselectively increased in both ulcerative colitis and Crohn's disease. J Pathol. 2003;199:28–35.

Barbara G, Xing Z, Hogaboam CM, Gauldie J, Collins SM. Interleukin 10 gene transfer prevents experimental colitis in rats. Gut. 2000;46:344-349.

Bent S. Herbal medicine in the United States: review of efficacy, safety, and regulation: grand rounds at University of California, San Francisco Medical Center. J Gen Intern Med. 2008;23:854-859.

Beuth J, Braun JM. Modulation of murine tumor growth and colonization by bromelaine, an extract of the pineapple plant (Ananas comosum L.). In Vivo. 2005;19:483-485.

Bickers DR, Athar M. Oxidative stress in the pathogenesis of skin disease. J Invest Dermatol. 2006 126: 2565-2575.

Birben E, Sahiner UM, Sackesen C, Erzurum S, Kalayci O. Oxidative stress and antioxidant defense. World Allergy Organ. J. 2012; 5:9-19.

Block E. The chemistry of garlic and onions. Sci Am. 1985 ;252:114-119.

Blonski W, Buchner AM, Lichtenstein GR. Inflammatory bowel disease therapy: current state-of-the-art. Curr Opin Gastroenterol. 2011;27:346-357.

Borchardt JK. The beginnings of drug therapy: Ancient mesopotamian medicine, Drug News Perspect. 2002;15:187–192.

Borrelli F, Aviello G, Romano B, Orlando P, Capasso R, Maiello F, Guadagno F, Petrosino S, Capasso F, Di Marzo V, Izzo AA. Cannabidiol, a safe and non-psychotropic ingredient of the marijuana plant Cannabis sativa, is protective in a murine model of colitis. J Mol Med. 2009; 87:1111-1121.

Borrelli F, Capasso F, Capasso R, Ascione V, Aviello G, Longo R, Izzo AA. Effect of Boswellia serrata on intestinal motility in rodents: inhibition of diarrhoea without constipation. Br J Pharmacol. 2006;148:553–560.

Borrelli F, Capasso R, Izzo AA. Garlic (Allium sativum L.): adverse effects and drug interactions in humans. Mol Nutr Food Res. 2007;51:1386-1397.

Bradford MM. A rapid and sensitive method for the quantitation of microgram quantities of protein utilizing the principle of protein–dye binding. Anal Biochem.1976;72:248–254.

Calvo-Gomez O, Morales-Lopez J, Lopez MG. Solid-phase microextraction-gas chromatographic-mass spectrometric analysis of garlic oil obtained by hydrodistillation. J. Chromatogr. A. 2004;1036:91–93.

Canadanovic-Brunet JM, Djilas SM, Cetkovic GS, Tumbas VT. Freeradical scavenging of wormwood (Arthemisia absinthium L) extracts. J Sci Food Agric.2005; 85: 265–272.

Capasso F, Gaginella TS, Grandolini G, Izzo AA. Phytotherapy. A Quick Reference to Herbal Medicine. Berlin, Springer-Verlag, 2003.

Capasso R, Borrelli F, Cascio MG, Aviello G, Huben K, Zjawiony JK, Marini P, Romano B, Di Marzo V, Capasso F, Izzo AA. Inhibitory effect of salvinorin A, from Salvia divinorum, on ileitis-induced hypermotility: cross-talk between kappa-opioid and cannabinoid CB(1) receptors. Br J Pharmacol. 2008;155:681-689.

Capasso R, Izzo AA, Fezza F, Pinto A, Capasso F, Mascolo N, Di Marzo V. Inhibitory effect of palmitoylethanolamide on gastrointestinal motility in mice. Br J Pharmacol. 2001;134:945-50.

Cascio MG, Gauson LA, Stevenson LA, Ross RA, Pertwee RG. Evidence that the plant annabinoid cannabigerol is a highly potent alpha2-adrenoceptor agonist and moderately potent 5HT1A receptor antagonist. Br J Pharmacol. 2010;159:129-141.

Chiang YH, Jen LN, Su HY, Lii CK, Sheen LY, Liu CT. Effects of garlic oil and two of its major organosulfur compounds, diallyl disulfide and diallyl trisulfide, on intestinal damage in rats injected with endotoxin. Toxicol Appl Pharmacol. 2006;213:46-54.

Chobotova, K., Vernallis, A.B., Majid, F.A., Bromelain's activity and potential as an anti-cancer agent: Current evidence and perspectives. Cancer Lett. 2010; 290:148-156.

Clavel T, Haller D. Bacteria- and host-derived mechanisms to control intestinal epithelial cell homeostasis: implications for chronic inflammation. Inflamm Bowel Dis. 2007;13:1153–1164.

Colasanti BK. A comparison of the ocular and central effects of delta 9-tetrahydrocannabinol and cannabigerol. J Ocul Pharmacol. 1990;6:259-69.

Collins AR. The Comet assay for DNA damage and repair: principles, applications, and limitations. Mol Biotechnol 2004; 26:249-261.

Conde de la Rosa L, Schoemaker MH, Vrenken TE, Buist-Homan M, Havinga R, Jansen PL, Moshage H.Superoxide anions and hydrogen peroxide induce hepatocyte death by different mechanisms: involvement of JNK and ERK MAP kinases. J Hepatol. 2006; 44: 918-929.

Cosnes J, Gower-Rousseau C, Seksik P, Cortot A. Epidemiology and natural history of inflammatory bowel diseases. Gastroenterology. 2011;140:1785-94.

Cragg GM, Newman DJ. Plants as a source of anti-cancer agents. J Ethnopharmacol. 2005;100:72-79.

Cragg GM, Newman DJ. Natural products: A continuing source of novel drug leads. Biochimica et Biophysica Acta. 2013. [Epub ahead of print].

Cunningham D, Atkin W, Lenz HJ, Lynch HT, Minsky B, Nordlinger B, Starling N. Colorectal cancer. Lancet. 2010;375:1030-1047.

D'Argenio G, Valenti M, Scaglione G, Cosenza V, Sorrentini I, Di Marzo V. Up-regulation of anandamide levels as an endogenous mechanism and a pharmacological strategy to limit colon inflammation. FASEB J. 2006;20:568–570.

De Petrocellis L, Ligresti A, Moriello AS, Allarà M, Bisogno T, Petrosino S, Stott CG, Di Marzo V. Effects of cannabinoids and cannabinoid-enriched Cannabis extracts on TRP channels and endocannabinoid metabolic enzymes. Br J Pharmacol. 2011;163:1479-1494.

De Petrocellis L, Orlando P, Moriello AS, Aviello G, Stott C, Izzo AA, Di Marzo V. Cannabinoid actions at TRPV channels: effects on TRPV3 and TRPV4 and their potential relevance to gastrointestinal inflammation. Acta Physiol 2012;204:255-266.

Deiana S, Watanabe A, Yamasaki Y, Amada N, Arthur M, Fleming S, Woodcock H, Dorward P, Pigliacampo B, Close S, Platt B, Riedel G. Plasma and brain pharmacokinetic profile of cannabidiol (CBD), cannabidivarine (CBDV), Δ-9-tetrahydrocannabivarin (THCV) and cannabigerol (CBG) in rats and mice following oral and intraperitoneal administration and CBD action on obsessive-compulsive behaviour. Psychopharmacology 2012;219:859-873.

Dhar ML, Dhar MM, Dhawan BN, Mehrotra BN, Ray C. Screening of Indian plants for biological activity: I. Indian J Exp Biol. 1968; 6: 232-247.

Dryden GW Jr, Deaciuc I, Arteel G, McClain CJ. Clinical implications of oxidative stress and antioxidant therapy. Curr Gastroenterol Rep. 2005; 7: 308-316.

Efferth, T., Signal Transduction Pathways of the Epidermal Growth Factor Receptor in Colorectal Cancer and their Inhibition by Small Molecules. Curr. Med. Chem. 2012;19: 5735-5744.

Ekbom A, Helmick C, Zack M, Adami HO. Ulcerative colitis and colorectal cancer. A population-based study. N Engl J Med. 1990;323:1228-1233.

Ernst B, Thurnheer M, Schultes B. Copper deficiency after gastric bypass surgery. Obesity (Silver Spring). 2009;17:1980-1981.

Esterbauer H, Cheeseman KH. Determination of aldehydic lipid peroxidation products: malonaldehyde and 4-hydroxynonenal. Methods Enzymol 1990;186:407-421.

Gálvez J, Garrido M, Merlos M, Torres MI, Zarzuelo A. Intestinal anti-inflammatory activity of UR-12746, a novel 5-ASA conjugate, on acute and chronic experimental colitis in the rat. Br J Pharmacol. 2000;130:1949-1959.

Goldblum SE, Wu KM, Jay M. Lung myeloperoxidase as a measure of pulmonary leukostasis in rabbits. J Appl Physiol 1985;59:1471–1480.

Goldstone AB, Liochev SI, Fridovich I. Inactivation of copper, zinc superoxide dismutase by H_2O_2: mechanism of protection. Free Radic Biol Med. 2006;41:1860-1863.

Gu X, Zhu YZ. Therapeutic applications of organosulfur compounds as novel hydrogen sulfide donors and/or mediators. Expert Rev Clin Pharmacol. 2011;4:123-133.

Hale LP, Greer PK, Trinh CT, Gottfried MR. Treatment with oral bromelain decreases colonic inflammation in the IL-10-deficient murine model of inflammatory bowel disease. Clin Immunol. 2005;116:135-142.

Half E, Arber N. Colon cancer: preventive agents and the present status of chemoprevention. Expert Opin Pharmacother. 2009;10:211-219.

Hart C, Cohen R, Norwood M, Stebbing J. The emerging harm of antioxidants in carcinogenesis. Future Oncol. 2012;8:535-548.

Hill AJ, Williams CM, Whalley BJ, Stephens GJ. Phytocannabinoids as novel therapeutic agents in CNS disorders. Pharmacol Ther. 2012;133:79-97.

Hilsden RJ, Verhoef MJ, Best A, Pocobelli G. Complementary and alternative medicine use by Canadian patients with inflammatory bowel disease: results from a national survey. Am J Gastroenterol. 2003;98:1563-1568.

Hoermannsperger G, Clavel T, Hoffmann M, Reiff C, Kelly D, Loh G, Blaut M, Hölzlwimmer G, Laschinger M, Haller D. Post-translational inhibition of IP-10 secretion in IEC by probiotic bacteria: impact on chronic inflammation. PLoS One. 2009;4:e4365.

Holzer P. Transient receptor potential (TRP) channels as drug targets for diseases of the digestive system. Pharmacol Ther. 2011;131:142-170.

Hou JK, El-Serag H, Thirumurthi S. Distribution and manifestations of inflammatory bowel disease in Asians, Hispanics, and African Americans: a systematic review. Am J Gastroenterol. 2009;104:2100-2109.

Huang KC The pharmacology of chinese herbs, 2nd ed. CRC Press, Boca Raton, FL, 1999.

Hunter MM, Wang A, Hirota CL, McKay DM. Neutralizing anti-IL-10 antibody blocks the protective effect of tapeworm infection in a murine model of chemically induced colitis. J. Immunol. 2005;174:7368–7375.

Hyun J, Lee G, Brown JB, Grimm GR, Tang Y, Mittal N, Dirisina R, Zhang Z, FryerJP , Weinstock JV, Luster AD, Barrett TA Anti-interferon-inducible chemokine, CXCL10, reduces colitis by impairing T helper-1 induction and recruitment in mice. Inflamm Bowel Dis. 2005;11:799–805.

Iciek MB, Kowalczyk-Pachel D, Kwiecień I, Dudek MB. Effects of different garlic-derived allyl sulfides on peroxidative processes and anaerobic sulfur metabolism in mouse liver. Phytother Res. 2012;26:425-31.

Ito R, Shin-Ya M, Kishida T, Urano A, Takada R, Sakagami J, Imanishi J, Kita M, Ueda Y, Iwakura Y, Kataoka K, Okanoue T, Mazda O. Interferon-gamma is causatively involved in experimental inflammatory bowel disease in mice. Clin Exp Immunol 2006;146:330-338.

Izzo AA, Borrelli F, Capasso R, Di Marzo V, Mechoulam R. Non-psychotropic plant cannabinoids: new therapeutic opportunities from an ancient herb. Trends Pharmacol Sci. 2009;30:515-527.

Izzo AA, Capasso R, Aviello G, Borrelli F, Romano B, Piscitelli F, Gallo L, Capasso F, Orlando P, Di Marzo V. Inhibitory effect of cannabichromene, a major non-psychotropic cannabinoid extracted from Cannabis sativa, on inflammation-induced hypermotility in mice. Br J Pharmacol. 2012;166:1444-1460.

Jacob C, Yang PC, Darmoul D, Amadesi S, Saito T, Cottrell GS, Coelho AM, Singh P, Grady EF, Perdue M, Bunnett NW. Mast cell tryptase controls paracellular permeability of the intestine. Role of protease-activated receptor 2 and beta-arrestins. J Biol Chem. 2005; 280:31936-1948.

Jamontt JM, Molleman A, Pertwee RG, Parsons ME. The effects of Delta-tetrahydrocannabinol and cannabidiol alone and in combination on damage, inflammation and in vitro motility disturbances in rat colitis. Br J Pharmacol. 2010;160:712-723.

Jones NP, Siegle GJ, Proud L, Silk JS, Hardy D, Keljo DJ, Dahl RE, Szigethy E.Impact of inflammatory bowel disease and high-dose steroid exposure on pupillary responses to negative information in pediatric depression. Psychosom Med. 2011;73:151-157.

Kalayarasan S, Prabhu PN, Sriram N, Manikandan R, Arumugam M, Sudhandiran G. Diallyl sulfide enhances antioxidants and inhibits inflammation through the activation of Nrf2 against gentamicin-induced nephrotoxicity in Wistar rats. Eur J Pharmacol. 2009;606:162-171.

Kalra, N., Bhui, K., Roy, P., Srivastava, S. et al., Regulation of p53, nuclear factor kappaB and cyclooxygenase-2 expression by bromelain through targeting mitogen-activated protein kinase pathway in mouse skin. Toxicol. Appl. Pharmacol. 2008;226:30-37.

Kapoor LD. Handbook of Ayurvedic Medicinal Plants; CRC Press. Boca Raton,1990.

Karihtala P, Soini Y Reactive oxygen species and antioxidant mechanisms in human tissues and their relation to malignancies. APMIS 2007;115:81-103.

Kefaloyianni E, Gaitanaki C, Beis I. ERK1/2 and p38-MAPK signalling pathways, through MSK1, are involved in NF-kappaB transactivation during oxidative stress in skeletal myoblasts. Cell Signal. 2006;18: 2238–2251.

Kelso EB, Lockhart JC, Hembrough Tet al. Therapeutic promise of proteinase-activated receptor-2 antagonism in joint inflammation. J Pharmacol Exp Ther. 2006;316:1017–1024.

Kim H. Oxidative stress in Helicobacter pylori-induced gastric cell injury. Inflammopharmacology. 2005;13: 63-74.

Kolios G, Valatas V, Ward SG. Nitric oxide in inflammatory bowel disease: a universal messenger in an unsolved puzzle. Immunology. 2004;113:427-437.

Kruidenier, L., and HW. Verspaget. Review article: oxidative stress as a pathogenic factor in inflammatory bowel disease--radicals or ridiculous? Aliment Pharmacol Ther 2002;16:1997-2015.

Kulich SM, Chu CT. Role of reactive oxygen species in ERK phosphorylation and 6-hydroxydopamine cytotoxicity. J Biosci. 2003;28:83-89.

Kupchan SM, Britton RW, Ziegler MF, Sigel CW. Bruceantin, a new potent antileukemic simaroubolide from Brucea antidysenterica. J Org Chem.1973;38:178–179.

Kuthan H, Haussmann HJ, Werringloer J. A spectrophotometric assay for superoxide dismutase activities in crude tissue fractions. Biochem J. 1986;237:175–180.

Lahat A, Lang A, Ben-Horin S. Impact of cannabis treatment on the quality of life, weight and clinical disease activity in inflammatory bowel disease patients: a pilot prospective study. Digestion. 2012;85:1-8.

Lal S, Prasad N, Ryan M, Tangri S, Silverberg MS, Gordon A, Steinhart H. Cannabis use amongst patients with inflammatory bowel disease. Eur J Gastroenterol Hepatol. 2011;23:891-896.

Lee HS, Lee CH, Tsai HC, Salter DM. Inhibition of cyclooxygenase 2 expression by diallyl sulfide on joint inflammation induced by urate crystal and IL-1beta. Osteoarthritis Cartilage. 2009;17:91-99.

Leyon PV, Lini CC, Kuttan G. Inhibitory effect of Boerhaavia diffusa on experimental metastasis by B16F10 melanoma in C57BL/6 mice. Life Sci. 2005;76:1339-1349.

Liu LN, Mei QB, Liu L, Zhang F, Liu ZG, Wang ZP, Wang RT Protective effects of Rheum tanguticum polysaccharide against hydrogen peroxide-induced intestinal epithelial cell injury. World J Gastroenterol. 2005;11:1503-1507.

Madsen K. Combining T cells and IL-10: a new therapy for Crohn's disease? Gastroenterology. 2002;123:2140-2144.

Madsen K. Combining T cells and IL-10: a new therapy for Crohn's disease? Gastroenterology2002;123:2140-2144.

Markowitz SD, Bertagnolli MM. Molecular origins of cancer: molecular basis of colorectal cancer. N Engl J Med. 2009;361:2449–2460.

Massa F, Marsicano G, Hermann H, Cannich A, Monory K, Cravatt BF, Ferri GL, Sibaev A, Storr M, Lutz B. The endogenous cannabinoid system protects against colonic inflammation. J Clin Invest. 2004;113:1202-1209.

Maurer, H.R., Bromelain: biochemistry, pharmacology and medical use. Cell. Mol. Life Sci. 2001; 58:1234-1245.

Mechoulam R, Ben-Shabat S From gan-zi-gun-nu to anandamide and 2-arachidonoylglycerol: the ongoing story of cannabis. Nat Prod Rep. 1999;16:131–143.

Molodecky NA, Soon IS, Rabi DM, Ghali WA, Ferris M, Chernoff G, Benchimol EI, Panaccione R, Ghosh S, Barkema HW, Kaplan GG. Increasing incidence and prevalence of the inflammatory bowel diseases with time, based on systematic review. Gastroenterology. 2012;142:46-54.

Moncada S, Higgs A, Furchgott R. International Union of Pharmacology Nomenclature in Nitric Oxide Research. Pharmacol Rev. 1997;49:137-142.

Mosmann T. Rapid colorimetric assay for cellular growth and survival: application to proliferation and cytotoxicity assays. J Immunol Methods.1983;65:55–63.

Mynott, T.L., Ladhams, A., Scarmato, P., Engwerda, C.R., Bromelain, from pineapple stems, proteolytically blocks activation of extracellular regulated kinase-2 in T cells. J. Immunol. 1999;163: 2568-2575.

Naftali T, Lev LB, Yablecovitch D, Half E, Konikoff FM. Treatment of Crohn's disease with cannabis: an observational study. Isr Med Assoc J. 2011;13:455-458.

Nakabeppu Y, Sakumi K, Sakamoto K, Tsuchimoto D, Tsuzuki T, Nakatsu Y. Mutagenesis and carcinogenesis caused by the oxidation of nucleic acids. Biol Chem. 2006;387: 373-379.

Onken JE, Greer PK, Calingaert B, Hale LP. Bromelain treatment decreases secretion of pro-inflammatory cytokines and chemokines by colon biopsies in vitro. Clin Immunol. 2008;126:345-352.

Orsini RA. Plastic Surgery Educational Foundation Technology Assessment Committee. Bromelain. Plast Reconstr Surg. 2006;118:1640-1644.

Osanai M, Nishikiori N, Murata M, Chiba H, Kojima T, Sawada N. Cellular retinoic acid bioavailability determines epithelial integrity: Role of retinoic acid receptor alpha agonists in colitis. Mol Pharmacol. 2007;71:250-258.

Palmer RM, Ashton DS, Moncada S. Vascular endothelial cells synthesize nitric oxide from L-arginine. Nature. 1988;333:664-666.

Pari L, Amarnath Satheesh M. Antidiabetic effect of Boerhaavia diffusa: effect on serum and tissue lipids in experimental diabetes. J Med Food. 2004;7:472-476.

Pavan R, Jain S, Shraddha, Kumar A. Properties and therapeutic application of bromelain: a review. Biotechnol Res Int. 2012;2012:976203.

Pfaffl MW. A new mathematical model for relative quantification in real-time RT-PCR. Nucleic Acids Res. 2001;29:e45.

Pol O, Puig MM. Reversal of tolerance to the antitransit effects of morphine during acute intestinal inflammation in mice. Br J Pharmacol. 1997; 122:1216-1222.

Pollastro F, Taglialatela-Scafati O, Allarà M, Muñoz E, Di Marzo V, De Petrocellis L, Appendino G. Bioactive prenylogous cannabinoid from fiber hemp (Cannabis sativa). J Nat Prod. 2011;74:2019-2022.

Rahier NJ, Cheng K, Gao R, Eisenhauer BM, Hecht SM. Synthesis of 14-azacamptothecin, a water-soluble topoisomerase I poison. Org Lett. 2005;7:835-837.

Rahimi R, Mozaffari S, Abdollahi M. On the use of herbal medicines in management of inflammatory bowel diseases: a systematic review of animal and human studies. Dig Dis Sci. 2009;54:471-480.

Rahman I, Biswas SK, Kode A. Oxidant and antioxidant balance in the airways and airway diseases. Eur J Pharmacol 2006; 533: 222-239.

Rahman M, Selvarajan K, Hasan MR, Chan AP, Jin C, Kim J, Chan SK, Le ND, Kim YB, Tai IT. Inhibition of COX-2 in colon cancer modulates tumor growth and MDR-1 expression to enhance tumor regression in therapy-refractory cancers in vivo. Neoplasia. 2012;14:624-633.

Ramasarma T. Emergence of oxyl radicals as selective oxidants. Indian J Biochem Biophys. 2012;49:295-305.

Reddy VB, Lerner EA. Plant cysteine proteases that evoke itch activate protease-activated receptors. Br J Dermatol. 2010;163:532-535.

Rego AC, Santos MS, Oliveira CR. Influence of the antioxidants vitamin E and idebenone on retinal cell injury mediated by chemical ischemia, hypoglycemia, or oxidative stress. Free Radic Biol Med. 1999;26:1405-1417.

Rock EM, Goodwin JM, Limebeer CL, Breuer A, Pertwee RG, Mechoulam R, Parker LA. Interaction between non-psychotropic cannabinoids in marihuana: effect of cannabigerol (CBG) on the anti-nausea or anti-emetic effects of cannabidiol (CBD) in rats and shrews. Psychopharmacology (Berl). 2011;215:505-512.

Romano B, Borrelli F, Fasolino I, Capasso R, Piscitelli F, Cascio M, Pertwee R, Coppola D, Vassallo L, Orlando P, Di Marzo V, Izzo A. The cannabinoid TRPA1 agonist cannabichromene inhibits nitric oxide production in macrophages and ameliorates murine colitis. Br J Pharmacol. 2013 Feb 4. doi: 10.1111/bph.12120.[Epub ahead of print].

Ruhaak LR, Felth J, Karlsson PC, Rafter JJ, Verpoorte R, Bohlin L. Evaluation of the cyclooxygenase inhibiting effects of six major cannabinoids isolated from Cannabis sativa. Biol Pharm Bull. 2011;34:774-778.

Ruiz P, Shkoda A, Kim SC, Sartor RB, Haller D. IL-10 gene deficient mice lack

TGFß/Smad signalling and fail to inhibit proinflammatory gene expression in intestinal epithelial cells after the colonisation with colitogenic Enterococcus faecalis. J Immunol. 2005;174:2990–2999.

Sachidanandam K, Fagan SC, Ergul A. Oxidative stress and cardiovascular disease: antioxidants and unresolved issues. Cardiovasc Drug Rev. 2005;23:115-132.

Samuelsson Gunnar. Drugs of Natural Origin. A textbook of Farmacognosy, 4th revised edition, 1999.

Sargent DJ, Patiyil S, Yothers G, Haller DG, Gray R, Benedetti J, et al. End Points for colon cancer adjuvant trials: observations and recommendations based on individual patient data from 20, 898 patients enrolled onto 18 randomized trials from the ACCENT group. J Clin Oncol. 2007;25:4569-4574.

Sato K, Ninomiya H, Ohkura S, Ozaki H, Nasu T. Impairment of PAR-2-mediated relaxation system in colonic smooth muscle after intestinal inflammation. Br J Pharmacol 2006; 148: 200-7.

Sewell JL, Inadomi JM, Yee HF Jr. Race and inflammatory bowel disease in an urban healthcare system. Dig Dis Sci. 2010;55:3479-3487.

Shi M, Yang H, Motley ED, Guo Z Overexpression of Cu/Zn-superoxide dismutase and/or catalase in mice inhibits aorta smooth muscle cell proliferation. Am J Hypertens. 2004;17:450-456.

Shivashankar R, Loftus EV Jr, Tremaine WJ, Bongartz T, Harmsen WS, Zinsmeister AR, Matteson EL. Incidence of spondyloarthropathy in patients with Crohn's disease: a population-based study. J Rheumatol. 2012;39:2148-2152.

Shivashankar R, Loftus EV Jr, Tremaine WJ, Bongartz T, Harmsen WS, Zinsmeister AR, Matteson EL. Incidence of spondyloarthropathy in patients with Crohn's disease: a population-based study. J Rheumatol. 2012;39:2148-2152.

Siegel R, Naishadham D, Jemal A. Cancer statistics. CA Cancer J Clin. 2013;63:11-30.

Strober W, Fuss IJ. Proinflammatory cytokines in the pathogenesis of inflammatory bowel diseases. Gastroenterology. 2011;140:1756-1767.

Suzuki K, Kawauchi Y, Palaniyandi SS, Veeraveedu PT, Fujii M, Yamagiwa S, Yoneyama H, Han GD, Kawachi H, Okada Y, Ajioka Y, Watanabe K, Hosono M, Asakura H, Aoyagi Y, Narumi S. Blockade of interferon-gamma-inducible protein-10 attenuates chronic experimental colitis by blocking cellular trafficking and protecting intestinal epithelial cells. Pathol Int. 2007;57:413–420.

Taussig SJ, Batkin S. Bromelain, the enzyme complex of pineapple (Ananas comosus) and its clinical application. An update. J Ethnopharmacol. 1988;22:191-203.

Triantafillidis JK, Nasioulas G, Kosmidis PA. Colorectal cancer and inflammatory

bowel disease: epidemiology, risk factors, mechanisms of carcinogenesis and prevention strategies. Anticancer Res. 2009;29:2727-2737.

Turner CE, Elsohly MA, Boeren EG. Constituents of Cannabis sativa L. XVII. A review of the natural constituents. J Nat Prod. 1980;43:169-234.

Valko M, Rhodes CJ, Moncola J, Izakovic M, Mazura M . Free radicals, metals and antioxidants in oxidative stress-induced cancer. Chemico-Biological Interactions. 2006;160:1-40.

Vantaggiato C, Formentini I, Bondanza A, Bonini C, Naldini L, Brambilla R. ERK1 and ERK2 mitogen-activated protein kinases affect Ras-dependent cell signaling differentially. J Biol 2006;5:14.

Wallace JL. Physiological and pathophysiological roles of hydrogen sulfide in the gastrointestinal tract. Antioxid Redox Signal. 2010;12:1125-1133.

Wang HC, Pao J, Lin SY, Sheen LY. Molecular mechanisms of garlic-derived allyl sulfides in the inhibition of skin cancer progression. Ann N Y Acad Sci. 2012;1271:44-52.

Watterlot L, Rochat T, Sokol H, Cherbuy C, Bouloufa I, Lefevre F, Gratadoux JJ, Honvo-Hueto E, Chilmonczyk S, Blugeon S, Corthier G, Langella P, Bermudez-Humaran LG. Intragastric administration of a superoxide dismutase-producing recombinant Lactobacillus casei BL23 strain attenuates DSS colitis in mice. Int. J. Food Microbiol. 2010;144:35-41.

Weigelt B, Downward J. Genomic Determinants of PI3K Pathway Inhibitor Response in Cancer. Front Oncol. 2012; 2:109.

Willcox JK, Ash SL, Catignani GLAntioxidants and prevention of chronic disease. Crit Rev Food Sci Nutr. 2004;44:275-295.

Wolpin BM, Mayer RJ. Systemic treatment of colorectal cancer. Gastroenterology. 2008;134:1296-1310.

Woo HM, Kang JH, Kawada T, Yoo H, Sung MK, Yu R. Active spice-derived components can inhibit inflammatory responses of adipose tissue in obesity by suppressing inflammatory actions of macrophages and release of monocyte chemoattractant protein-1 from adipocytes. Life Sci. 2007;80:926-31.

Xavier RJ, Podolsky DK Unravelling the pathogenesis of inflammatory bowel disease. Nature. 2007;448:427–434.

Yang CS, Wang H, Li GX, Yang Z, Guan F, Jin H. Cancer prevention by tea: Evidence from laboratory studies. Pharmacol Res. 2011;64:113-122.